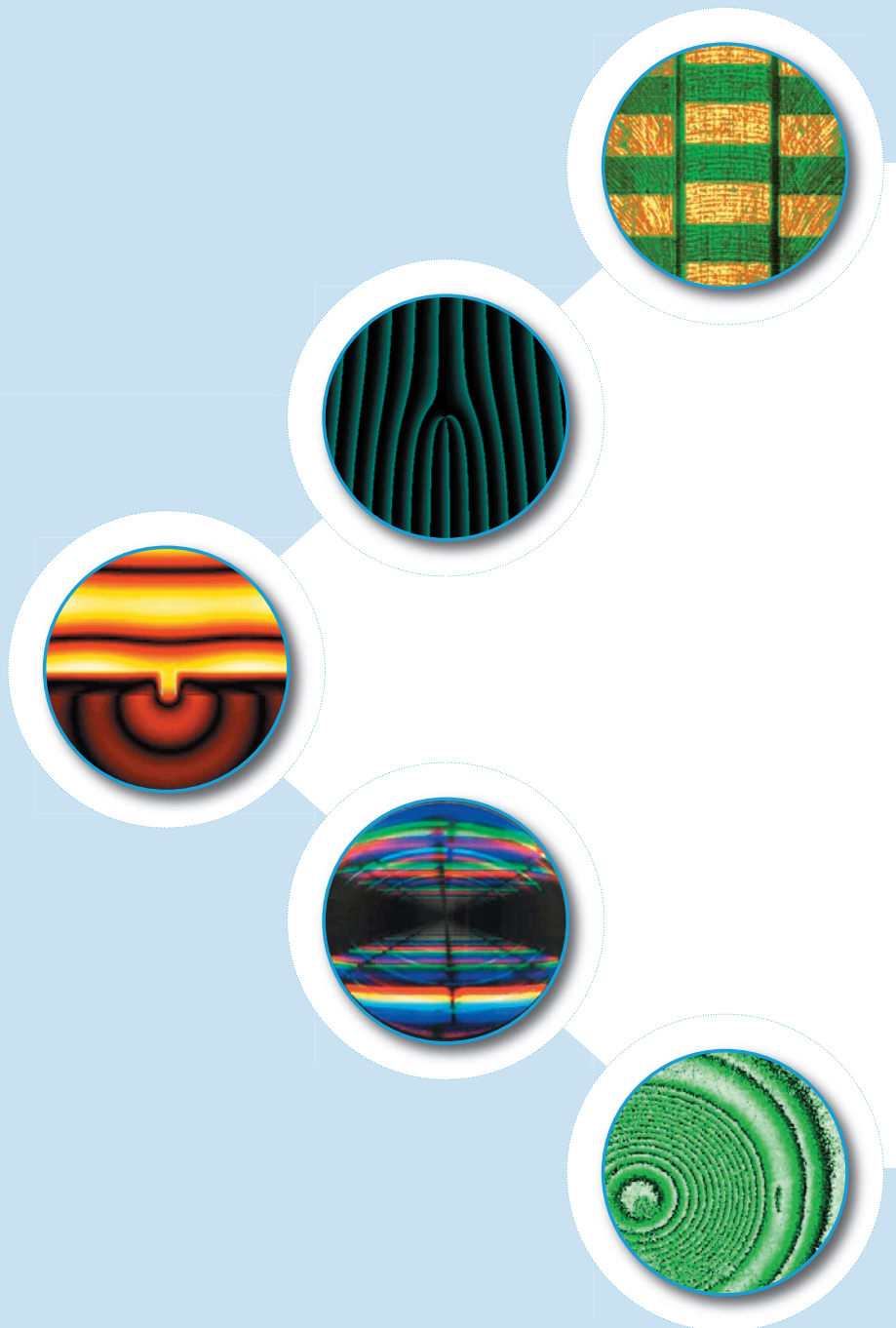




annual report
2003 / 2004

INSTITUT FÜR
TECHNISCHE OPTIK
UNIVERSITÄT STUTTGART



INSTITUT FÜR TECHNISCHE OPTIK
UNIVERSITÄT STUTTGART
Prof. Dr. W. Osten



Pfaffenwaldring 9
D-70569 Stuttgart
Tel.: +49(0)711 685-6075
Fax: +49(0)711 685-6586
<http://www.uni-stuttgart.de/ito>

ANNUAL REPORT 2003/2004

Dear Reader,

This is the first edition of the ITO research report since the change of the Institute Director in 2002. At the end of August 2002 and after 23 years of successful work for the Institute and for the international optics community Prof. Hans Tiziani retired. On the 1st September 2002 the position of Institute Director was handed over to me. Since then more than 2 years have passed and it is again time to report on the activities of ITO in the field of Applied Optics.

In the modern world we still rely on some golden rules. One of them – well known from the sports world - says “*Don't change a winning team*”. If we change this a little by replacing the word team by the word concept, I would also apply this rule to my personal understanding of the running of science in our highly competitive world. Thus continuity together with careful renewing and modernization is the basis that determines the direction of the whole team at the Institute. As part of the Faculty of Mechanical Engineering, the Institute represents Stuttgart University in the field of Engineering Optics in research and education. Together with our national and international partners, our research work focuses on the exploration of new measurement and design principles and their implementation in new optical components, sensors and sensor systems. One of our central goals is the extension of existing limits by combining modelling, simulation and experimental data acquisition within actively controlled measurement processes.

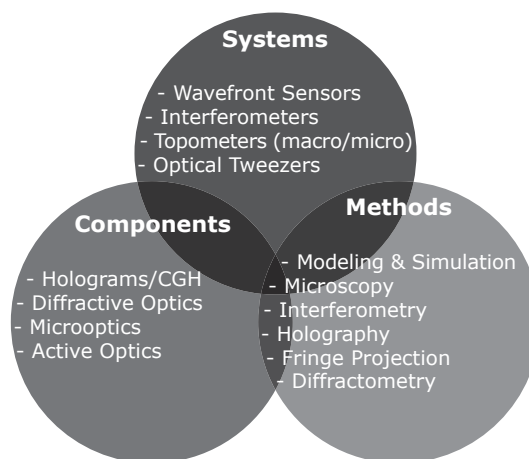
The five main research areas of the Institute can be summarized as:

- the investigation and implementation of new sensors and procedures for the 3D measurement of optical, technical and biological surfaces in macro, micro and nano scales,
- the design of active optical components and algorithms for the spatio-temporal manipulation and control of complex wavefronts including amplitude, phase and polarization,
- the development of new strategies for the high resolution measurement of sub-wavelength scale structures by the combination of rigorous physical modelling, computer-aided simulation and experimental data acquisition,
- the design and fabrication of customer-specific diffractive optics and the investigation of new measurement concepts for the testing of optical components, in particular, aspheric lenses, and
- the investigation and application of coherent optical measurement methods for the full-field and non-destructive investigation of technical and biological components with respect to static and dynamic deformations, 3D-shapes, internal imperfections and material properties.

These five research aims are each pursued by one of the five research groups which make up the Institute. Together with the strong interactions between these groups, this gives the Institute a strength in depth over a broad range of optics activities. The considerable number of research projects that are referred to in this report reflects the success of this approach. Along with the fulfilment of these research projects the Institute is currently undergoing a modernisation of the equipment and infrastructure. The most important activity concerns the construction of a new cleanroom where the fabrication of diffractive optical elements and the high resolution optical metrology will find an adequate technological basis and environment. This is planned for completion in May 2006.

To cope with our ambitious and widely spanned approach in Applied Optics a deep understanding of the physics of optics needs to be combined with practical engineering implementation. The fulfilment of this boundary condition means a daily challenge for all members of the staff. However, a good mixture of graduates in physics and engineering, a vital and innovative scientific climate that considers the interdisciplinary cooperation with numerous national and international institutes and a continuous observation of the technological and scientific progress – the traditional features of the ITO - are a good basis to meet these and future challenges. May this report once again convince our sponsors, customers and partners of this.

Wolfgang Osten



Applied optical methods and their implementations in new optical components, sensors and sensor systems.

Index

Institute structure

| | |
|-----------------------------|----|
| Team and structure | 08 |
| Staff of the Institute..... | 10 |
| Studying optics..... | 13 |
| The research groups..... | 14 |

Research projects

3D-Surface Metrology

| | |
|---|----|
| Hybrid microoptic sensors using the chromatic-confocal focus detection principle (HymoSens) .. | 18 |
| <i>A. Ruprecht, C. Pruss, H. J. Tizjani, W. Osten</i> | |
| Micro optical components: Fast parallel characterization of micro optic arrays | 19 |
| <i>T. Wiesendanger, Y. Yasuno, S. Reuter, A. Ruprecht, H.J. Tizjani</i> | |
| Integration of optical measurement techniques for laser welding process control (INESS)..... | 20 |
| <i>T. Wiesendanger, A. Ruprecht, K. Körner, H.J. Tizjani, W. Osten</i> | |
| Full Field, Fast Confocal Laser Microscopy for Measuring the Mechanical Properties of Cortical... 22 | |
| <i>BonéT. Wiesendanger, A. Ruprecht, G. Pedrini, K. Körner, H.J. Tizjani, W. Osten, P. Zaslansky, S. Weiner</i> | |
| Aberration correction in a confocal microscope (METAMO)..... | 23 |
| <i>Y. Yasuno, T.F. Wiesendanger, A.K. Ruprecht, C. Pruss, H.J. Tizjani</i> | |
| Microscopic three-dimensional topometry with LCOS displays..... | 24 |
| <i>C. Kobler, K.-P. Proll, J.-M. Nivet, K. Körner, H. J. Tizjani, W. Osten</i> | |
| Evaluation and Characterization of Liquid Crystal SLMs for Digital Comparative Holography (DISCO).. | 26 |
| <i>C. Kobler, X. Schwab, K.-P. Proll, W. Osten</i> | |
| Collaboration with industry: A new white light interferometer..... | 27 |
| <i>U. Droste, K. Körner, A. Goretzky, W. Osten, P. Lehmann (Mabr GmbH)</i> | |
| Depth-Scanning Fringe Projection (3D-MicroScan) | 28 |
| <i>U. Droste, K. Körner, H.J. Tizjani, W. Osten</i> | |
| Direct Calibration Scheme for the Depth-Scanning Fringe Projection (3D-MicroScan) | 30 |
| <i>J. M. Nivet, U. Droste, K. Körner, H. J. Tizjani, W. Osten</i> | |

Active Optical Systems

| | |
|--|----|
| Detection of contamination on technical surfaces..... | 34 |
| <i>W.Gorski, T.Haist, H.J.Tizjani, W.Osten</i> | |
| Phase-only light modulation: Wavefront shaping tests with piston micro mirror arrays | 35 |
| <i>J. Liesener, W. Osten</i> | |
| Alternative aspheric testing: Interferometer with a tiltable reference wave (CCUPOB) | 36 |
| <i>J. Liesener, C. Pruf, H.J. Tizjani</i> | |

| | |
|---|----|
| Current spatial light modulators: Market analysis and tests on electrowetting and LC lenses..... | 37 |
| <i>J. Liesener, L. Seifert, B. Rühb</i> | |
| Holographic Tweezers: Active Micro-Manipulation (AMIMA)..... | 38 |
| <i>M. Reichert, W. Górski, T. Haist, H.J. Tiziani, W. Osten</i> | |
| Holographic Tweezers: Force Measurement in holographic tweezers..... | 39 |
| <i>M. Reichert, S. Zwick, T. Haist, H.J. Tiziani, W. Osten</i> | |
| Adaptive Shack-Hartmann sensor: A comparison of wavefront reconstruction algorithms (METAMO) .. | 40 |
| <i>L. Seifert, H.J. Tiziani, W. Osten</i> | |
| High Resolution Metrology and Simulation | |
| Rigorous Simulations at the ITO – The Program Package MicroSim..... | 42 |
| <i>S. Rafler, N. Kernien, T. Schuster, M. Totzeck, W. Osten</i> | |
| Rigorous diffraction simulation: A comparison of RCWA, FDTD and FEM (RISOM)..... | 44 |
| <i>R. Berger, J. Kauffmann, N. Kernien, H.J. Tiziani, W. Osten</i> | |
| Both a blessing and a curse: Physical optical effects in high resolution metrology (NanoEdge) .. | 45 |
| <i>N. Kernien, H.J. Tiziani, W. Osten</i> | |
| Scatterometry and diffractometry for nanoelectronic devices (ABBILD)..... | 46 |
| <i>T. Schuster, N. Kernien, J. Kauffmann, W. Osten</i> | |
| Focus-shaping using phase-singularities: Highly sensitive defect detection in the sub-lambda range | 48 |
| <i>N. Kernien, A. Tavrov, H.J. Tiziani, W. Osten</i> | |
| Polarisation measurements for diffractometry (RISOM)..... | 49 |
| <i>J. Kauffmann, J. Bader, S. Meining, N. Kernien, W. Osten, H.J. Tiziani</i> | |
| Tensor-tomographic 3d reconstruction of the anisotropic refractive index inhomogeneity in glass blanks (RISOM) | 50 |
| <i>J. Kauffmann, N. Kernien, W. Osten, H.J. Tiziani</i> | |
| Interferometry and Diffractive Optics | |
| Absolute Calibration of Aspheric Null Tests (CCUPOB)..... | 54 |
| <i>C. Pruss, S. Reichelt, H.J. Tiziani</i> | |
| An Adaptive Null Lens using Membrane Mirrors (METAMO)..... | 55 |
| <i>C. Pruss, C. Leroux, H.J. Tiziani, W. Osten</i> | |
| An Adaptive Phase Mask for Wavefront Coding | 56 |
| <i>C. Pruss, C. Leroux, H.J. Tiziani, W. Osten</i> | |
| Refractive and Hybrid Microoptic Design: Minimally invasive systems for combustion analysis... | 57 |
| <i>R. Reichle, C. Pruss, H.J. Tiziani, W. Osten, F. Zimmermann (PCI), C. Schulz (PCI)</i> | |
| Fabrication of high resolution diffractive elements by direct laser writing | 58 |
| <i>C. Pruss, V. Korolkov, T. Schoder, J. Westhauser, H.J. Tiziani, W. Osten</i> | |
| Interferometry at different optical wavelengths | 59 |
| <i>C. Pruss, S. Reichelt, H.J. Tiziani</i> | |

Coherent Measurement Techniques

| | |
|---|----|
| Digital holographic interferometry for the investigation of the elastic properties of bone..... | 62 |
| <i>G. Pedrini, I. Alexeenko, P. Zaslansky, W. Osten</i> | |
| Applications of short-coherence digital holography in microscopy..... | 64 |
| <i>G. Pedrini, L. Martínez-León, W. Osten</i> | |
| Pulsed digital holographic interferometry for endoscopic investigations (HoEnd)..... | 66 |
| <i>G. Pedrini, I. Alexeenko, W. Osten</i> | |
| Online surveillance of dynamical processes by using a moving system based on pulsed digital holographic interferometry..... | 68 |
| <i>G. Pedrini, I. Alexeenko, U. Schnars, W. Osten</i> | |
| Wave front reconstruction from a sequence of holograms recorded at different planes..... | 70 |
| <i>G. Pedrini, Y. Zhang, W. Osten</i> | |
| Compensation of unwanted deviations in Comparative Digital Holography (KOMA)..... | 72 |
| <i>X. Schnab, G. Pedrini, W. Osten</i> | |

Publications 2002 - 2004

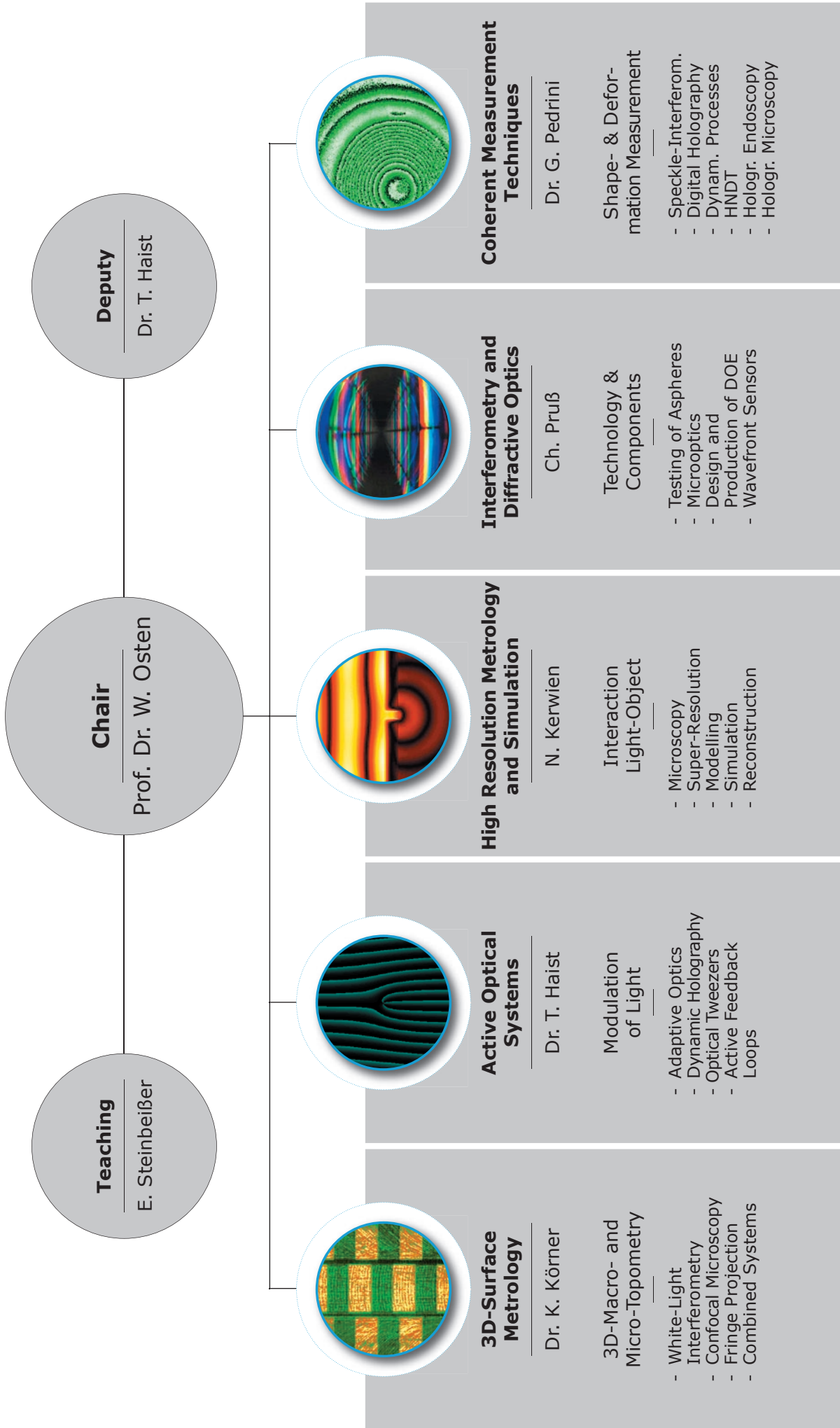
| | |
|---|----|
| Invited lectures on international conferences..... | 74 |
| Editorial Work..... | 75 |
| Reviewed papers..... | 76 |
| Conference proceedings and journals..... | 78 |
| Patents..... | 83 |
| Doctorial Thesis, Diploma Thesis & Student Research Projects..... | 84 |

Colloquia & Conferences

| | |
|---|----|
| Fest-Kolloquium Optik 2003..... | 86 |
| Optik-Kolloquium 2004..... | 87 |
| Organized International Conferences: 2002 – 2004..... | 88 |

Institute structure





Staff of the Institute

Please note the telephonumbers will be changing early in 2006. For the new number add "6" after "685"
(e.g. "+49 (0) 711 685 6074" becomes "+49 (0) 711 685 6 6074")

Director

Prof. Dr. Wolfgang Osten _____ +49 (0) 711 685-6075 _____ osten@ito.uni-stuttgart.de

Emeritus

Prof. Dr. Hans Tiziani _____ +49 (0) 711 685-6077 _____ tiziani@ito.uni-stuttgart.de

Secretary

Gabriele Großhans _____ +49 (0) 711 685-6074 _____ grosshans@ito.uni-stuttgart.de

Ruth Edelmann _____ +49 (0) 711 685-6074 _____ edelmann@ito.uni-stuttgart.de

Christa Wolf _____ +49 (0) 711 685-6083 _____ wolf@ito.uni-stuttgart.de

Studys

Erich Steinbeißer _____ +49 (0) 711 685-6068 _____ steinbeisser@ito.uni-stuttgart.de

Research Assistants

3D-Surface Metrology

Dr. Klaus Körner (leader) _____ +49 (0) 711 685-6082 _____ koerner@ito.uni-stuttgart.de

Reinhard Berger _____ +49 (0) 711 685-6835 _____ berger@ito.uni-stuttgart.de

Ulrich Droste _____ +49 (0) 711 685-6835 _____ droste@ito.uni-stuttgart.de

Christian Kohler _____ +49 (0) 711 685-6835 _____ kohler@ito.uni-stuttgart.de

Dr. Evangelos Papastathopoulos _____ +49 (0) 711 685-6082 _____ itoepapa@ito.uni-stuttgart.de

Aiko Ruprecht _____ +49 (0) 711 685-6594 _____ ruprecht@ito.uni-stuttgart.de

Tobias Wiesendanger _____ +49 (0) 711 685-6594 _____ wiesendanger@ito.uni-stuttgart.de

Active Optical Systems

Dr. Tobias Haist (leader) _____ +49 (0) 711 685-6069 _____ haist@ito.uni-stuttgart.de

Dr. Witold Gorski _____ +49 (0) 711 685-6069 _____ gorski@ito.uni-stuttgart.de

Jan Liesener _____ +49 (0) 711 685-6071 _____ liesener@ito.uni-stuttgart.de

Lars Seifert _____ +49 (0) 711 685-6071 _____ seifert@ito.uni-stuttgart.de

Marcus Reicherter _____ +49 (0) 711 685-6069 _____ reicherter@ito.uni-stuttgart.de

Susanne Zwick _____ +49 (0) 711 685-6069 _____ zwick@ito.uni-stuttgart.de

High Resolution Metrology and Simulation

Norbert Kerwien (leader) _____ +49 (0) 711 685-6065 _____ kerwien@ito.uni-stuttgart.de

Jochen Kauffmann _____ +49 (0) 711 685-6553 _____ kauffmann@ito.uni-stuttgart.de

Stephan Rafler _____ +49 (0) 711 685-6553 _____ rafler@ito.uni-stuttgart.de

Thomas Schuster _____ +49 (0) 711 685-6065 _____ schuster@ito.uni-stuttgart.de

Interferometry and Diffractive Optics

Christof Pruß (leader) _____ +49 (0) 711 685-6066 _____ pruss@ito.uni-stuttgart.de

Markus Freudenreich _____ +49 (0) 711 685-6066 _____ freudenreich@ito.uni-stuttgart.de

René Reichle _____ +49 (0) 711 685-6066 _____ reichle@ito.uni-stuttgart.de

Thomas Schoder _____ +49 (0) 711 685-6064 _____ schoder@ito.uni-stuttgart.de

Johann Westhauser _____ +49 (0) 711 685-6064 _____ westhauser@ito.uni-stuttgart.de

Coherent Measurement Techniques

Dr. Giancarlo Pedrini (leader) _____ +49 (0) 711 685-6078 _____ pedrini@ito.uni-stuttgart.de

Dr. Roger Groves _____ +49 (0) 711 685-6073 _____ groves@ito.uni-stuttgart.de

Xavier Schwab _____ +49 (0) 711 685-6076 _____ schwab@ito.uni-stuttgart.de

Dr. Fucai Zhang _____ +49 (0) 711 685-6076 _____ fucai@ito.uni-stuttgart.de

Software Engineering & Technicians

Andreas Goretzky _____ +49 (0) 711 685-6070 _____ goretzky@ito.uni-stuttgart.de

Ralph Knoll _____ +49 (0) 711 685-6067 _____ knoll@ito.uni-stuttgart.de

Andreas Lorenz _____ +49 (0) 711 685-6089 _____ lorenz@ito.uni-stuttgart.de

 Past members of the staff (2003 – 2004)

| | | |
|------------------------------|-------------------------------|---------------------------|
| Igor Alexeenko | Dr. Matthias Fleischer | Dr. Stefan Franz |
| Ralf Gärtner | Dr. Jens Korallus | Michael Krämer |
| Stefanie Krug | Jean-Marc Nivet | Dr. Michael Pahlke |
| Dr. Klaus-Peter Proll | Dr. Stephan Reichelt | Eva Rosenthal |
| Dr. Alexandre Tavrov | | |

 Guest Scientists

| | | |
|--------------------------------|---|------------------------------------|
| Prof. Mikhail Gusev | Kaliningrad State University, Russia | 9/2002 – 11/2002 |
| Dr. Yan Zhang | Capital Normal University, Beijing, PR China | 11/2002 – 10/2003 |
| Dr. Lluís Martínez León | Universitat Jaume I, Castelló, Spain | 7/2003 – 1/2004 |
| Dr. Andrés Márquez Ruiz | Universidad de Alicante, Spain | 6/2004 – 7/2004 |
| Dr. Victor Korolkov | IA&E Sibirian Branch of the Russian Academy of Sciences, Novosibirsk, Russia | 8/2002 – 3/2003 3/2004 – 9/2004 |

 Foreign Guests visiting the Institute: 2002 - 2004

| | | |
|-------------------------------------|---|----------------|
| Dr. Joanna Schmit | Veeco Process Metrology, Tucson, USA | September 2002 |
| Prof. Dr. Bahram Javidi | University of Connecticut, USA | November 2002 |
| Prof. Dr. Michail Gusev | Kaliningrad State Univ., Russia | November 2002 |
| Dr. V. Tornari | F.O.R.T.H., Heraklion, Greece | December 2002 |
| Prof. Dr. T. Lasser | Swiss Federal Institute of Technology, Lausanne, Suisse | December 2002 |
| Prof. Steve Weiner | Weizmann Institute of Science, Rehovot, Israel | June 2003 |
| Prof. Armando Albertazzi | Univ. Florianopolis, Florianopolis, Brasil | June 2003 |
| Prof. Kazuyoshi Itoh | Osaka University, Osaka, Japan | June 2003 |
| Dr. Christophe Gorecki | Universite de Franche-Comté, Becancon, France | July 2003 |
| Dr. Jim Trollinger | Metrolaser Inc., Irvine, USA | August 2003 |
| Prof. Dr. Qifeng Yu | National University of Defense Technology, Changsha, P.R. China | January 2004 |
| Dr. Fernando Mendoza-Santoyo | Centro de Investigaciones en Optica, Leon, Mexico | September 2004 |
| Dr. Roger Groves | Cranfield University, Bedfordshire, England | September 2004 |
| Prof. Dr. Yuriy Shugui | Russian Academy of Sciences, Novosibirsk, Russia | October 2004 |
| Prof. Zoltan Füzessy | Budapest University of Technology and Economics, Budapest, Hungary | November 2004 |
| Dr. Ference Gyimesi | Budapest University of Technology and Economics, Budapest, Hungary | November 2004 |

Studying optics

Our curriculum is primarily directed towards the students in upper-level courses (“Hauptdiplom”) of Mechanical Engineering, Mechatronics, and Technology Management. We especially recommend the course option “Microsystems and precision engineering”.

We also welcome students from other courses, such as “Physics” and “Engineering Cybernetics”.

Concerning the main subject “Engineering Optics” we offer the following

Core lectures:

- **fundamentals of engineering optics** (Prof. Dr. W. Osten)

basic laws and components: optical imaging with lenses, mirrors, and prisms; basic optical set-ups; optical systems and devices (the human eye, magnifying glasses, microscopes, and telescopes); physical optics, physical limits of optical images, resolution of optical devices; geometrical and chromatic aberrations and their influence on picture quality and basic laws of photometry.

- **optical measurement techniques and procedures** (Prof. Dr. W. Osten)

basics of geometrical optics and physical optics; holography; speckle; components and systems: light sources, lenses, mirrors, prisms, apertures, light modulators, the human eye and other detectors; measuring errors; measuring techniques based on geometrical optics: measuring microscopes and telescopes, structured illumination, application of Moiré-phenomenon; measuring techniques based on physical optics: interferometrical measurement techniques, holographic interferometry, speckle measurement techniques.

- **optical information processing** (Prof. Dr. W. Osten)

Fourier theory of optical imaging; basics of wave theory, coherence, frequency analysis of optical systems, holography and speckle, spectrum-analysis and optical filtering; digital image processing: basics of methods and applications.

Elective lectures

- optical phenomena in nature and everyday life (Dr. T. Haist)

- opto-electronical image-sensor and digital photography (Dr. K. Lenhardt)

- coherence and polarisation in optics / optics of thin films, surfaces and crystals (Dr. K. Leonhardt)

- optical lithography / measuring techniques for micro-structures (Dr. M. Totzeck)

- design and calculation of optical systems (Dr. H. Zügge)

Additional studies

- project work and theses within our field of research

- practical course “optics-laboratory”
 - speckle measurement
 - digital image processing
 - computer aided design of optical systems
 - measurement of the spectral power distribution

- practical course “optical measurement techniques”
 - 3D surface measurements applying fringe projection
 - digital holography
 - 2D-interferometry and measurement
 - quality inspection of photo-objectives with the MTF measuring system

- common lab for mechanical engineering (APMB)

The research groups



3D-Surface Metrology

The objective of the group is the analysis and the implementation of new principles for the acquisition of optical 3D-surface data of engineering and biological objects over a wide scale. Our main focus is on the enhancement of the metering capacity by a combination of physical models and optimized system design.

Current research activities are:

- 3D-measurement applying fringe projection and deflectometry (macroscopic and microscopic)
- adaptive techniques using spatial light modulators
- confocal microscopy
- white light interferometry
- combined sensors and data interpretation strategies

Contact: ofm@ito.uni-stuttgart.de



Active Optical Systems

The objective of our work is the development of flexible optical systems in order to enable new applications, especially within the field of scientific and industrial metrology. To achieve this goal, we make use of different modern light modulation technologies and computer-based methods. One focus of our work lies in the application of holographic methods based on liquid crystal displays and micromechanical systems for various applications ranging from optical tweezers to aberration control and testing of aspherical surfaces.

Main research areas:

- active wavefront modulation
- adaptive optics
- active wavefront sensors
- dynamic holography
- components, algorithms, and strategies

Contact: aos@ito.uni-stuttgart.de



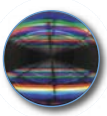
High Resolution Metrology and Simulation

The Goal of this research group is the investigation of the interaction of light with 3d object structures in the micro and nano domain. Along with experimental research, one major aspect is the rigorous modelling and simulation as an integral part of the active metrology process. The analysis of all information channels of the electromagnetic field (intensity, phase, polarisation state of light) allows us to obtain sub-wavelength information about the structure.

ITO has developed a modularised program package called MicroSim for:

- the rigorous computing of the light-object interaction using RCWA
- the visualisation of the near and farfield in 2D and 3D
- the simulation of the microscopic imaging process

Contact: hms@ito.uni-stuttgart.de



Interferometry and Diffractive Optics

The goal of our research activity is to explore new measurement concepts using diffractive optics. One important application is the testing of optical surfaces, in particular, aspheric lenses. For this purpose we design and produce computer generated holograms (CGH). At the same time, we develop flexible measurement techniques that enhance or even replace static null correctors. In addition to CGH for interferometry, our in house production facilities allow to produce diffractive elements and micro-optics for a wide variety of applications such as UV-measurement systems, beam shaping applications and wavefront sensing.

Our research areas include:

- diffractive optics
- dynamic wavefront coding
- interferometry
- testing of aspheric surfaces

Contact: ide@ito.uni-stuttgart.de



Coherent Measurement Techniques

Our research objective is the analysis and application of methods based on coherent optics for the measurement of 3D-shape and deformation and to determine the material properties of technical objects and biological tissues. Aside from the quantitative measurements of form and deformation, methods for non-destructive material testing are also analysed and applied.

Research areas include:

- digital holography
- pulsed holographic interferometry
- dynamic strain measurements on biological samples
- shape measurement
- wavefront reconstruction
- holographic non-destructive testing
- endoscopy

Contact: kom@ito.uni-stuttgart.de

3D-Surface Metrology

Hybrid microoptic sensors using the chromatic-confocal focus detection principle (HymoSens)

Supported by: BMBF (FZK: 02P D2551)

Micro optical components: Fast parallel characterization of micro optic arrays

Supported by: German Ministry of Education and

Research (BMBF); FKZ: 13N7479 / 1

Integration of optical measurement techniques for laser welding process control (INESS)

Supported by: BMBF; INESS (Integration of optical measurement techniques for laser welding process control), FKZ: 02PD2523

Full Field, Fast Confocal Laser Microscopy for Measuring the Mechanical Properties of Cortical Bone

Supported by: Alfred Krupp von Bohlen und Halbach-Stiftung

Aberration correction in a confocal microscope (METAMO)

Supported by: Landesstiftung Baden-Württemberg, Project: "Metamo"

Microscopic three-dimensional topometry with LCOS displays

Supported by: Deutsche Forschungsgemeinschaft (DFG) under contract Ti 119/37-1 "Adaptive Sensorik zur Bestimmung der Mikrogeometrie"

Evaluation and Characterization of Liquid Crystal SLMs for Digital Comparative Holography (DISCO)

Supported by: The German Ministry for Education and Research (BMBF) under the contract 13N8095 as subcontract of BLAS, Bremen

Collaboration with industry: A new white light interferometer

In collaboration with: Mabir GmbH

Depth-Scanning Fringe Projection (3D-MicroScan)

Supported by: BMBF 3D-MicroScan 16SV942

Direct Calibration Scheme for the Depth-Scanning Fringe Projection (3D-MicroScan)

Supported by: BMBF 3D-MicroScan 16SV942

Hybrid microoptic sensors using the chromatic-confocal focus detection principle (HymoSens)

A. Ruprecht, C. Pruss, H. J. Tiziani, W. Osten

Miniaturized point sensor

Increasing demands for checking tolerances in small mechanical and optical precision components require improved measurement techniques. In particular, components with a complex geometry, such as small holes or channels, are difficult to access using state of the art tactile measurement systems. Optical measurement systems have the advantage that no mechanical forces occur during the measurement, which could distort or displace a miniaturized sensor head and therefore influence the result.

The main focus of this project is to develop a miniaturized optical sensor for this application. The sensor makes use of the chromatic-confocal measurement principle, which has no need for a mechanical depth scan. Therefore, a chromatic-confocal point sensor can be designed without any moving parts. This knowledge was used to design a miniaturized sensor head with an outer diameter smaller than two millimeters (see Fig. 1 and Fig. 2). A special feature of the sensor head is its capability to measure with a 90 degree redirection. This enables us to measure surfaces within small holes with high accuracy.

A diffractive element is applied to achieve the necessary chromatic dispartment of the light. The diffractive microoptic is produced by the ITO using photolithographic processes and reactive ion etching of the structure of thin substrates of fused silica.

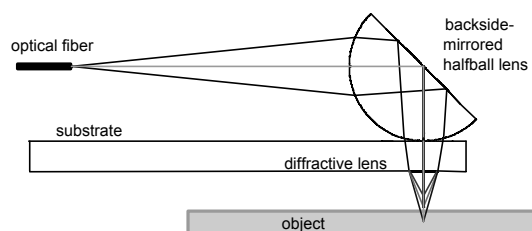


Fig. 1: Principle of the optical setup of the miniaturized point sensor: Optical fiber, microlens, redirection-mirror, diffractive lens

The alignment structures and mounts between the different optical elements are produced by the Institut für Mikrostrukturtechnik (Forschungszentrum Karlsruhe) from PMMA using deep X-ray lithography, this is the first step of the LIGA process (Direct LIGA). The LIGA technique (German acronym for lithography, electroplating and molding) utilizes x-ray synchrotron radiation and provides a high performance for manufacturing micro compo-

nents and systems with close tolerances and high aspect ratios (large structural height ($> 1000 \mu\text{m}$)).

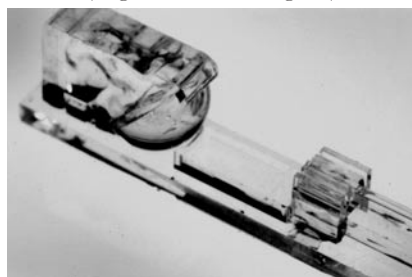


Fig. 2: Photo of the miniaturized point sensor (Forschungszentrum Karlsruhe)

Chromatic confocal area sensor

Confocal microscopy is a widespread method to measure volume structures or surface topographies. It has a growing impact on the measurement of technical micro-structures. In comparison to confocal laser scanners, a chromatic-confocal setup achieves a complete parallelization of the depth scan by using white-light and chromatic effects of the focusing lenses.

The maximum parallelization is achieved by measuring a complete area instead of a point or a line. We realized such a setup by using a colour camera as an area-spectrometer. This sensor is capable of one-shot measurements and fast high precision measurements in a large measurement volume. Therefore, one can choose between high speed measurements and fast measurements with increased axial resolution without any change in the setup. In the high resolution mode, it is also possible to get information about the colour distribution on the object surface.

Supported by: BMBF (FZK: 02P D2551)

References:

- [1] A. K. Ruprecht, T. F. Wiesendanger, H. J. Tiziani "Chromatic confocal microscopy with finite pinhole size" *Opt. Lett.* 29 (18), 2130-2132, 2004
- [2] P. Lücke, A. Last, J. Mohr, A. Ruprecht, W. Osten, H. J. Tiziani; P. Lehmann, "Confocal microoptical distance-sensor for precision metrology", *Optical Sensing, Proceedings of SPIE Vol. #5459-22*, Strasbourg, 27-30 April 2004
- [3] A. K. Ruprecht, K.-P. Proll, J. Kauffmann, H. J. Tiziani, W. Osten, "Multi Wavelength Systems in Optical 3-D Metrology", 6th Int. Conference for Optical Technologies, Optical Sensors and Measuring Techniques (OPTO 2004), Nürnberg, 25.-27. Mai 2004, page 101-106

Micro optical components: Fast parallel characterization of micro optic arrays

T. Wiesendanger, Y. Yasuno, S. Reuter, A. Ruprecht, H.J. Tiziani

The importance of micro-optical arrays, e.g. for the collimation of diode-lasers for Optical Networks or for Hartmann-Shack sensors, is increasing. The most important fabrication errors are void elements, these are deviations of the focal length and aberrations. A good knowledge of the optical properties of the micro lenses is essential for the quality control of the micro lens fabrication.

For this industrial application, a very robust system which evaluates arrays of some thousands lenses in a few seconds is needed. All existing measurement systems (Mechanical stylus profilometry, Twyman-Green interferometry, Shack-Hartmann-sensors, atomic force microscopy) have in common that the micro lenses are tested serially. Therefore a 100%-quality control is not feasible. Interferometric techniques moreover demand a high mechanical stability of the setup. Our approach is based on the confocal principle: The array to test plays the role of the front objective in a confocal microscope (Fig. 1).

We illuminate the total microlens array (MLA) with collimated light ($\lambda=633$ nm) from a single mode fiber (F) working as a point light source. A flat mirror (M) is placed in the focal plane of the microlens-array. We image the pupils of the microlenses with the tubelens (L_T), through the confocal pinhole (P), onto the camera (CCD). During the measurement the mirror is shifted along the optical axis through the focal plane of the array.

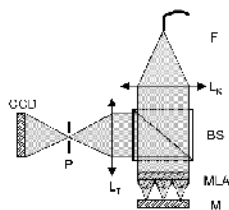


Fig. 1: Optical Setup

A CCD image is stored for each position of the mirror. It is well known that the axial response of a confocal setup also possesses inherent information about the aberrations: The maximum value of the intensity is shifted axially, the FWHM-value increases and characteristic side lobes occur if the lenses are not perfect (Fig. 2). We use this fact to determine the aberration of microlens arrays. Void elements or deviations of the focal length are also detected. In contrast to other measuring techniques, the two-dimensional information of the wavefront is not available in our case, we have the one-dimensional axial response instead. We obtain a fast, alignment insensitive and parallel measuring system.

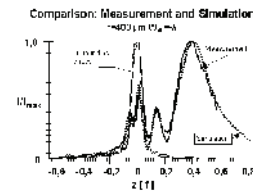


Fig. 2: Axial confocal signals

For evaluation of the system we produced a diffractive microlens-array with well defined deviations. The deviations are void elements, lenses with spherical aberration and lenses with defocus. Fig. 2 shows the axial responses for an aberrated microlens (focal length $f=400$ μm , numerical aperture $\text{NA}=0.15$, spherical aberration $W40=-\lambda$). For comparison the axial responses of the surrounding microlenses featuring no defined aberrations and a simulation of the axial response of an aberrated microlens are displayed. For evaluation of the axial response a Neural Network was used [3]. The Neural Network can determine spherical aberration coefficients in the range from -0.7λ , to 0.3λ , with less than 1 % RMS error. This system demands only a few tens of seconds of operation time, including for measurement and computation, to determine the aberrations of a 100×100 microlens array.

Supported by: German Ministry of Education and Research (BMBF); FKZ: 13N7479 /1

References:

- [1] Yasuno Y, Wiesendanger, T.F., Yatagai, T., Ruprecht, A.K. and Tiziani, H.J., "Aberration measurement from confocal axial intensity response using neural network", *Opt. Exp.* 10, 1451-1457 (2002)
- [2] T. Wiesendanger, Y. Yasuno, A. Ruprecht, T. Yatagai and H. Tiziani, "Characterization of Microoptic Arrays by Evaluation of the Axial Confocal Response", *Opt. Rev.* 10, 301-302 (2003)
- [3] Y. Yasuno, T. Wiesendanger, A. Ruprecht, T. Yatagai and H.J. Tiziani, "Determination of Aberration Coefficient of Microoptic Arrays from Axial Confocal Response by Neural Method", *Opt. Rev.* 10, 318-320 (2003)

Integration of optical measurement techniques for laser welding process control (INESS)

T. Wiesendanger, A. Ruprecht, K. Körner, H.J. Tiziani, W. Osten

A Keyhole-Sensor for in-process-control of laser welding

Laser beam welding has gained an increasing acceptance in industry, due to its high penetration depth over weld width ratio, small heat effects and high welding speed (about 15m/min). In laser welding process control one of the most important parameters is the depth of the weld. There are already techniques which determine the welding depth, but these systems are based on secondary process radiation where the welding depth is measured indirectly. Therefore, a system for the direct measurement of the welding depth is needed. The highly dynamic processes in the welding zone, especially inside the keyhole, require a very fast measurement system of at least 1 kHz measuring frequency. The desired measurement range is 1 mm.

To our knowledge, there is no system that performs a direct measurement of the welding depth in a cw welding process. Confocal microscopy is a very robust method widely used in biology and with increasing importance for topographical measurements of technical surfaces. It is robust with respect to vibrations. To obtain the confocal axial response curve, we have to scan the sample axially. The desired measurement speed and the axial scanning range make it impossible to move the sample or the objective axially. Therefore, a fast scanning of the focus is required. We use a small pentaprism mounted on a vibrating tuning fork, to modulate the optical path length in the setup (cf. Fig. 1).

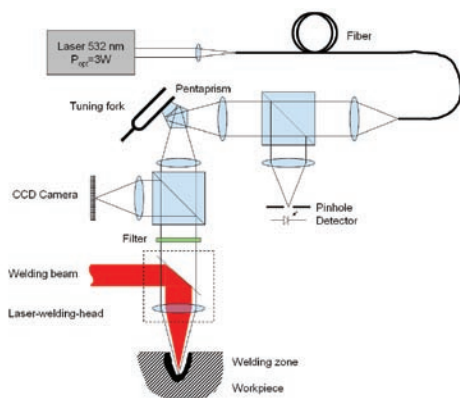


Fig. 1: Optical Setup of the Keyhole-Sensor

Thus, we achieve an axial scan of the focus spot. As the moving mass is comparatively small, we can run the system at high measurement frequencies and over large measurement ranges. As a light source, we

use a high power disk laser (wavelength: 532 nm, optical power: 3 W), which is coupled into a multimode fiber (diameter: 50 μm). After collimation to a beam diameter of 15 mm and passing through a beam splitter, the light is focused into a pentaprism (cf. Fig. 2), which is mounted on the vibrating tuning fork.

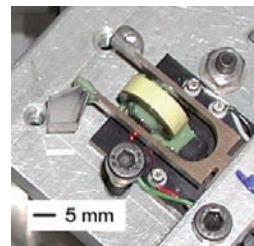


Fig. 2: Pentaprism mounted on a tuning fork

The tuning fork oscillates at its natural frequency of 768 Hz. By the oscillation of the prism, the optical path length is modulated. We successfully tested mechanical amplitudes of the prism up to $\pm 110 \mu\text{m}$. After passing the pentaprism, the light is collimated by a lens again and enters the commercial laser welding head. The laser welding head contains a beam splitter and a front lens. As the welding laser is also delivers collimated light to the welding head, the welding laser focus is within the measurement range. Due to the change in the optical path length caused by the oscillating prism, the axial position of the sensor focus is modulated correspondingly.



Fig. 3: Integration into the Laser welding cell

The effective measurement range is 1.5 mm at a measurement frequency of 1.536 kHz. Each time the focus is exactly on the surface of the object, the reflected light passes through the pinhole and is detected by a Photodiode. Otherwise, if the focus is either below or above the surface of the object, most of the reflected light is blocked by the pinhole and it can thus not reach the photodiode.

A Chromatic-confocal line sensor for weld seam testing

The topography of the weld seam can give additional information about the quality of the welding process. To accomplish a high throughput, short measurement times are demanded. The chromatic-confocal approach enables the parallelization of the complete depth-scan of confocal topography measurements. Therefore, mechanical movement can be reduced, or completely avoided, and the measurement times are shortened. Chromatic-confocal point sensors are already commercially available but they need lateral scanning in the x- and y-directions to measure the surface topography. We achieved a further parallelization in the x-direction by realizing a chromatic-confocal line sensor using a line focus and a spectrometer. This configuration has the advantage that cylindrical work pieces can be measured by rotating the work piece. The rotation is already performed during the welding process.

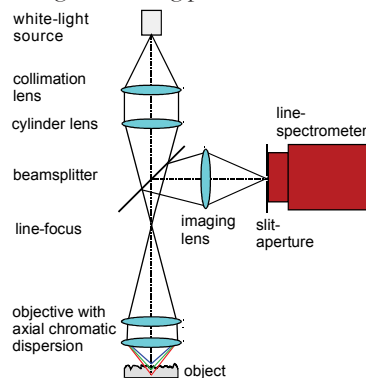


Fig. 4: Optical setup of the line sensor

The setup is shown in Fig. 4. Polychromatic light from a Xenon arc lamp is coupled into a multimode fiber. The light from this fiber is collimated and then focused by a cylinder lens to form a line focus, which is imaged onto the object. The reflected light is imaged via the beam splitter onto a slit aperture. This slit aperture is the confocal aperture, which blocks the defocused light and stray light. At the same time it is the entrance slit of a spectrometer. In contrast to the point sensor, the light along the line is not integrated but the lateral information about the object is used. Therefore, we used a line spectrometer, which is able to maintain the lateral resolution. We used a spectral range from 450 nm to 700 nm, and a spectrometer with a relatively low spectral resolution to limit the amount of measurement data. The topography along the focal line can be measured with a single spectroscopic image.

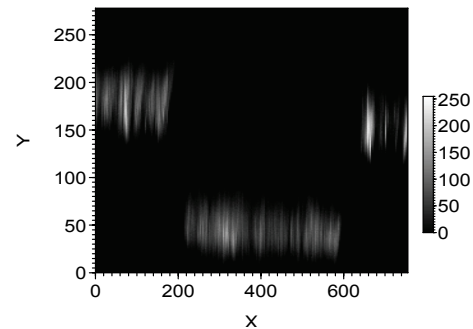


Fig. 5: Depth discriminated spectral image of a trench

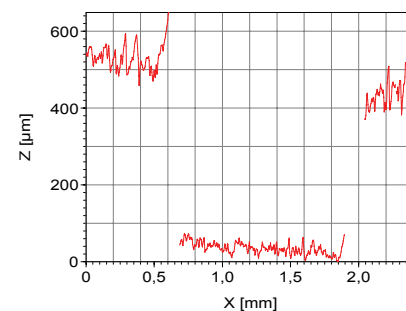


Fig. 6: Corresponding line profile of the trench (cf. Fig. 5)

Fig. 5 shows a trench of app. 400 μm depth in a rough metal surface. The y-axis is the spectroscopic axis and the x-axis denotes the lateral distribution along the line focus. The corresponding topography, calculated from the spectroscopic image, is plotted in Fig. 6.

Supported by: BMBF: INESS (Integration of optical measurement techniques for laser welding process control), FKZ: 02PD2523

References:

- [1] Wiesendanger, T., Körner, K., Ruprecht, A., Windecker, R., Tiziani, H.J., Osten, W., "Fast confocal point-sensor for in-process control of laser welding", ICLAOM'03, International Conference on Laser Applications and Optical Metrology, New Delhi, 2003
- [2] Ruprecht, A., Körner, K., Wiesendanger, T., Tiziani, H.J., Osten, W., "Chromatic confocal detection for high speed micro-topography measurements", Electronic Imaging, Proceedings of SPIE Vol. #5302-6, San Jose (CA), p. 53-60, 2004
- [3] Ruprecht, A., Wiesendanger, T., Tiziani, H.J., "Chromatic confocal microscopy with finite pinhole size" Opt. Lett. 29 (18), 2130-2132, 2004
- [4] Wiesendanger, T., Körner, K., Ruprecht, A., Tiziani, H.J., Osten, W., "Fast confocal point-sensor for in-process control of laser welding", ISMQ2004, 8th International Symposium on Measurement and Quality Control in Production, Erlangen, Germany, 2004

Full Field, Fast Confocal Laser Microscopy for Measuring the Mechanical Properties of Cortical Bone

T. Wiesendanger, A. Ruprecht, G. Pedrini, K. Körner, H.J. Tiziani, W. Osten, P. Zaslansky, S. Weiner

Facing the fact of growing life expectancies of humans, bone diseases are an ever growing menace. To overcome this problem, accurate knowledge about the internal structure of the bone tissue is essential.

Confocal microscopy is a well established technique in biology, medicine and materials science due to its depth discriminating property. At the 'Institut für Technische Optik' this method is used to determine three-dimensional high-resolved surface topographies of technical objects. In order to study the internal materials properties of bone, the confocal evaluation technique was adapted in order to visualize structures underneath the bone surface.

Bone tissue is translucent and light can penetrate several tens of micrometers inside the sample. This property allows us to detect sub-surface microfractures and other structures. The confocal measurements on bone tissue were performed using a confocal microscope with a rotating microlens disk. This system was developed at our institute. The principle of the system is shown in Figure 1.

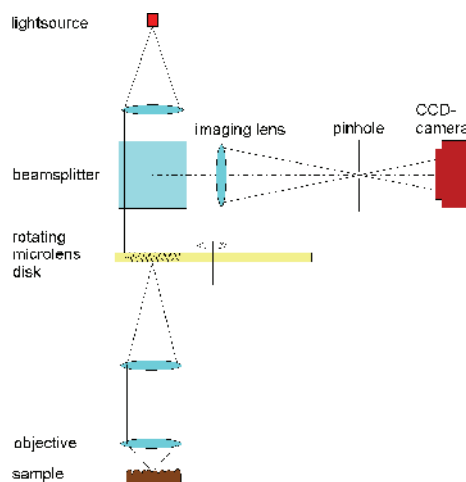


Fig. 1: Principle of the confocal microscope with rotating microlens disk

Unlike other confocal microscopes with a rotating Nipkov disk with a low light efficiency of about 1%, this setup uses 60% of the light. Consequently, the system can operate with a LED at low costs and without problems of speckling.

The measurement and evaluation routines had to be adapted to the new task for acquisition of volume data. A deconvolution routine was added. Images can be successfully obtained from depths down to 80 microns with an axial resolution in the submicron range. The system can be used to perform measurements of stressed bone samples, as the microscope can acquire images of a whole plane in a single measurement, and automatically scan through the desired volume.

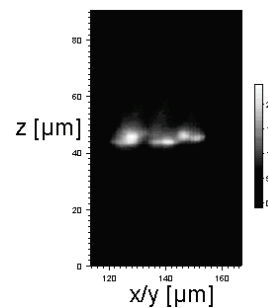


Fig. 2: Intensity on a single line in depth

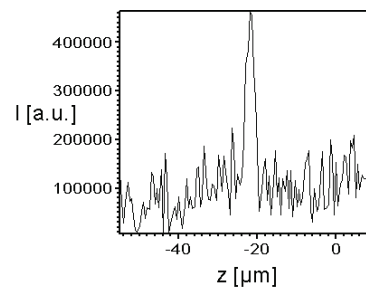


Fig. 3: Confocal axial response signal in bone tissue

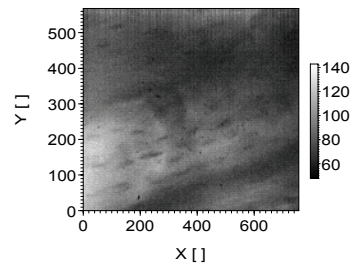


Fig. 4: Osteocyte lacunae, 55 μm under the bone surface

Supported by: Alfried Krupp von Bohlen und Halbach-Stiftung

Aberration correction in a confocal microscope (METAMO)

Y. Yasuno, T.F. Wiesendanger, A.K. Ruprecht, C. Pruss, H.J. Tiziani

Confocal microscopy is a measurement technique widely used in biological and technical applications. In case of the deployment of a monochromatic light source a time consuming axial scan is inevitable. Moreover when performing measurements underneath a refractive index mismatching layer we have to cope with aberrations, especially spherical aberration which degrades the signal quality and thus also the measurement accuracy. To overcome these problems we integrate an adaptive mirror into a confocal microscope. The adaptive mirror is used to perform the fast axial scan as well as the aberration correction. To optimize the shape of the adaptive mirror we introduce an optimization criterion which we call Wavefront-Information-Entropy-Method (WIEM). In contrast to most other criteria in this context, WIEM represents a single numerical value which is ideal for the optimization algorithm. As an optimization algorithm we use a genetic algorithm. Fig. 1 shows the optical setup. The adaptive mirror is shown in Fig. 2. Measurement results using the adaptive mirror for the axial scan are displayed in Fig. 3. Fig. 4 depicts the confocal signal before and after optimization.

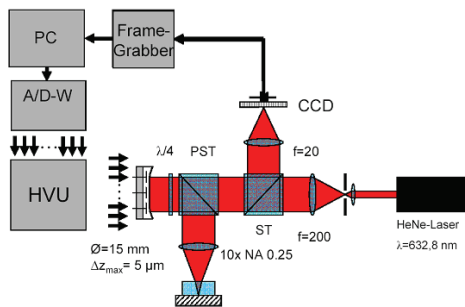


Fig. 1: Optical setup

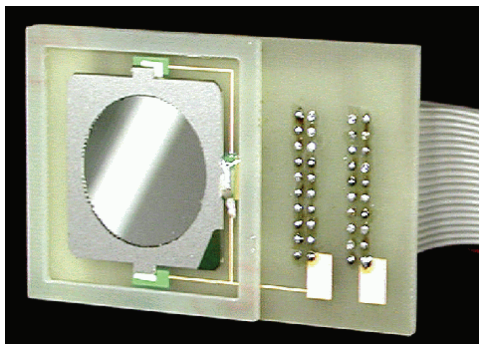


Fig. 2: Adaptive Mirror

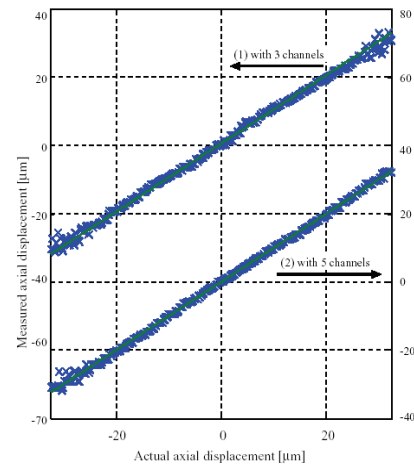


Fig. 3: Axial scan using the adaptive mirror

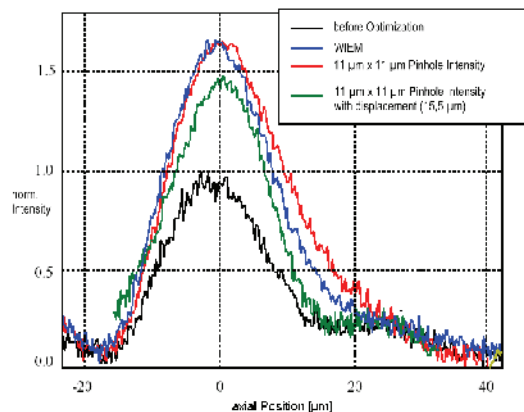


Fig. 4: Aberration Correction

Supported by: Landesstiftung Baden-Württemberg,
Project: "Metamo"

References:

- [1] Y. Yasuno, T. F. Wiesendanger, S. Makita, A. K. Ruprecht, T. Yatagai and H. J. Tiziani, "Non-mechanically-axial-scanning confocal microscope using adaptive mirror switching", *Optics Express* 11, 54-60, (2003)
- [2] Y. Yasuno, T.F. Wiesendanger, A.K. Ruprecht, S. Makita, T. Yatagai and H.J. Tiziani, "Wavefront-flatness evaluation by wavefront-correlation-information-entropy method and its application for adaptive confocal microscope", *Optics Communications* 232, 91-97, (2004)

Microscopic three-dimensional topometry with LCOS displays

C. Kohler, K.-P. Proll, J.-M. Nivet, K. Körner, H. J. Tiziani, W. Osten

The optical measurement of three-dimensional microtopography is an important field for the control of industrial processes. Different measurement principles have been developed for various requirements, such as measurement field size, lateral and depth resolution, and measurement time. Common methods are confocal microscopy [1], white-light interferometry [2], [3], and microscopic fringe projection based on the principle of triangulation [4]-[8]. While confocal microscopy and white-light interferometry offer resolutions down to the nanometer-range, the microscopic fringe projection offers a fast and robust method for measurement field sizes from ca. 1 mm² up to several square centimeters with a depth resolution in the micrometer-range. For the generation of the fringes, mechanical Ronchi gratings [4]-[7], the digital micromirror device (DMD, developed by Texas Instruments) or transmissive twisted nematic liquid crystal displays (LCD) [9] have been used. Pixelated devices like the DMD or LCDs offer more flexibility compared to mechanical gratings. With these elements, the fringe period can be adapted to the object under test. They also permit the adaptation of the fringe brightness to a locally varying brightness of the measurement scene [8].

The measurement setup

In order to apply the LCOS display as a fringe projection device, we used an experimental setup that has proven to be very suitable for microscopic fringe projection [4]-[8]. The measurement principle is illustrated in Fig. 1. The setup is based on a Leica MZ 12.5 stereo microscope with a zoom range from 0.8 to 10.0 and interchangeable objectives with magnifications of 0.63 x, 1.0 x, and 1.6 x, respectively. This gives us the possibility of varying the measurement field size from 21.2 x 15.7 mm² down to 0.83 x 0.62 mm².

As a detector, we used a digital CMOS camera Photonfocus model MV-D1024k with 1024 x 1024 pixels, a pixel pitch of 10.6 μm, and a gray scale resolution of 8 bits. The pixel clock of the camera was 80 MHz. Both exposure time and frame time could be changed by software in steps of 50 ns. This enabled us to adjust the exposure time to exact multiples of the projection time of the LCOS display (16.67 ms for 60 Hz) resulting in virtually flicker free images. For the acquisition of images, the CMOS sensor could be programmed to read

out only the desired regions of interest (ROI). Hence, the measurement of parts of the measurement field was possible.

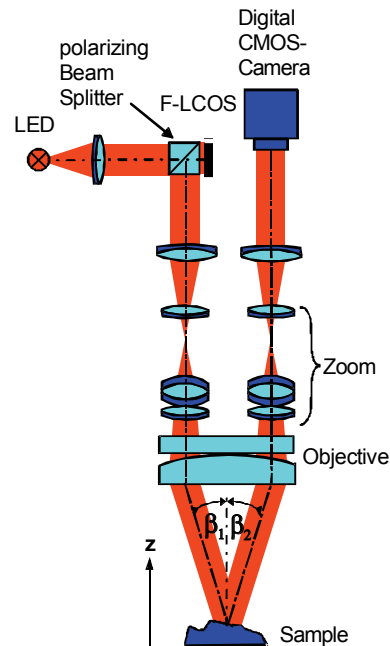


Fig. 1: Scheme of the stereomicroscope used for the measurements

Measurements

In order to demonstrate the performance of the LCOS measurement system, we conducted measurements on several technical surfaces. For all the measurements we present here, we used a 4 bucket algorithm with a preceding 8 bit Gray code sequence to unwrap the phase. The period of the sinusoidal fringes was 12 LCOS pixels.

The full triangulation angle $\beta_r = \beta_1 + \beta_2$ varies slightly over the measurement field, leading to a lowly varying z resolution ($\pm 5\%$). In order to compensate this variation, we conducted a sensitivity calibration according to Ref. [7]. The calibration was done by moving the stereo microscope to different z positions above a reference mirror with a translation stage. At each position, the absolute phase was measured. From these measurements, a sensitivity field could be calculated which represents the relationship between the change in height and the change in the phase. As a reference, we used the measured phase for the position in the middle of the depth of sharpness, i.e. $z = 0$.

Fig. 3 shows the topography of a roughness standard fabricated by HALLE Feinwerktechnik with a mean roughness of $R_a = 3.40 \mu\text{m}$ (manufacturer's data). The measurement was conducted with the 1.0 x objective and a zoom factor of 4.0 resulting in a measurement field size of $3.18 \times 2.35 \text{ mm}^2$ and a z resolution of $0.43 \mu\text{m}$.

Fig. 3 shows the topographies of two different chrome-plated steel sheets exhibiting different surface textures. These measurements were made with the 1.6 x lens and a zoom factor of 8.0. The measurement field size and the height resolution were $1.04 \times 0.77 \text{ mm}^2$ and $0.085 \mu\text{m}$, respectively.

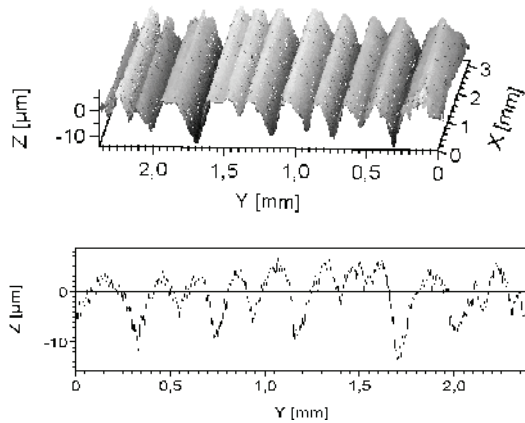


Fig. 2: 3D plot of the topography of a roughness normal with a mean roughness of $R_a = 3.40 \mu\text{m}$ and a section through the topography at $x = 2.0$

Conclusions

We have shown that the application of an LCOS display as the fringe generating element in a stereo microscope makes measurements with high accuracy possible. In combination with a CMOS camera, the achievable z resolution is in the micrometer range. Since the switching time of the ferroelectric liquid crystal layer is below $100 \mu\text{s}$, the theoretical limitation of the measurement time is the frame rate of the projected images. Thus, LCOS displays have a very high potential for future high speed measurement applications.

Supported by: Deutsche Forschungsgemeinschaft (DFG) under contract Ti 119/37-1 "Adaptive Sensorik zur Bestimmung der Mikrogeometrie"

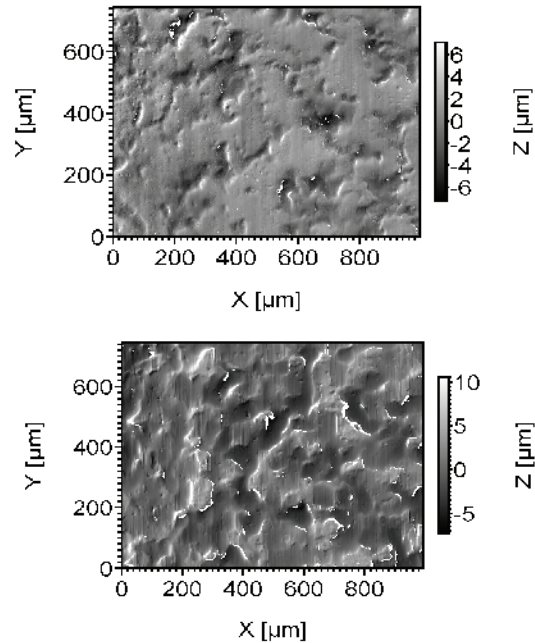


Fig. 3: Topographies of two chrome-plated steel sheets. Height values are gray level encoded

References:

- [1] D. Steudle, M. Wegner, H. J. Tiziani, "Confocal principle for macro- and microscopic surface and defect analysis", *Opt. Eng.* 39 (1) 32-39 (2000)
- [2] R. Windecker, M. Fleischer, H. J. Tiziani, "White-light interferometry with an extended zoom range", *JOSA* 46, 1123-1135 (1999)
- [3] R. Windecker, H. J. Tiziani, "Optical roughness measurements using extended white-light interferometry", *Opt. Eng.* 38(6) 1081-1087 (1999)
- [4] K. Leonhardt, U. Droste, H. J. Tiziani, "Microshape and rough-surface analysis by fringe projection", *Appl. Opt.* 33, 7477-7488 (1994)
- [5] R. Windecker, M. Fleischer, H. J. Tiziani, "Three-dimensional topometry with stereo microscopes", *Opt. Eng.* 36(12) 3372-3377 (1997)
- [6] R. Windecker, S. Franz, H. J. Tiziani, "Optical roughness measurements with fringe projection", *Appl. Opt.* 38 (13) 2837-2842 (1999)
- [7] R. Windecker, M. Fleischer, S. Franz, H. J. Tiziani, "Testing micro devices with fringe projection and white-light interferometry", *Optics and Lasers in Engineering* 36, 141-154 (2001)
- [8] K.-P. Proll, J.-M. Nivet, C. Volland, H. J. Tiziani, "Application of a liquid-crystal spatial light modulator for brightness adaptation in microscopic topometry", *Appl. Opt.* 39(34), 6430-6435 (2000)
- [9] K.-P. Proll, J.-M. Nivet, K. Körner, H. J. Tiziani, "Microscopic three-dimensional topometry with ferroelectric liquid-crystal-on-silicon displays", *Appl. Opt.* 42(10) 1773-1778 (2003)

Evaluation and Characterization of Liquid Crystal SLMs for Digital Comparative Holography (DISCO)

C. Kohler, X. Schwab, K.-P. Proll, W. Osten

For industrial applications, fast technologies for shape comparison between a master and a test object are needed. This task can be fulfilled with the help of comparative digital holography, which is the concern of the BMBF project DISCO (Distant Shape Control by Comparative Digital Holography). For the reconstruction of the recorded master hologram, a SLM is used. As the development of SLMs for this purpose is too expensive, commercially available elements are used. These elements are especially made for devices like projectors and are deployed as amplitude modulators. To be able to use the more efficient phase holograms, a phase modulator is needed. Therefore, the available SLMs can be applied, but they have to be characterized in detail. Their phase shifting properties and the according amplitude modulation have to be known to use them as phase modulators. In addition the knowledge of their Jones-Matrix [1] is a great advantage if further simulations or polarisation calculations should be made. ITO had the task of characterizing the SLMs. A modularized

test bench, which can easily be adjusted for the different measurements, was set up. At the moment it's possible to measure the following properties:

- Phase shift
- Amplitude modulation
- Diffraction efficiency
- Contrast
- Display homogeneity
- Jones-Matrix

All the measurements can be made by varying the direction of the incident light, as the illumination setup can be rotated around the axis of the display (See Fig. 1).

For the phase shift measurement, different methods were implemented and evaluated. The most preferable method to be found was the double slit experiment.

In figure 2, the image and the result of a phase shift measurement are presented. The result shows the comparison of two different displays for two different polarizer / analyzer combinations.

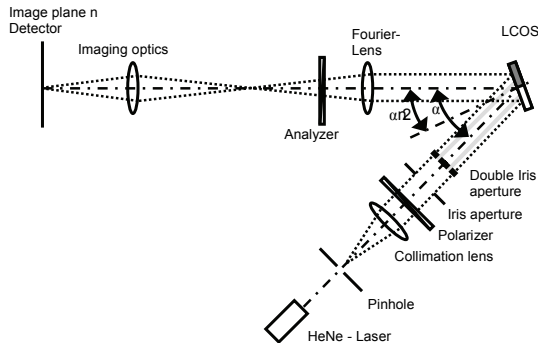


Fig. 1: Test bench in the configuration for phase shift measurements

Supported by: The German Ministry for Education and Research (BMBF) under the contract 13N8095 as sub-contract of BIAS, Bremen

References:

- [1] Dipl.-Ing. Klaus Leonhardt, "Kontrast, Helligkeit und Streifenversetzung in Interferometern mit unterschiedlich polarisierten Teilstäbchen", Universität Stuttgart, PhD. Thesis, 1972

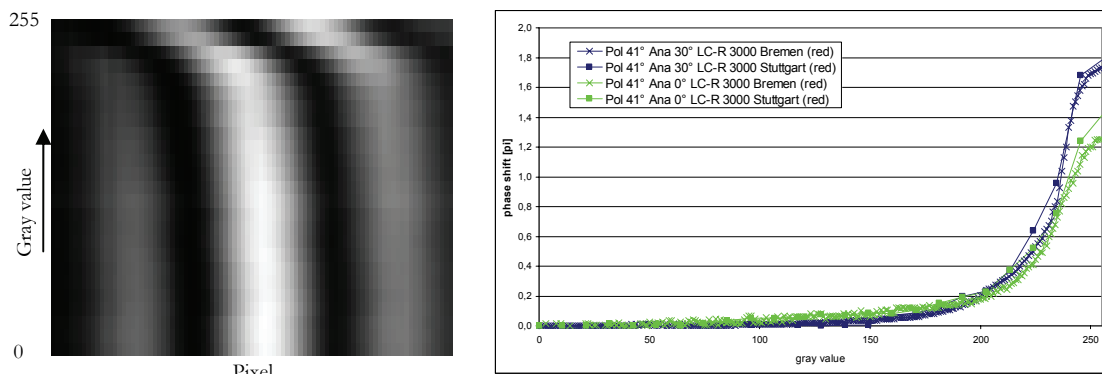


Fig. 2: **Left:** Image of a phase shift measurement, each line represents the interference pattern of one gray level
Right: Results of the phase shift measurement of two different displays

Collaboration with industry: A new white light interferometer

U. Droste, K. Körner, A. Goretzky, W. Osten, P. Lehmann (Mahr GmbH)

In collaboration with the company Mahr GmbH in Göttingen, a new white light interferometer “MarSurf WS 1” for contactless 3-D measurements was developed, by which a vertically resolution of 0.1 nm can be achieved. The ITO provided a software library for initial testing of the interferometer.

By the use of a short coherent light source it is possible to measure objects with steps. The optical setup follows the design of a classical Mirau interferometer, apart from that only a light source with low-coherence is employed. The reference field of the interferometer is integrated in the Mirau objective, reducing signifi-

cantly the size of the sensor. During the measurement, the Mirau objective is moved along the vertical axis, and a sequence of images is acquired, used to calculate the 3-D topography of the object.

The sensor can be applied in micro inspections rooms as well in the production. By use of an innovative algorithm to analyse the measured signals specular like lenses and mirrors as well as rough objects can be measured. The material of the object is thereby irrelevant for the measurement, objects made of glass, paper, lacquer, metals or fluids can be addressed.

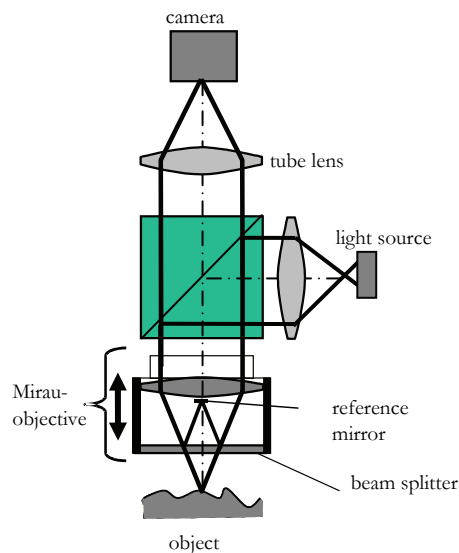


Fig. 1: Principle of a Mirau type white light interferometer

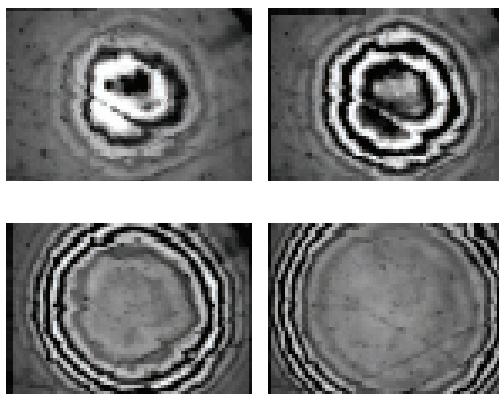


Fig. 2: Interferograms in several depths of focussing

References:

- [1] MarSurf WS 1-flyer
- [2] www.mahr.com



Fig. 3: Photo of the white light interferometer MarSurf WS 1

Depth-Scanning Fringe Projection (3D-MicroScan)

U. Droste, K. Körner, H.J. Tiziani, W. Osten

Today, the fringe projection technique is a commonly used method for various 3-D profiling, 3-D shape, or 3-D scene measurement techniques, based on the projection of a grating onto the surface of an object. The deformation of the fringe pattern observed from a different direction contains the information for determining the height map [1][2][3].

We are currently introducing a new depth-scanning triangulation method for absolute 3-D profiling of a macroscopic scene based on fringe projection technique. A scanning focal plane allows the phase to be determined for any desired depth range of the measurement volume. Furthermore, the limitations in the depth of focus that occur when using projected light techniques will be overcome, allowing a larger aperture and therefore better use of light. Additionally, we use a small angle of triangulation to reduce shadowing in the scene.

The projection and detection channels of the DSFP setup are laid out as two nearly identical, and parallel, optical paths as shown in Fig. 1 [4]-[8]. For projection, we use a Ronchi grating illuminated by a collimated white light source. An image-sided telecentric lens (L) with relatively high aperture is used to image the Ronchi grating into the object space. The optical path of the detection channel only differs in that a CCD-array takes the place of the Ronchi grating. It makes use of an identical lens, labelled D. Both Ronchi grating and CCD-array are mounted on a single high precision translation stage, whose axis is parallel to the optical axis of the measurement system. Furthermore, those devices are aligned, so that their planes of focus coincide. Thus, by simultaneously shifting the Ronchi grating and the CCD-camera along the z_A -axis in the array space, we shift this plane out of focus throughout the whole depth of the measurement volume. An additional lateral shift of the Ronchi grating along the x_A -axis produces the time-dependent intensity variation onto the CCD-array, which is needed to detect the phase variation.

By using image-sided telecentric lenses, we can practically overcome the lateral shifting of imaged points when the magnification is slightly modified, e. g. due to (de)focusing. For the detection lens D, this means that an object point is imaged at the same position of the CCD-array (i.e. onto the same pixel), when the image is slightly defocused.

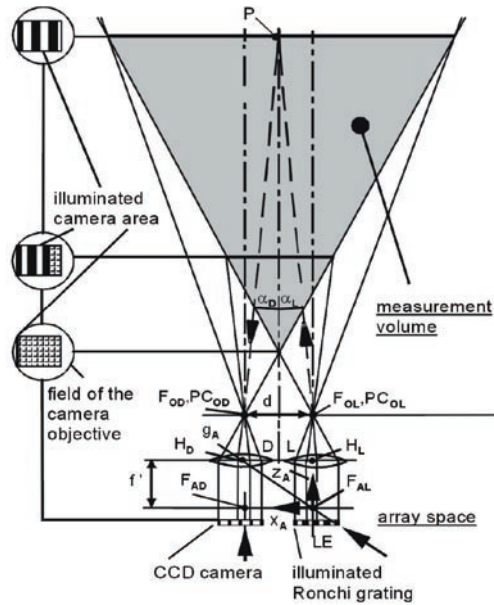


Fig. 1: Optical layout of the sensor for the depth-scanning fringe projection technique (DSFP) with a scanning objective L for illumination and an objective D for detection. The pupil centres are PCOL and PCOD, respectively.

Therefore, the modulated periodic intensity signal I that is detected by each individual pixel of the CCD-array can be interpreted as a signal type, commonly known from the short coherence interferometry [9]:

$$I = I_0 \left\{ 1 + m \left[z_A - z_{AP} \right] \cos \left[2\pi \left\{ \frac{z_A - z_{AP}}{\lambda_{TA}} \right\} + \varphi_0 + \Delta\varphi \right] \right\} \quad (1)$$

where m is the modulation function, z_A is the component of the translation of the grating and of the CCD camera chip in the z_A -direction, z_{AP} is the z_A -coordinate of the image position of an object at point P that is illuminated by a light emitting point LE of the grating plane. The distance d is the basis of triangulation of the measurement arrangement and p is the grating period. The lines of the grating are parallel to the y_A -coordinate. The unknown start position of the grating is described by φ_0 , $\Delta\varphi$ is a slowly varying phase term dependent on distortions due to the objectives.

In our experimental setup, the Ronchi grating is shifted exactly parallel to the oblique straight line g_A in the array space. The wavelength of triangulation in the array space depends only on the geometry of the optical arrangement and can be expressed as:

$$\lambda_{TA} = \frac{pf'}{d} \quad (2)$$

where f' is the focal length for the identical objectives for illumination (L) and detection (D). With the knowledge of the other geometric-optical parameters of the setup, the pixel pitch of the CCD camera, and the scale ratio β_p for the sharp imaging of the grating into the point P in object space, the lateral coordinates (x_{OP} , y_{OP}) of the point P can be also calculated. The position z_{AP} of the image point of P is given by Newton's formula with:

$$z_{AP} = -\frac{f'^2}{z_{OP}} \quad (3)$$

where z_{OP} is the z_O -position of the object point P in object space.

The best focus position is calculated from the maximum of the envelope that is stored in the envelope field, Z_E , giving information about the fringe order. Finally, the calculation procedure provides the exact phase at the maximum of the envelope. The algorithms used are explained in detail in Refs. [8] and [9].

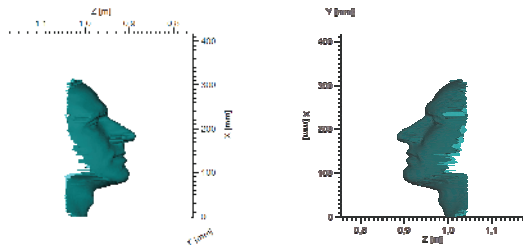


Fig. 2: Measurement result of a human face from one point of view

In Fig. 2 we show a result of a measurement with the depth-scanning fringe projection of a human face from one point of view.

Supported by: BMBF 3D-MicroScan 16SV942

References:

- [1] Osten, W., Jüptner, W., "New Light Sources and Sensors for Active Optical 3D-Inspection", SPIE 3897, pp. 314-27, 1999
- [2] Osten, W., "Application of optical shape measurement for the nondestructive evaluation of complex objects", Opt. Eng. 39, pp. 232-43, 2000
- [3] Tiziani, H. J., "Macro- and microscopic surface measurement", in Fringe'01, Jüptner W., Osten W. (Eds.), Proc. 4th Int. Workshop on Automatic Processing of Fringe Patterns. Elsevier, pp. 15-24, 2001
- [4] Körner, K., DE 198 46 145 A1.
- [5] Körner, K., Droste, U., Windecker, R., Fleischer, M., Tiziani, H. J., Bothe, T., Osten, W., "Projection of structured light in object planes of varying depths for absolute 3-D profiling in a triangulation setup", Proc. Laser'01, SPIE 4398, pp. 23-34, 2001
- [6] Körner, K., Windecker, R., Fleischer, M., Tiziani, H. J., "One-grating projection for absolute 3-D profiling", Opt. Eng. 40, pp. 1653-1660, 2001
- [7] Körner, K., Windecker, R., "Absolute macroscopic 3-D measurements with the innovative depth-scanning fringe projection technique (DSFP)". Optik 112, pp. 433-441, 2001
- [8] Körner, K., Droste, U., Windecker, R., Fleischer, M., Tiziani, H. J., Bothe, T., Osten, W., "Depth-Scanning fringe projection for absolute 3-D profiling", in Fringe'01, Jüptner, W., Osten, W. (Eds.), Proc. 4th Int. Workshop on Automatic Processing of Fringe Patterns. Elsevier, pp. 394-401, 2001
- [9] Windecker, R., Körner, K., Fleischer, M., Droste, U., Tiziani, H. J., "Generalized signal evaluation for white-light interferometry and scanning fringe projection", in Fringe'01, Jüptner, W., Osten, W. (Eds.), Proc. 4th Int. Workshop on Automatic Processing of Fringe Patterns. Elsevier, pp. 173-180, 2001

Direct Calibration Scheme for the Depth-Scanning Fringe Projection (3D-MicroScan)

J. M. Nivet, U. Droste, K. Körner, H. J. Tiziani, W. Osten

We adapted the direct calibration approach to perform both lateral and depth calibration of a depth scanning fringe projection setup. This approach enables us to introduce the dependency of the lateral calibration functions to magnification in the form of the z' -coordinate, and thus to tackle the problem of the lateral calibration of a focusing system for the first time [1].

The direct calibration of this setup is performed in array space. It is based on the determination of three transformations T_x , T_y and T_z between the measured coordinates $\hat{P}_i(\hat{x}_i', \hat{y}_i', \hat{z}_i')$ and the corresponding distortion free coordinates $P_i'(x_i', y_i', z_i')$, according to eq. (1):

$$P' \begin{cases} x' = T_x(\hat{x}', \hat{y}', \hat{z}') \\ y' = T_y(\hat{x}', \hat{y}', \hat{z}') \\ z' = T_z(\hat{x}', \hat{y}', \hat{z}') \end{cases} \quad (1)$$

Polynomial transformations as shown in eq. (2) and (2.a) proved to be suitable for this task.

$$\begin{aligned} T_x: x' &= \sum_i^M \sum_j^N \sum_k^P a_{ijk} \cdot \hat{x}'^i \cdot \hat{y}'^j \cdot \hat{z}'^k \\ T_y: y' &= \sum_i^M \sum_j^N \sum_k^P b_{ijk} \cdot \hat{x}'^i \cdot \hat{y}'^j \cdot \hat{z}'^k \\ T_z: z' &= \sum_i^M \sum_j^N \sum_k^P c_{ijk} \cdot \hat{x}'^i \cdot \hat{y}'^j \cdot \hat{z}'^k \end{aligned} \quad (2)$$

whereby

$$\frac{i}{M} + \frac{j}{N} + \frac{k}{P} \leq 1 \quad (2a)$$

The transformations, T_x and T_y , of the lateral calibration use all three measured \hat{z}_i' coordinates $(\hat{x}_i', \hat{y}_i', \hat{z}_i')$. In contrast, for the depth calibration transformation, T_z , the calibrated lateral coordinates, x_i' and y_i' , in combination with the measured \hat{z}_i' coordinate are used. Following this approach, the lateral and the depth calibration can be decoupled. This is a commonly used procedure for calibration of 3-D measurement systems because it leads to more stable and easier to interpret results. The additional condition introduced by eq. (2a) was also used to reduce the number of polynomial coefficients to be determined, leading thus to a shorter computation time. Introducing eq. (2.a) does not affect the accuracy, which was achieved by using only eq. (2).

In order to determine the coefficients, a_{ijk} , b_{ijk} and c_{ijk} , of the polynomial transformations, the coordinates of control points can be identified for

the coordinates measured with the depth scanning fringe setup. We will shortly show this identification for the case of the transformation T_x . In the case of T_y and T_z the identification can be processed in a similar way. Utilizing eq. (2) and (2a), with a number of n different control points, leads to a linear system of n equations, which can be expressed following the formalism of linear algebra:

$$X' = \hat{X}' A \quad (3)$$

where $X' = (x'_1, x'_2, \dots, x'_n)^T$ is the vector of the coordinates of the control points used as reference values, $A = (a_{000}, \dots, a_{ijk}, \dots, a_{MNP})^T$ is the vector of the polynomial coefficients, and \hat{X}' is the design matrix, built according to eq. (2). \hat{X}' has the form:

$$\hat{X}' = \begin{bmatrix} \hat{x}'_1^0 \hat{y}'_1^0 \hat{z}'_1^0 & \dots & \dots & \hat{x}'_1^M \hat{y}'_1^N \hat{z}'_1^P \\ \vdots & \ddots & \ddots & \vdots \\ & & \hat{x}'_i^i \hat{y}'_i^j \hat{z}'_i^k & \\ \vdots & \ddots & \ddots & \vdots \\ \hat{x}'_n^0 \hat{y}'_n^0 \hat{z}'_n^0 & \dots & \dots & \hat{x}'_n^M \hat{y}'_n^N \hat{z}'_n^P \end{bmatrix} \quad (4)$$

This system of equations can be solved provided the number of known set of coordinates (x_i', y_i', z_i') and measured sets of coordinates $(\hat{x}_i', \hat{y}_i', \hat{z}_i')$ is equal to or exceeds the number of unknown coefficients a_{ijk} . A large set of known and measured coordinates leads to better results since the influence of the measurement uncertainty is partly compensated by redundancy. According to eq. (3) the vector A can be expressed by:

$$A = (\hat{X}'^T \hat{X}')^{-1} \hat{X}'^T X' \quad (5)$$

A well known and numerically stable method to solve eq. (2) consists of computing a QR decomposition of \hat{X}' , where $\hat{X}' = QR$. Q is an orthogonal matrix and R is an upper triangular matrix. This leads to:

$$R \cdot A = Q^T \cdot X' \quad (6)$$

Since R is an upper triangular matrix, eq. (6) can be solved for A by back-substitution.

We conducted several series of measurements to prove the quality of the calibration. For each series, the depth of the calibrated volume was about 300 mm. This is limited by the range of our translation stage. We covered working distances ranging from 600 mm up to 1300 mm.

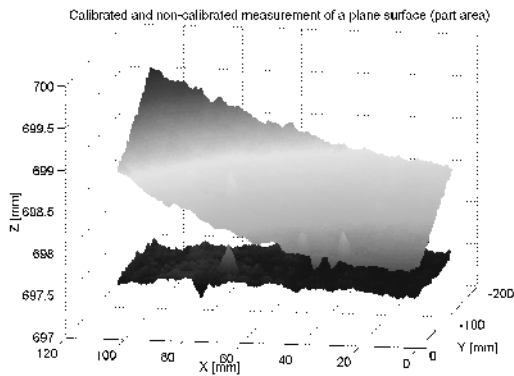


Fig. 1: Calibrated measurement of a plane surface (part of the area is shown) in comparison to the corresponding non-calibrated set of data. The reduction of the plane distortion due to the imaging is clearly observable.

After intensive investigation, the best combination for the grade of the polynomial transformations proved to be equal to 4 for the lateral calibration as well as for the depth calibration (i. e. $M = N = P = 4$ referring to eq. (2)). Using these values, we achieved a depth accuracy of $z_{\text{RMS}} < 0.1 \text{ mm}$ at a distance of $z \approx 800 \text{ mm}$ which corresponds to an accuracy of $z_{\text{RMS}}/z \leq 1:8000$ or

$z_{\text{RMS}}/\text{diag} \leq 1:5000$. Those relative accuracy values were also verified over the whole calibrated depth range. Further investigations proved the lateral mean relative accuracy to be about 0.5 pixels over the whole calibrated range, compared to about 1.5 pixels for non calibrated data. This corresponds to an average lateral accuracy of 0.3 mm at a distance $z = 800 \text{ mm}$ for calibrated data. We also investigated the long term stability of our setup and found that a set of calibration coefficients may be employed without significant loss of accuracy even after the system has been powered down for several days, provided thermal stability is reached.

Supported by: BMBF 3D-MicroScan 16SV942

References:

- [1] Nivet, J.-M., Körner, K., Droste, U., Fleischer, M., Tiziani, H.-J., Osten, W., "Depth-scanning Fringe projection technique (DSFP) with 3-D calibration", In: Optical Measurement Systems for Industrial Inspection III, Proceedings of the SPIE, Vol. 5144, pp. 443-450, 2003

Active Optical Systems

Detection of contamination on technical surfaces

Supported by: Bundesministerium für Wirtschaft und Arbeit (BMWA), Ref.No. 16IN0152

Phase-only light modulation: Wavefront shaping tests with piston micro mirror arrays

Supported by: the European Space Agency's Technology Research Program, ESTEC, contract no. 16632/02/NL/PA

Alternative aspheric testing: Interferometer with a tiltable reference wave (CCUPOB)

Supported by: BMBF FKZ 13N7861

Current spatial light modulators: Market analysis and tests on electrowetting and LC lenses

–

Holographic Tweezers: Active Micro-Manipulation (AMIMA)

Supported by: Landesstiftung Baden-Württemberg, Project AMIMA

Holographic Tweezers: Force Measurement in holographic tweezers

Supported by: Deutsche Forschungsgemeinschaft (DFG), Ti-119-40-1

Adaptive Shack-Hartmann sensor: A comparison of wavefront reconstruction algorithms (METAMO)

Supported by Landesstiftung Baden-Württemberg, Project "METAMO"

Detection of contamination on technical surfaces

W.Gorski, T.Haist, H.J.Tiziani, W.Osten

Manufacturing of metallic parts includes several mechanical processing steps such as cutting, bending, shaping etc. All of these operations are performed in a short time due to mass production requirements. One of the most important quality parameters is the cleanliness of the parts produced. This issue includes the presence of particles and oil on the surface, which could reduce, or even make impossible, normal usage of the components.

The project was realized within a consortium of industrial partners, with the Fraunhofer Institut (IPA) and with ITO. The target device was a modular, medium-cost system for real-time testing of metallic parts in fast (up to 0.3m/s) motion.

The system operates in the so called *inline* mode, with the maximum resolution depending on the speed of movement of the part under test and the acquisition frequency. The configuration for the system includes two channels, for detection of particles and oil layers (Fig. 1).

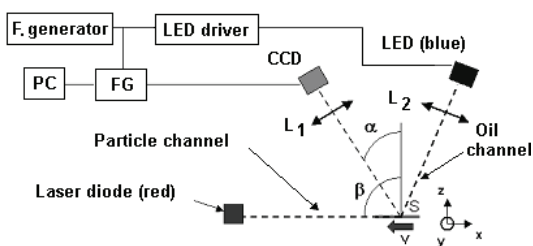


Fig. 1: Configuration of the measurement system: $\alpha = 35^\circ \pm 5^\circ$, $\beta = 88...90^\circ$, S – tested surface, v – up to 0.3 m/s

The particle detection channel consists of an intense (40mW) laser diode module, which illuminates the tested surface at an angle of nearly 90° . The light is scattered from the particle towards the camera. In the oil layer detection channel, the tested surface is illuminated by an intense LED (5W electrical power) at an angle similar to the observation angle. The change in the intensity indicates the presence of oil contamination. The wavelength in the particle channel is matched to the sensitivity characteristics of the camera and is 650 nm, while in the oil detection channel the wavelength is determined by the absorption curve of a typical oil, and is 455nm. The line camera is a Dalsa Piranha 2P2, 1024 pixels, (8 bit mode). It is coupled with the computer (PC) by a MVTitan frame grabber (Matrix Vision). The field of view is 20 mm. The illumination for the oil detection channel is strobed and synchronized with the acquisition sequence by the help of an external function generator and a driver. As a result, lines corresponding to each channel are interlaced, therefore the data analysis for both channels is

performed in nearly the same time. The total cost of all system components is 8500 €.

To evaluate the system performance, a special test object, with etched phantom **particles** in different sizes, was designed and manufactured. According to the evaluation results, the minimum size of the particle depends of the line acquisition frequency. For frequencies lower than 1 kHz it is $7.5 \mu\text{m}$, while from 1 to 15 kHz it is $10 \mu\text{m}$, and from 15 to 60 kHz it is $17 \mu\text{m}$ (Fig.2). The maximum speed of the tested element is 0.3 m/s. The evaluation of the oil detection channel was performed with externally prepared and certified probes. The minimum detectable thickness of the oil layer is below $1 \mu\text{m}$.

Software controls the acquisition and synchronization, enables calibration of the system, and allows the testing of elements with complex geometry and various roughnesses (e.g. USB plugs). The algorithm was optimised for high speed. It is also possible to select several areas of interest on the surface of each part that is tested.

Further improvement of the system performance can be achieved by increasing the amount of light in the particle channel and using 10 bits signal processing.

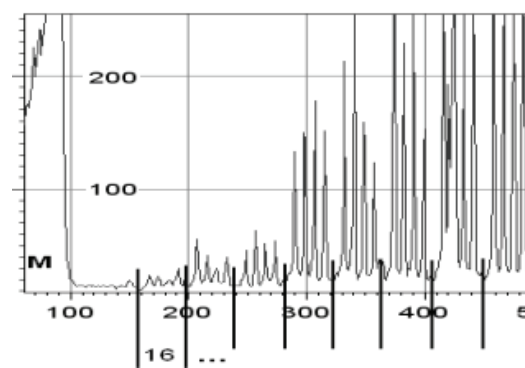


Fig.2: Example results for the particle channel evaluation at $f=1\text{kHz}$. Row 16 corresponds to a particle size of $7.5 \mu\text{m}$.

Supported by: Bundesministerium für Wirtschaft und Arbeit (BMWA), Ref.No. 16IN0152

References:

- [1] M.Dorndorf, W.Gorski, T.Haist: „KOMBISENS – Ein Sensorsystem zur Detektion von partikulären und filmischen Kontaminationen auf technischen Oberflächen“, presented in: „Reinigungsprozesse bei der Metallbearbeitung 2003“, Fraunhofer IPA Technologieforum F98, 9 Dezember 2003, Stuttgart
- [2] „Parts 2 Clean“ - Fachmesse für industrielle Teilereinigung und Teiltrocknung, 26 –28.10.2004, Friedrichshafen

Phase-only light modulation: Wavefront shaping tests with piston micro mirror arrays

J. Liesener, W. Osten

Spatial light modulators (SLMs) are key elements in the field of active and adaptive optics, where a precise control of light fields is demanded. The removal of aberrations in optical systems requires, for example, a modulator that can influence the phase of light fields, thus forming the shape of the outgoing wavefront. Currently deformable membrane mirrors are widely-used though their spatial resolution is very limited.

A new SLM, a micro mirror array (MMA) developed by the IPMS (Institut für Photonische Mikrosysteme) at the Fraunhofer Gesellschaft (www.ipms.fraunhofer.de) consists of an array of 240x200 micromirrors (40 μ m in size) that can be individually controlled. They move in a piston-like motion perpendicular to their surfaces (see fig. 1). The movement of a single mirror is induced by applying a voltage to the electrode underlying the pixel, resulting in an equilibrium between the electrostatic force and the restoring force of the suspension arms. The continuous deflection range is up to 400nm, so that a 2π phase shift for any visible wavelength is possible.

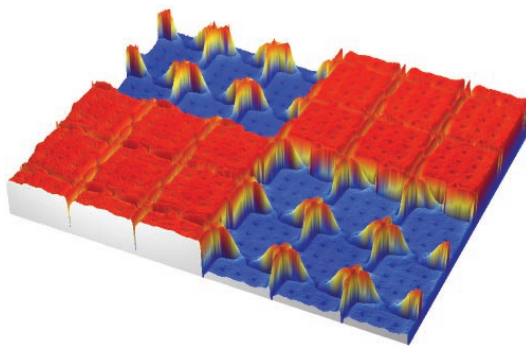


Fig. 1: View of deflected and undeflected micro-mirrors, measured with a white light interferometer, showing the surface height

A breadboard was set up to test the MMA's wavefront shaping capabilities. For this purpose artificially induced aberrations, with an error of up to 9 times the wavelength, were compensated for by the MMA. The quality of the wavefront error compensation was judged by measuring the coupling efficiency achieved when coupling into a monomode fiber. Several methods to obtain the correct mirror positions were applied, among them interferometry, Shack-Hartmann measurements, which display the remaining wavefront error, and iterative methods that use only the coupling efficiency as a measurement. The optical setup (see Fig. 2) was designed so that only minor changes were necessary to switch between the different methods.

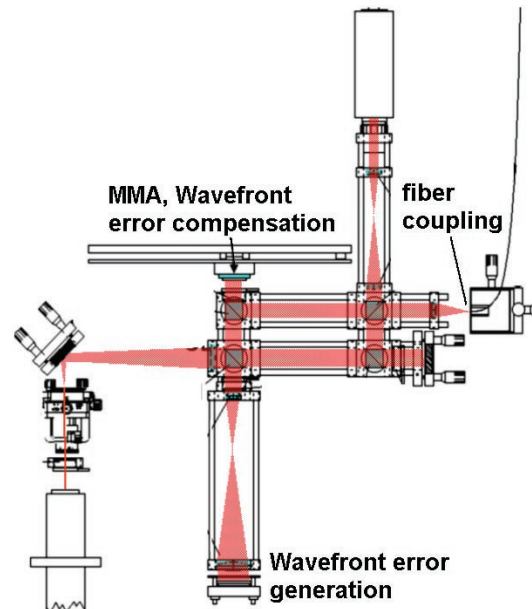


Fig. 2: Optical setup for wavefront optimization tests

For low wavefront errors the achieved coupling efficiencies were above 60% and were therefore immediately below the expected theoretical limit for the given setup. Compared to flip mirrors with binary operation (also tested within the project) the efficiency was, as expected, significantly higher. A clear advantage of this technique over deformable membrane mirrors (previously tested by the project partner EADS astrium) lies in the correction of high spatial frequency errors or even errors with phase steps.

Supported by: the European Space Agency's Technology Research Program, ESTEC, contract no. 16632/02/NL/PA

References:

- [1] Liesener, J., Hupfer, W.J., Gehner, A., Wallace, K., "Tests on micromirror arrays for adaptive optics", Proc. SPIE, 5553, p. 319-329, 2004
- [2] Liesener, J., Seifert, L., Tiziani, H.J., Osten, W., "Active wavefront sensing and control with SLMs", Proc. SPIE 5532, pp.147-158, 2004

Alternative aspheric testing: Interferometer with a tiltable reference wave (CCUPOB)

J. Liesener, C. Pruß, H.J. Tiziani

A section of the BMBF project “Asphärenprüfung mit computergenerierten Hologrammen (CGHs)” was the investigation of flexible aspheric testing methods that do not require the fabrication of CGHs for every asphere type. A strong emphasis was placed on an interferometer in which the angle of the reference wave could be controlled in a very defined way. This is so that areas of the fringes in the interferogram can be evaluated which could not be resolved by the previous image sensor. The results of several measurements under varying reference wave angles were stitched at the end of the process.

The interferometer is depicted in fig. 2. Light reflected by the lens under test and by the light following the reference path is brought to interfere on the camera chip. The varying reference wave angles are realized by switching between point sources, each with a different lateral position on the phase-shifting point source array (PPA, description below).

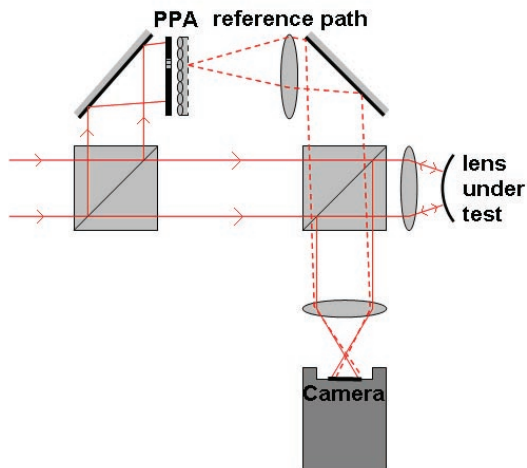


Fig. 1: Flexible interferometer setup for aspheric testing. The reference wave angle can be modified so that different areas of the interferogram can be evaluated.

The PPA was developed within the project. (patent DE 10325601). It is an array of point sources that can be individually switched. It consists of three layers, namely a liquid crystal micro display (LCD), a microlens array (MLA) and an array of pinholes (PHA) that are placed at the focus of the microlenses.

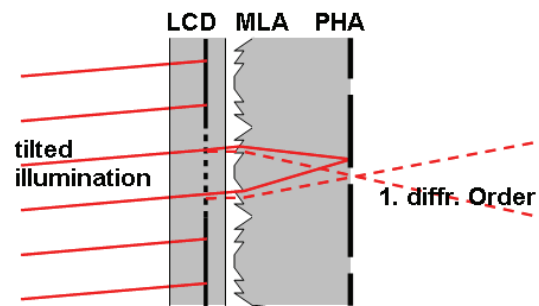


Fig. 2: Phase-shifting point source array (PPA) consisting of liquid crystal display (LCD), microlens array (MLA) and pinhole array (PHA).

The LCD is to be illuminated at a slight angle, so that, in order to activate one of the point sources, a local grating needs to be written into the LCD. Only the first diffraction order of the light diffracted by the local grating is focused, by the microlens, through the corresponding pinhole to form a point source. In addition to the intensity, the phase of the light emitted by the point sources can be changed. The phase is shifted in several steps by laterally shifting the local LCD-grating. In this way conventional phase shifting algorithms for the phase retrieval can be applied.

Using the test setup a lens was tested that required the recording of interferograms with 25 different reference wave angles. Almost seamless stitching was possible. The measurement error was below 1/10 rms at in the surface.

Future work will focus on a more accurately adjustable optical setup and on calibration strategies.

Supported by: BMBF FKZ 13N7861

References:

- [1] Liesener, J., Tiziani, H.J., "Interferometer with dynamic reference", Proc. SPIE 5252, p. 264-271, 2004.

Current spatial light modulators: Market analysis and tests on electrowetting and LC lenses

J. Liesener, L. Seifert, B. R uth

The aim of this industry-commissioned study was to assess the suitability of current spatial light modulators for focussing purposes. The study was divided into two parts.

The first part consisted of a market analysis and a technology review in which the relevant issues for an industrial application of several modulator types were examined. The list of modulators included pixelated liquid crystal displays, membrane mirrors, electrowetting lenses and continuous liquid crystal (LC) lenses. The topics of interest were the functional principle of the modulators, the state of the art, future developments, the patent situation, the availability and specifications such as aperture diameter, tunable focal length range, operation cycle time and wavefront error.

The second part of the study was an experimental investigation carried out within a student research project for which both an electrowetting lens and an LC lens were supplied by the industrial partner. Both lens types were in the prototype stage by the time of the investigation. An electrowetting lens (see fig. 1) uses two isodensity liquids, one is an insulator while the other is a conductor. The variation of voltage leads to a change of curvature of the liquid-liquid interface, which in turn leads to a change of the focal length of the lens. The electrowetting lens was purchased from varioptic (France).

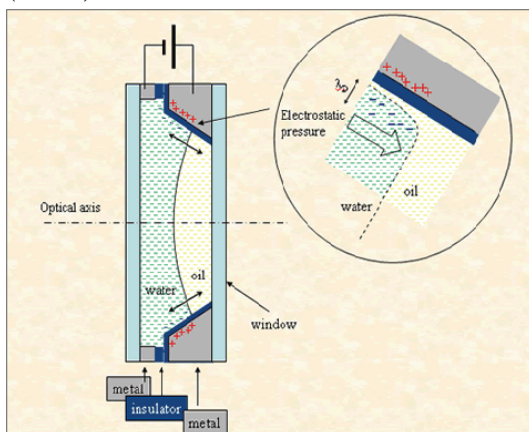


Fig. 1: Principle sketch of an electrowetting lens (source: [1])

The liquid crystal lens has a convex cavity filled with a liquid crystal enclosed between two glass substrates with two transparent conductive layers that act as electrodes. The amplitude as well as the frequency of the applied voltage influence the orientation and therefore the refractive index distribution within the liquid crystal. This enables the focusing of the beam that passes through the lens. The lens (fig. 2) is made by OKO Technologies (Netherlands).



Fig. 2: Liquid crystal lens (photo from [2])

References:

- [1] www.varioptic.com
- [2] G. Vdovin et al, "On the possibility of intraocular adaptive optics", *Optics Express*, 11, p. 810-817, (2003)

Holographic Tweezers: Active Micro-Manipulation (AMIMA)

M. Reicherter, W. Górski, T. Haist, H.J. Tiziani, W. Osten

One of the driving forces of scientific and technological progress is the increasing ability to work on smaller and smaller scales. Optical tweezers are a tool for such kinds of manipulations. In optical tweezers a focused beam of light is used to trap particles which have a size ranging from some hundred nanometres to several tens of micrometers. Holographic tweezers are an important extension of this tool. They incorporate a spatial light modulator (SLM), such as a digital micro-mirror device (DMD) or a liquid crystal device (LCDs). They have many advantages over conventional tweezers including the ability to move many particles independently of each other, without using mechanically moving parts such as mirrors and movable lenses. The holographic approach allows us to move the particles not only in the lateral direction but also along the optical axis. In addition to that it makes an aberration correction possible.

In the project AMIMA two different methods of aberration correction were developed. The first method is based on the principle of an artificial point source as is known from astronomy. The micro-particles are trapped and positioned by the holographic tweezers which acts as a lens that creates a spot. This can be regarded as a point source. The light coming from that point source is analysed by a Shack-Hartmann-Sensor. If there are no aberrations, neither from the setup nor from the sample volume, the analysed wavefront would be spherical. Any deviation from the spherical shape is recorded and used to compute a correction hologram. This hologram and the trapping hologram are superimposed and displayed on the SLM. A crucial aspect of this method is the filtering out of the illumination light which misses the particle and therefore does not contribute to the point source. This can be achieved either by using an aperture or by an obscuration shown in figure 1. A third approach was tried using fluorescent particles and an appropriate filter. This is very elegant approach, but we did not have a camera

that was sensitive enough camera at the wavelength of the fluorescence. With this point source method using an aperture we were able to correct for $4\ \mu\text{m} \pm 0,25\ \mu\text{m}$ defocus in a first experiment.

The second method is an iterative optimisation approach. A randomly generated, or one from an educated guess, hologram is displayed on the SLM. To generate a feedback loop, one has to analyze the image and decide if the correction hologram obtained leads to an improvement. If an improvement has occurred, subsequent changes to the correction hologram will be smaller. If not the next hologram is calculated with a significantly changed parameter set. Figure 2 shows an example of this method.

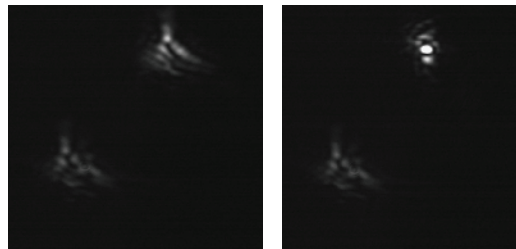


Fig. 2: Uncorrected 0. und 1. order of the trapping laser (left) Corrected 1. order (right)

The image on the left shows the zeroth and first order of the trapping beam. Strong aberrations can be seen which result mainly from the astigmatism of the diode laser used. After manually adapting the correction hologram, the first order is improved significantly. Further steps include the automation of the method.

Supported by: Landesstiftung Baden-Württemberg, project AMIMA

References:

- [1] M. Reicherter, W. Górski, T. Haist, W. Osten, "Dynamic correction of aberrations in microscopic imaging systems using an artificial point source", Proc. SPIE 5462 (5) 33, S. 68 2004

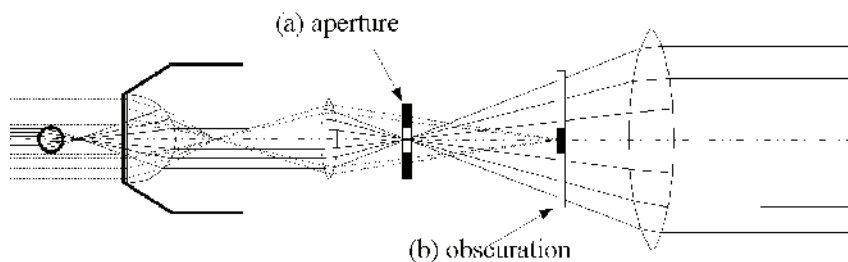


Fig. 1: Filtering out the illumination light

Holographic Tweezers: Force Measurement in holographic tweezers

M. Reicherter, S. Zwick, T. Haist, H.J. Tiziani, W. Osten

An important application of optical tweezers is their use as a force transducer. This is one of the most sensitive techniques for force measurement. It is capable of detecting forces in the region of femto Newtons. The ability to measure force in that range is of great interest especially in micro-biological applications [1].

The principle of force measurement in optical tweezers is based on a precise determination of the position of a trapped micro-particle within the optical trap. The optical trap constituted by a Gaussian beam can be considered as a force potential. If an external force acts on the particle it is drawn out of its equilibrium position in the centre of the potential. Detecting this distance gives a measure of the external force.

There are several possibilities to calibrate the force potential. The most straightforward method to determine the depth of the potential is to move a trapped particle at different speeds and to measure when it is lost from the trap. However this only gives the maximum trapping force but does not deliver information about the shape of the force potential. This can be achieved, for example, by using the Brownian motion of the particle within the trap. By imaging the particle on a quadrant photodiode, its position is recorded with nanometer precision. Alternatively interference between the trapping beam, which hits the particle, and an unmodified portion can be recorded. This approach has several advantages as Rohrbach[2] explains. Figure 1a depicts the recording of the lateral position of a 3 μm polystyrene particle within the trap. The histogram shown in figure 1b gives the probability $p(x)$ of finding the particle at a specific deflection from its equilibrium position. Using the Boltzmann distribution $p(x) dx = C \exp(-E/(k_B T))$ [3] one is able to compute the potential E . The potential (dotted line) and a harmonic fit (solid line) to it is shown in figure 1c.

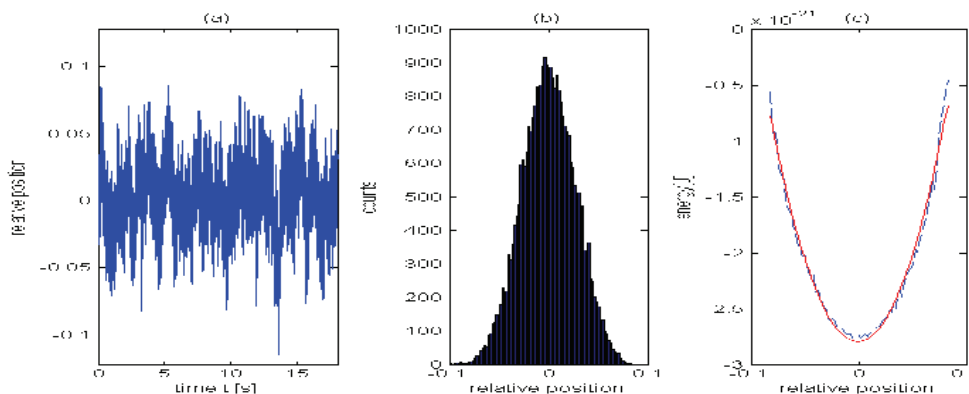


Fig. 1: Determination of the force potential using Brownian motion and Boltzmann statistics

We also investigated an image processing based approach[4]. The particle position is detected using a normalized correlation of a particle template and the current image. Figure 2 displays a comparison of the potential determined by the interference and the image processing method.

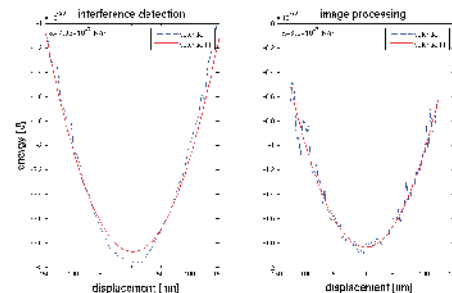


Fig. 2: Comparison of the two calibration methods investigated

Comparing the two methods the image processing with a data acquisition of about 50Hz is much slower than the quadrant diode. However it is simpler to implement and it is potentially better suited for the detection of the positions of several particles simultaneously.

Supported by: Deutsche Forschungsgemeinschaft (DFG), Ti-119-40-1

References:

- [1] W. Singer et al.: "3D-Force Calibration of Optical Tweezers for Mechanical Stimulation of Surfactant-Releasing Lung Cells", Laser Physics (11) 11, 2001, p 1217
- [2] A. Rohrbach et al.: "Trapping and tracking a local probe with a photonic force microscope", Rev. Scient. Instr. (75) 6, 2004
- [3] E.-L. Florin et al.: "Photonic force microscope calibration by thermal noise analysis", Appl. Phys. A (66), p 75, 1998
- [4] S. Zwick : „Grundlegende Untersuchungen zur hochgenauen Positionsbestimmung in holografischen Pinzetten“, Diplomarbeit ITO, 2005

Adaptive Shack-Hartmann sensor: A comparison of wavefront reconstruction algorithms (METAMO)

L. Seifert, H.J. Tiziani, W. Osten

The adaptive Shack-Hartmann sensor (aSHS) is a modification of the conventional Shack-Hartmann wavefront sensor (SHS). Instead of the static diffractive, or refractive, microlens array in the conventional sensor a programmable spatial light modulator (SLM) is used. The result is a far more flexible sensor which can be quickly adapted to solve different measurement tasks [1].

Wavefront reconstruction is the process of restoring the phase values from the measured wavefront slopes. There are differences in the reconstruction process between the conventional and the adaptive sensor. Because of the low resolution of the SLM in the aSHS, the number of microlenses is limited. Therefore a restriction of the measurement area to a circle should be avoided. This is often done in the conventional sensor. Furthermore the measured slope is a value that is integrated over the area of one microlens. Because of the relatively large size of a single microlens in the aSHS, the measured derivative can not be interpreted as the gradient at the center of the lens. A high fitting accuracy with the aSHS is only possible after taking these issues into account.

There are mainly two types of reconstruction algorithms: matrix inversion and iterative methods. The latter are often used in real time applications because they are fast. Matrix inversion methods are slower but more accurate.

We compared two matrix inversion reconstruction methods, particularly with regard to the aSHS, on the basis of fit accuracy, reconstruction time and the effect of noise and missing data points [2].

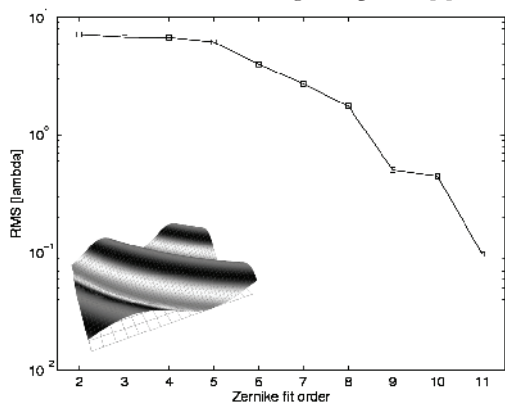


Fig. 1: RMS fit error of the Zernike reconstruction of a sin-shaped wavefront dependent of the fit order

Fitting the gradient data into Zernike modes is the classical SHS reconstruction algorithm. It is popular because the resulting coefficients represent important wavefront characteristics like tilt or third order aberra-

tions. The time to solve the equation system depends only on the number of Zernike modes used. The highest Zernike fit order, which can be used, is limited by the number of microlenses along the shorter side of the rectangular microlens array. We observed that the classical Zernike method is the best choice when fitting simple wavefronts. It is relatively fast and yields a high fit accuracy because of the global definition of the polynomials and their low noise vulnerability.

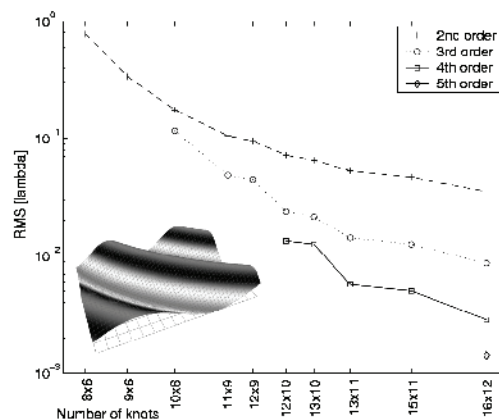


Fig. 2: RMS fit error of the B-Spline reconstruction of a sin-shaped wavefront dependent on the fit order and knot points

The novel reconstruction method is based on B-Spline surfaces. Unlike the Zernike algorithm, B-Spline fitting does not need a scaling to the unit circle. The locally defined base functions are more flexible than the global Zernike polynomials but also more vulnerable to noise. The solving time of the B-Spline equation system is not directly dependent on the order of the fit but on the number of knot points. The fit order in the x and y directions can be changed independently. This is particularly interesting for the aSHS, because the shorter side of the microlens array then does not limit the fit parameter along the longer side. We observed that the B-Spline reconstruction method is better suited for the rectangular aSHS and should be used when fitting more complex wavefronts (see Fig 1 and 2).

Supported by Landesstiftung Baden-Württemberg, Project "METAMO"

References:

- [1] L.Seifert, J.Liesener, H.J. Tiziani, "The adaptive Shack-Hartmann sensor", Opt. Com. 216, p.313-319, 2003
- [2] L. Seifert, H.J. Tiziani, W. Osten, "Wavefront reconstruction with the adaptive Shack-Hartmann sensor", Opt. Com. 245, p.255-269, 2005

High Resolution Metrology and Simulation

High Resolution Metrology and Simulation

–

Rigorous Simulations at the ITOThe Program Package MicroSim

–

Rigorous diffraction simulation: A comparison of RCWA, FDTD and FEM (RISOM)

Supported by: Landesstiftung Baden-Württemberg, Project: RISOM

Both a blessing and a curse: Physical optical effects in high resolution metrology (NanoEdge)

Supported by: BMBF; Nanoedge FKZ 13N7794

Scatterometry and diffractometry for nanoelectronic devices (ABBILD)

Supported by: BMBF, Project No. 01M3154D

Focus-shaping using phase-singularities: Highly sensitive defect detection in the sub-lambda range

Supported by: European Union, Craft 1999-70400

Polarisation measurements for diffractometry (RISOM)

Supported by: Landesstiftung Baden-Württemberg, Project RISOM

Tensor-tomographic 3d reconstruction of the anisotropic refractive index inhomogeneity in glass blanks (RISOM)

Supported by: Landesstiftung Baden-Württemberg, Project "RISOM"

Rigorous Simulations at the ITO

The Program Package MicroSim

S. Rafler, N. Kerwien, T. Schuster, M. Totzeck, W. Osten

Under development for many years at the ITO, the program package MicroSim forms the backbone for rigorous simulations in the working-group HMS [1]. The continuous advancement and extension of the program package in different fields of rigorous simulations is a crucial part of several running projects.

MicroSim is a package of numerical routines, which cover the solution of diffraction problems by rigorous methods, the calculation and visualization of the corresponding near-fields as well as microscopic far-field images.

The range of applications of MicroSim spreads from rigorous treatment of scatterometry and diffractometry for semiconductor industry [2] over near-field calculations up to systematic investigations of microscopic imaging techniques [4-5]. Further details can also be found in several project descriptions of this annual report (following pages).

MicroSim is completely written in MATLAB-code. This allows for necessary flexibility in a research environment. So, extensions and adoptions of the core code to different project related demands can be done quickly and easily.

Figure 1 shows the modular structure of MicroSim: there are three main modules for diffraction, near-field and far-field computation (i.e. imaging).

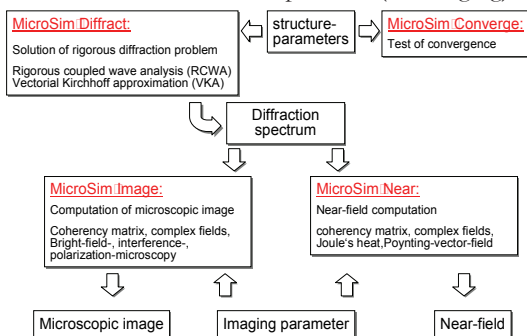


Fig. 1: Modular structure of MicroSim

The diffraction module MicroSim.Diffract is based on the rigorous coupled wave analysis (RCWA) in combination with the enhanced-transmittance-matrix approach. This approach provides the coupling of different grating layers. An arbitrary grating-shape is approximated by a staircase-like profile. Symmetries of the illumination or the grating structure are exploited to reduce computation time. For less demanding diffraction problems and for saving computation time, a semi-rigorous calculation method called the vectorial Kirchhoff approach is also implemented. In this approximation the vertical coupling of the electromagnetic field in the layers of the grating structure is calculated by means

of the thin-film-matrix-theory while the explicit lateral coupling in the layers-system is suppressed. The diffraction process itself is handled as in classical theory under full consideration of polarisation.

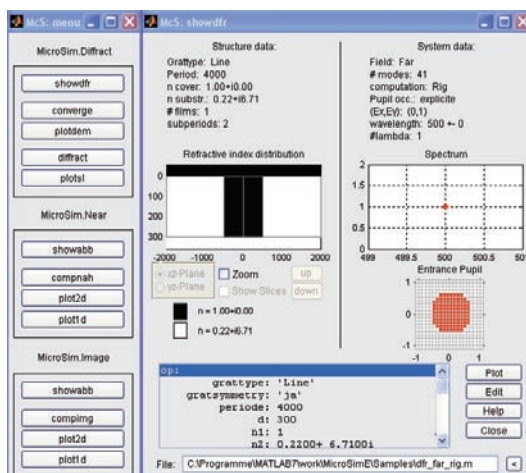


Fig. 2: typical Screenshot of input mask

MicroSim provides different classes of gratings in 2D and 3D. The implemented 2D structure types consist of line-gratings with multiple layers where in each layer the refraction index is piecewise constant but otherwise arbitrary. Slanted edges are approximated by staircases. In the 3D-case different predefined crosssections are implemented. These include circles and squares, ellipses and rectangles with different grating-periods in x- and y-direction. Recent developments enable us to compute structures with any given boundary in the framework of RCWA. The two-dimensional fourier-transform of these domains is done either via FFT with over-sampling or with a subdivision in rectangles and triangles which can then be handled analytically. This is necessary to achieve the desired accuracy.

In order to compute near- or far-fields for arbitrary illumination conditions, the diffraction spectrum has to be calculated for a bundle of different plain waves defined by a set of polarisation-states, wavelengths and angles of incidence. The parameters for the structure, illumination and computation are defined in a MATLAB-file and can be visualized and changed in a GUI. The whole operation of the program can be done via this GUI (see figure 2) or with batch-files for systematic variations of parameters in overnight-computations.

The diffraction spectrum computed with MicroSim.Diffract is the basis for the calculation of the corresponding near- and far-fields. It provides the complete necessary information in the pupil-plane of an imaging system.

In the case of microscopic far-field imaging MicroSim.Image calculates the electric field in the image-plane by superposition of all propagating waves of the diffraction spectrum falling into the aperture of the microscope lens. In the sense of Hopkins effective source this is done for each illuminating wave separately. Depending on the illumination conditions, the whole field distribution in the image-plane is obtained by summing up all field contributions originating from the set of incoming waves. This is done either coherently or incoherently. For this purpose the illumination entrance pupil is discretized with the size of the patches given by MicroSim.Diffract. The wavelength spectrum, amplitude and phase inside the pupil (aberrations) and polarisation of the illumination field can be given by predefined or user defined functions.

As the complete rigorous diffraction spectrum in the pupil-plane is accessible, different microscopic imaging techniques can be simulated by appropriate filtering in the pupil-plane. These include bright field microscopy under full consideration of (polarisation-dependent) aberrations and apodisations, dark-field imaging, Zernike-phase contrast, interference microscopy and different types of polarisation microscopy. An example is given in figure 3.

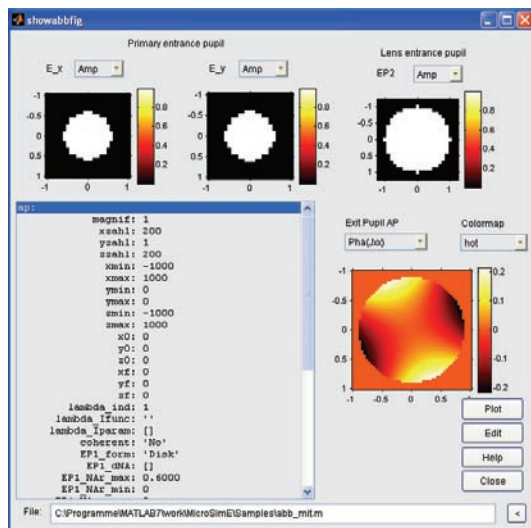


Fig. 3: GUI for microscopic image-simulation

Besides the various modes of far-field imaging also near-field computations provide a valuable tool to understand the basis of optical image formation. On the basis of the same ideas as described above MicroSim.Near creates near-field images by superposition of all modes obtained from the solution of the diffraction problem in the different regions of the

grating structure. In contrast to the far-field case this is done without any restriction to the numerical aperture of the imaging system in the grating region itself as well as in the cover and the substrate. Therefore the evanescent field components play a crucial role in image-formation as can be seen in figure 4.

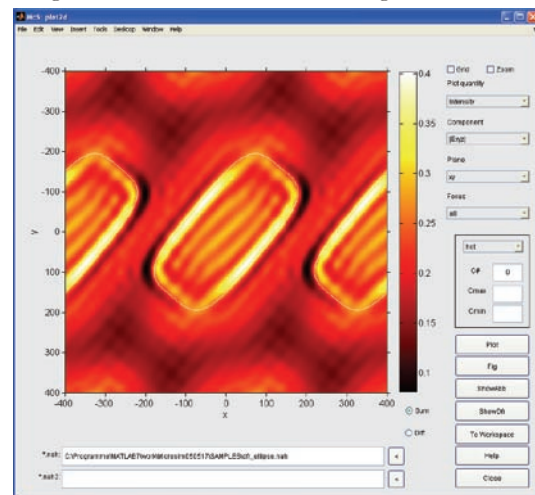


Fig. 4: Near field crosssection in topview

Those three modules form the basis of MicroSim. The focus of current developments is especially the implementation of alternative rigorous computation-methods of diffraction theory as well as providing interfaces for completely different methods like classical rigorous scattering-theory, FDTD and FEM simulations.

References:

- [1] M. Totzeck, "Numerical simulation of high-NA quantitative polarization microscopy and corresponding near-fields", *Optik*, 112 (2001) 381-390
- [2] T. Schuster, N. Kerwien, W. Osten, P. Reinig, M. Moert, T. Hingst, U. Mantz, "Effect of CD-fluctuations and side-wall roughness on scatterometry measurements." Conference on Lasers and Electro-Optics, CLEO Europe (2005)
- [3] N. Kerwien, A. Tavrov, J. Kauffmann, W. Osten, H.J. Tiziani, "Rapid quantitative phase imaging using phase retrieval for optical metrology of phase-shifting masks", *Proc of SPIE Vol 5144* (2003), pp. 105-114, *Optical Measurement Systems for Industrial Inspection III*, W. Osten, K. Creath, M. Kujawinska
- [4] A. Tavrov, M. Totzeck, N. Kerwien, H.J. Tiziani, "Rigorous coupled-wave analysis calculus of submicrometer interference pattern and resolving edge position versus signal to noise ratio" *Opt. Eng.* 41(8) (2002), pp. 1886-1892
- [5] N. Kerwien, E. Rosenthal, M. Totzeck, W. Osten, H.J. Tiziani, "Mueller matrix microscopy for high-resolution inspection of 2D-microstructures", *EOS Topical Meeting Advanced Imaging Techniques*, Delft 2003

Rigorous diffraction simulation: A comparison of RCWA, FDTD and FEM (RISOM)

R. Berger, J. Kauffmann, N. Kerwien, H.J. Tiziani, W. Osten

In metrology and in the design of optical systems rigorous simulations are needed, if the structures are in the scale of the wavelength or smaller. There are various simulation methods available to calculate the interaction of light with nanostructures and microstructures. At the moment we use Rigorous Coupled Wave Analysis (RCWA), the Finite Difference Time Domain method (FDTD) and the Finite Element Method (FEM). The various methods differ with respect to the technique of modelling and to the application area. Therefore we performed a comparison of the three methods [1].

At our Institute RCWA has been used to calculate the diffraction at gratings for several years. The structure is divided into different layers and the incident wave is composed of plane waves. The diffraction of every plane wave is calculated and the data combined. With this method it is also possible to evaluate the electromagnetic distribution of the light in the far field.

With the FDTD-method the modelling area is divided into a uniform net of nodes. The Maxwell-Equations are then spatially and temporally discretised in the same manner. This also allows us to investigate dynamic problems. To summarize, we had a good agreement between the simulations that were performed using the FDTD and the RCWA methods.

The Finite Element Method was first introduced for structural mechanics, but it can also be used in electrodynamics. We used the commercial program, FEMLAB, which has already a module for electromagnetic problems. In addition, it is possible to install a link to MATLAB and it is also possible to simulate anisotropic media. To compare the RCWA and FEM methods, we investigated a silicon grating, surrounded by air. Figure 1 shows the results for the TM-mode for the two methods. As it can be seen, the agreement of the simulations is high and there are only small differences inside the grating.

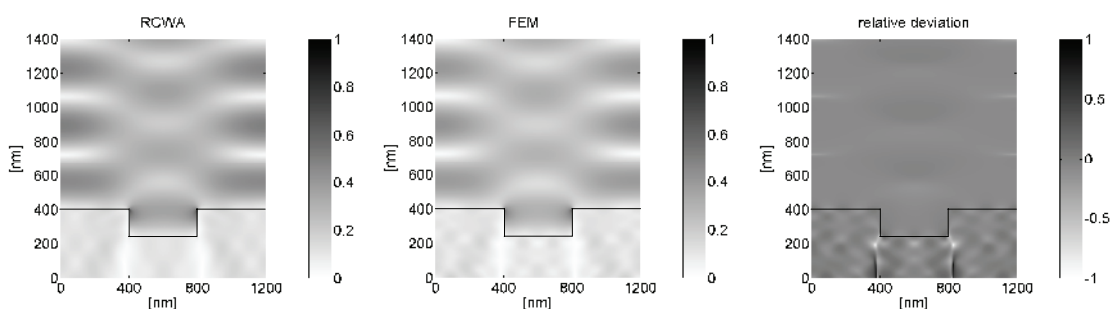


Fig. 1: Si-grating in air, TM-mode $\text{abs}(E_x)$

Another advantage of FEM can be seen in figure 2. It shows the simulation of a cosine grating, surrounded by air.

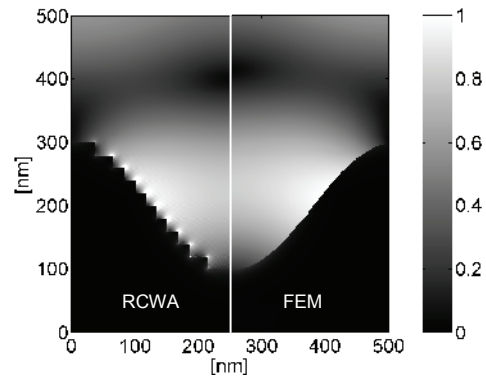


Fig. 2: Cosine grating in air, TM-mode $\text{norm}(E)$

Using RCWA (figure 2, left), the shape of the cosine function is approximated with steps. The electromagnetic field is increased at the tip of every step, which causes simulation errors. The described physical effect also occurs, when more steps are used for the approximation. With FEM, triangular elements are used to discretise the modeling area. Therefore gratings with a continuous shape, like the cosine function, can be approximated better with the FEM (figure 2, right).

Supported by: Landesstiftung Baden-Württemberg,
Project: RISOM

References:

- [1] Berger, R., Kauffmann, J., Kerwien, N., Osten, W., Tiziani, H.J., „Rigorse Beugungssimulation: Ein Vergleich zwischen RCWA, FDTD und der Finiten Elemente Methode“, DGaO-Proceedings P59, 2004

Both a blessing and a curse: Physical optical effects in high resolution metrology (NanoEdge)

N. Kerwien, H.J. Tiziani, W. Osten

Although diffraction limited in resolution to the range of the wavelength, optical measurement techniques compete successfully to other established metrology methods, like AFM or SEM that have inherently better physical resolution capabilities, down to approximately 1 nm in the later case. Among the well know technical advantages for optical measurements, are high throughput, excellent in-situ capabilities and a non-invasive character. A deep theoretical understanding of the light-object interaction in the framework of electrodynamics, and typically the large amount of a priori knowledge about the examined objects in different fields of semiconductor metrology, is responsible for the successful application of optical metrology techniques in the range well below the optical wavelength. In this case the high demand on the resolution requires a more precise model-based object reconstruction. The model takes geometrical data, shape and material composition of the object as well as parameters of the measurement system like polarisation state and coherence properties into account.

about. Figure 1 shows the microscopic focus-series of a 100 nm thick chromium edge simulated with Microsim. Incoherent illumination was used, with a wavelength of 248 nm in transmission, with an NA = 0.6, and for both the linear polarization parallel (TE) and linear polarization perpendicular (TM) cases relative to the edge. The boundary condition of the electro-dynamical problem results in different edge images. These concern the optimal focus-position, defined by the steepest ascent of the intensity-profile at 50% threshold, as well as the lateral position of the edge images. Both parameters are essential for high precision CD-measurement in the field of wafer metrology as well as for mask inspection. In the case of chromium at $\lambda = 248$ nm the displacement of the edge image is of the order of 10 nm, as can be seen on the right hand side of figure 1. The magnitude of this effect is strongly controlled by the wavelength and by the material composition of the surface under investigation. This displacement can increase up to 70 nm in the case of silicon at a wavelength of 248 nm.

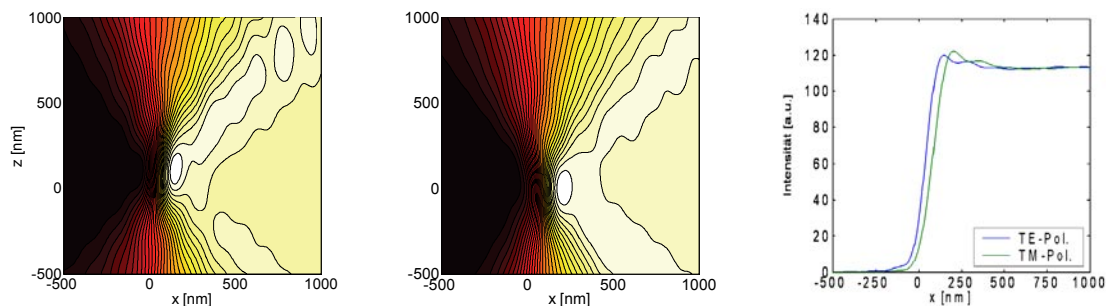


Fig. 1: Focus series of a 100 nm thick chromium edge in transmission at $\lambda = 248$ nm calculated with MicroSim: TE-Pol. **(left)** and TM-Pol. **(middle)**. The comparison shows clearly the variation of optimal focus (steepest flank angle) and different positions of the edge images **(right)** due to the dependence on polarisation.

The aim of the BMBF-project NanoEdge was the systematic experimental and numerical investigation of physical optical effects from the formation of an optical image. To these belong, for example, the well known proximity-effect, the polarization dependent line-width measurements, the resonance-effects in periodic media and the fundamental excitations such as surface-plasmons.

The insight gained was used in two ways. Firstly, in the consideration of these effects in optical metrology by means of rigorous model based imaging as well as experimental correction-procedures. Secondly, in the target use of electro-dynamical phenomena for light-sample-interaction for metrological purposes.

For further details concerning both strategies we refer you to the publications listed below.

Below, we would like to give a typical example of the fundamental effects that NanoEdge is concerned

Supported by: BMBF: Nanoedge FKZ 13N7794

References:

- [1] Kerwien, N., Tiziani, H.J., Osten, W., "Nutzung physikalisch optischer Effekte in der mikroskopischen Oberflächencharakterisierung", Final Report of BMBF-Project „NanoEdge“ FKZ 13N7794
- [2] Kerwien, N., Tavrov, A., Kauffmann, J., Osten, W., Tiziani, H.J., „Rapid quantitative phase imaging using phase retrieval for optical metrology of phase-shifting masks“, Proc of SPIE Vol 5144 (2003), pp. 105-114, Optical Measurement Systems for Industrial Inspection III, W. Osten, K. Creath, M. Kujawinska
- [3] Kerwien, N., Rosenthal, E., Totzeck, M., Osten, W., Tiziani, H.J., „Mueller matrix microscopy for high-resolution inspection of 2D-microstructures“, EOS Topical Meeting Advanced Imaging Techniques, Delft 2003

Scatterometry and diffractometry for nanoelectronic devices (ABBILD)

T. Schuster, N. Kerwien, J. Kauffmann, W. Osten

In the BMBF-project “ABBILD” the ITO is a subcontractor of Infineon Technologies. The aim of this project is to examine the capabilities of advanced strategies in the scatterometry and diffractometry, as fast and non-destructive measurement techniques to observe the geometry of complex nanostructures during the chip fabrication. Scatterometry and diffractometry are techniques in which geometric measurements of periodic nanostructures are made by investigating diffracted light. The term scatterometry is predominantly used if only the zeroth order is investigated, whereas diffractometry includes the measurement of higher diffraction orders. The measurands in each case can be the polarization resolved diffraction efficiencies or the ellipsometric angles as a function of the wavelength or as a function of the angle of incidence. If all but a few parameters of the nanogeometry of periodic structures are known with great precision, those few unknown parameters may be determined from the spectra by comparison between measurement and simulation.

One of the most widely-used methods for simulating diffraction at periodic structures is the rigorous coupled wave analysis (RCWA) [1][2][3]. One important task within this project is the extension of the Institute's simulation tool, MicroSim, to arbitrarily shaped crossed gratings. Furthermore simulation of the diffraction at complex crossed gratings showed that systematic computations for such structures are not possible with sufficient accuracy on a normal PC. Thus it turned out to be desirable to port Microsim to a modern 64 bit system which provides much more memory and computing power. Both tasks, the extension and the porting, are currently being worked on.

The capabilities of scatterometry and diffractometry were investigated by systematic RCWA computations with regard to the special structure geometries that Infineon is interested in. In this report we can just show some examples of those computations.

One example structure, with a rather complicated nanogeometry, is called DTMO (deep trench mask open) [4]. One unit cell of this periodic structure is depicted in Fig. 1. This structure consists basically of silicon oxide on a silicon substrate. The trench is 2 μm deep and 0.2 μm wide. The sidewall of the deep trench shows a bowing. The depth, Δb , is the parameter to be measured. Due to the enormous requirements of memory and computation power

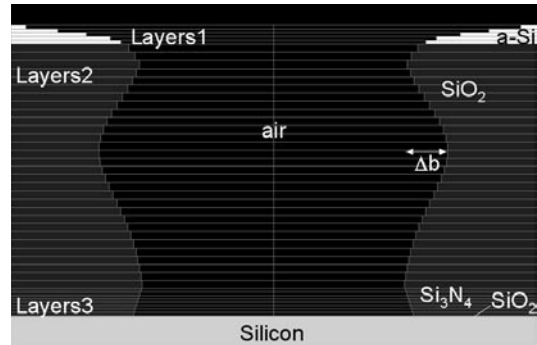


Fig. 1: DTMO structure

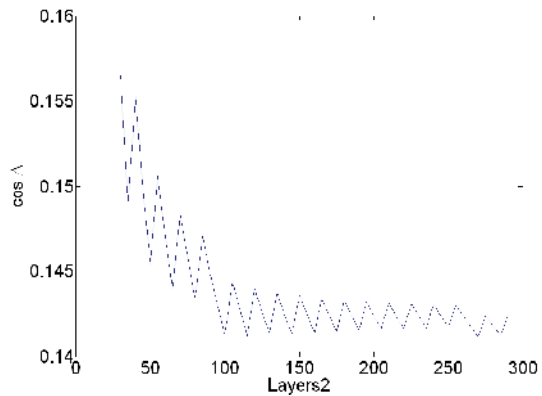


Fig. 2: Convergence with Layers2

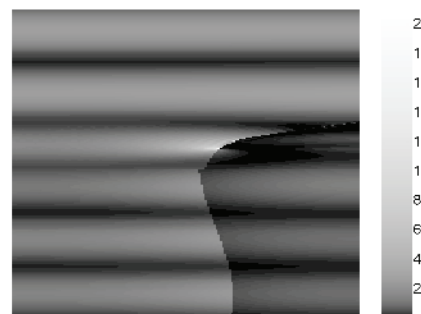


Fig. 3: Field enhancement at edges in an aSi layer

for crossed gratings, most of the computations were done instead for a line grating. On the one hand these computations, which were performed at the ITO, as well as at Infineon, showed that a measurement of this bowing depth is possible in principle. On the other hand they taught us that the spectra vary greatly, not only with the parameter to be determined but also with different other parameters such as the trench depth or the height of the maximum bowing. Thus a very exact modelling of the structure geometry is necessary, as well as a very exact knowledge and consistency of the parameters

that are assumed to be constant. The need for exact modelling leads to a rather large number of layers to be needed within the model. Fig. 2 shows a test series where the number of layers in the bowed region, denoted by "Layers2", is varied. This is assuming typical parameters for the experimental setup and sufficiently high values for the other layer numbers. The diagram shows, that according to the desired accuracy a more or less large number of layers has to be chosen.

The structure has also taught us a lot about the effect of slicing. There are two inherent limitations of the RCWA. The first one is the consideration of the lateral structure by Fourier expansion, which restricts the method to periodic structures. The second one is the slicing in the axial direction (perpendicular to the diffraction grating, usually denoted as the z-direction). For example the boundary of any oblique, or curved, trench or ridge sidewall is modelled as a staircase. This slicing contains two main drawbacks. Firstly, a great number of slices have to be chosen in order to model an oblique boundary with great precision. This makes it more difficult to do systematic computations of diffraction at crossed gratings. Secondly, the orientation of the sidewall boundary is (locally) always parallel to the z-axis. The first drawback is only a technical problem, which means that deep structures with oblique or curved sidewalls cannot be computed with sufficient accuracy within an acceptable time. For most relevant crossed gratings structures it is therefore impossible to choose a sufficient number of slices and, at the same time, a sufficient number of Fourier components. The second drawback is, in principle, a physical problem. The incorrect orientation of the boundary in the model affects mainly the field component that is perpendicular to the sidewall. As we know from Maxwell's equations this component is unsteady and thus "localizes" the boundary. At the edges, which are merely artifacts of the modelling and are not present in the real structures, a field enhancement is observed. This phenomenon is depicted in Fig. 3 using a logarithmic gray scale.

In addition to the previously mentioned systematic computation of spectra we made some more fundamental simulations. We studied the influence of lateral fluctuations of geometric measurements and sidewall roughness on the spectra. We modelled those fluctuations using the binomial distribution $P_{n,p}(v) = \frac{n!}{v!(n-v)!} p^v (1-p)^{n-v}$ assuming

the parameters $n=2$ and $p=1/2$. For each of the investigated structures we computed a series where we kept the measurement parameter constant and varied its standard deviation. In a second series we kept the standard deviation constant and varied the variable itself. For all investigated structures, we observed that a variation of the measurement parameter mainly influenced the peak positions in the wavelength spectra, whereas a variation of its standard deviation chiefly affected the peak heights. Thus the two influences can be separated in the measurement evaluation. It is possible to measure parameters (their mean values) even if they show a variation across the sample. Furthermore it is of course possible to do the opposite thing, i.e. to measure the standard deviation of a variable due to lateral fluctuations or sidewall roughness. This work will be presented in more detail in June [5].

In the next period of the project one important task will be the comparison between measurement and simulation. To this end, a research diffractometer has been modified with photoelastic modulators (PEMs) for fast and precise phase measurement.

Supported by: BMBF, Project No. 01M3154D

References:

- [1] Moharam, M.G., Grann E.B.; Pommet, D.A., Gaylord, T.K., "Formulation for stable and efficient implementation of the rigorous coupled-wave analysis of binary gratings", J. Opt. Soc. Am. A 12 (1995) No. 5, 1068-76
- [2] Moharam M.G., Pommet, D.A., Grann, E.B., Gaylord, T.K., "Stable implementation of the rigorous coupled-wave analysis for surface-relief gratings: enhanced transmittance matrix approach", J. Opt. Soc. Am. A 12 (1995) No. 5, 1077-86
- [3] Totzeck M., "Numerical simulation of high-NA quantitative polarization microscopy and corresponding near-fields", Optik 112 (2001) No. 9, 399-406
- [4] Reinig, P., Dost, R., Moert, M., Hingst, T., Mantz, U., Schuster, T., Kerwien, N., Kauffmann, J., Osten W., "Potential and limits of scatterometry: A study on bowed profiles and high aspect ratios", 2nd European Scatterometry Workshop, Porquerolles (France) 3-5 May 2004
- [5] Schuster, T., Kerwien, N., Osten, W., Reinig, P., Moert, M., Hingst, T., Mantz, U., "Effect of linewidth fluctuations and sidewall roughness in scatterometry", to be presented on the "Conference on Lasers and Electro-Optics" (CLEO Europe), Munich 12-17 June 2005

Focus-shaping using phase-singularities: Highly sensitive defect detection in the sub-lambda range

N. Kerwien, A. Tavrov, H.J. Tiziani, W. Osten

Pupil manipulation is a valuable tool for high resolution imaging. This concerns not only the manipulation of the exit-aperture of the imaging lens, as its done in Zernike phase contrast or in differential interference contrast for instance, but also for illumination control. In the later case we enter the wide field of the appropriate, or let us say, better adapted illumination in microscopy. Dark-field illumination is a prominent example. In the case of coherent pupil illumination, as used in confocal microscopy, phase manipulation introduces specific singularities that are of increasing interest. Such phase singularities are inherent properties of the resulting beam and are conserved in the propagation of the beam through free space and through ideal optical systems. Phase singularities are related to the symmetry properties of the forming system and can be associated with corresponding quantum numbers, such as parity or angular momentum. Because a dark region arises due to destructive interference, caused by singularities, such beams are often called dark beams. Perhaps the most prominent example in this field is the doughnut beam which forms as a consequence of a spiral singularity of π . In the investigations presented here we would like to concentrate on line singularities, which are generated by a phase mask with a linear phase-step of π , that intersect the symmetry-axis of the optical system in the pupil plane.

Besides the well known use for focus-shaping in the field of optical trapping, the special properties of phases-singularities in a high NA focus can also be exploited for metrological purposes. The advantage of dark beams is their particular sensitivity to phase objects and their ability to measure small isolated structures with simple detection schemes. They are therefore a promising tool for quantitative defect detection of single defects on flat surfaces, such as those arising during wafer inspection or in the characterisation of optical components such as laser mirrors.

We studied dark beam scans of different surface features and for various combinations of the illumination and detection numerical apertures. An example is given in figure 1. In the line scans a strong dependence on the incoming polarisation is apparent. Comparing the scans for single- and double-trench structures, the TM-Mode in particular varies strongly with the shape of the structure, due to better penetration capabilities into the structure in comparison with the TE-Mode. This general

feature is also true for sub-wavelength structures and can be used for sub-wavelength scale object recognition: A direct comparison of TE- and TM-polarisation reveals the potential of getting a more precise reconstruction of the structure under investigation. Apart from the investigations of the lateral resolution capabilities of dark beam microscopy, the axial resolution potential was also examined. Assuming that a two-cell photo detector with a dynamical range of 105 is the limiting factor for the signal to noise ratio (and therefore suppressing the optical noise associated with the surface roughness, which is usually dominant) the numerical investigations reveal detectable step-heights down to 0.2 nm. This is in the order of $\lambda/1000$ to $\lambda/10000$ and is therefore comparable to measurement accuracies achieved in advanced interferometry.

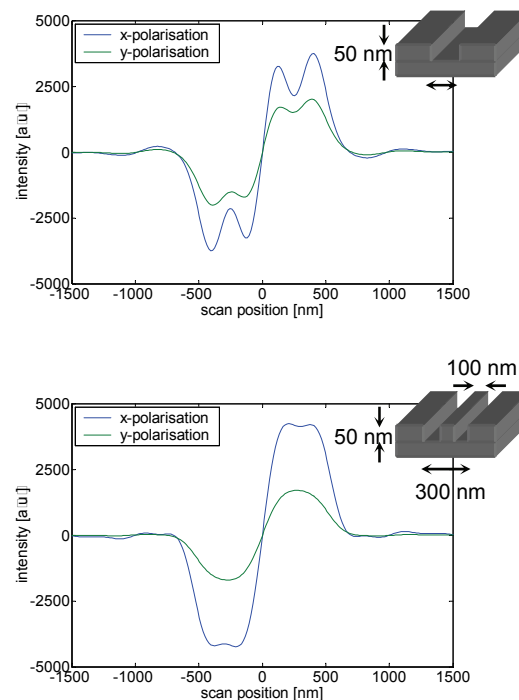


Fig. 1: Dark beam line scans on a Si-structure for different imaging and structure parameters. ($NA=0.9$, $\lambda=550$ nm)

Supported by: European Union, Craft 1999-70400

References:

- [1] Tavrov, A.; Kerwien, N.; Berger, R.; Tiziani, H.J., Totzeck, M., Spektor, B.; Shamir, J.; Toker, G.; Brunfeld, A.: Vector simulations of dark beam interaction with nano-scale surface features. Proc of SPIE Vol 5144 (2003), pp. 26-36

Polarisation measurements for diffractometry (RISOM)

J. Kauffmann, J. Bader, S. Meining, N. Kerwien, W. Osten,
H.J. Tiziani

The diffraction of light at structures with sizes in the scale of the wavelength influences the polarisation state of the light. This phenomenon is predicted by the Maxwell equations and can be calculated numerically by rigorous diffraction methods [1]. To characterize diffracting structures as, for example, diffractive optical elements (DOEs) experimentally diffractometers are used to measure the diffraction efficiency of the different diffraction orders. We have build such a diffractometer and constructed a polarisation measuring unit to measure the rigorous diffraction effects (Figure 1).

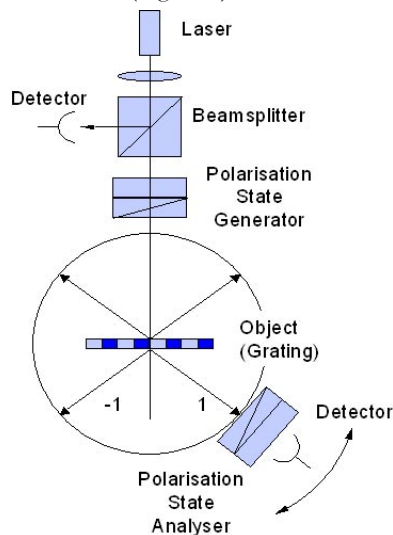


Fig. 1: Layout for the polarisation measuring diffractometer

A first approach is with circularly polarised input light and a polarizer to analyse the polarisation state at the detector. With this measurement the polarisation dependent attenuation is detected. To determine the ellipticity of the circularly polarised input light, for calibration purposes, measurements are performed for all polarizer positions without a measurement object. After the calibration the device under test is placed in the diffractometer. Figure 2 shows the polarisation dependent diffraction efficiency of a phase grating in fused silica.

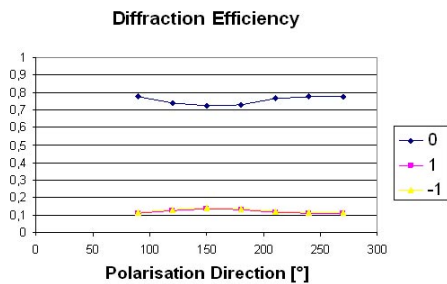


Fig. 2: Polarisation dependent diffraction efficiency of a DOE

To determine a more general form of the polarisation transfer function a different approach is currently implemented. Two photoelastic modulator – polarizer pairs, where the photoelastic modulators operate at different resonant frequencies, are used. The time-dependent intensity is analysed due to the lock-in principle at several frequencies so that the Müller matrix of the sample is obtained. With one configuration the nine elements of the matrix can be measured at the same time. When the azimuthal angles of the photoelastic modulators are changed the other elements are accessible. However the ellipsometric angles are already available from a single arrangement.

Supported by: Landesstiftung Baden-Württemberg,
project RISOM

References:

- [1] Berger R., Kauffmann J., Kerwien N., Osten W., Tiziani H.J., "Rigorous Beugungssimulation: Ein Vergleich zwischen RCWA, FDTD und der Finiten Elementen Methode", Proceeding der DGaO 2004, Bad Kreuznach

Tensor-tomographic 3d reconstruction of the anisotropic refractive index inhomogeneity in glass blanks (RISOM)

J. Kauffmann, N. Kerwien, W. Osten, H.J. Tiziani

For optical systems with the highest performance requirements even small inhomogeneities are disturbing. Inhomogeneities in glass blanks lead to a ray displacement and a phase retardation. Modelling the refractive index variation with a coplanar plate, as indicated in figure 1, shows that variations of the order of 10^6 can cause displacements in addition to phase retardations of about 100 nm. Similar results can be obtained when inhomogeneities in the anisotropic refractive index tensor is investigated. If the inhomogeneity is close to the image field the ray displacement is dominant in the vicinity of the pupil plane and the phase retardation is relevant.

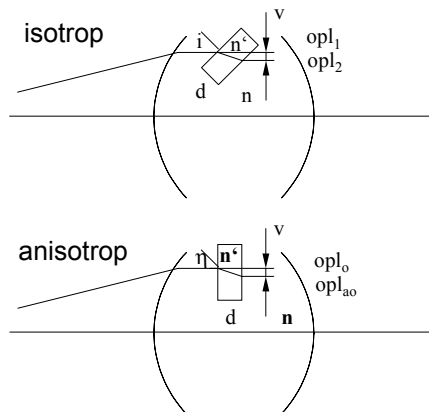


Fig. 1: Model to estimate the influence of inhomogeneities in **a)** the isotropic case **b)** the anisotropic case

To localize 3d anisotropic inhomogeneities in glass blanks we have developed a tensor tomographic reconstruction method [1]. It uses Jones matrices that are measured for individual rays with various projection directions. The results of the reconstructions are refractive index tensor fields. Figure 2 shows such a reconstruction. We started with a random distribution of the refractive index tensor elements (2a). Each tensor element is displayed as an individual sectional plot so that the nine diagrams compose the anisotropic inhomogeneity of a glass blank. In figure 2b the reconstruction is shown. With 10 projection directions and 17 by 17 measurements per direction, a cube of 15 by 15 by 15 cells has been reconstructed. After 1000 iteration steps the relative reconstruction deviation was smaller than 7.5%. Further investigations have shown that even with noise affecting the measurement data (about 10% noise) the reconstruction succeeds.

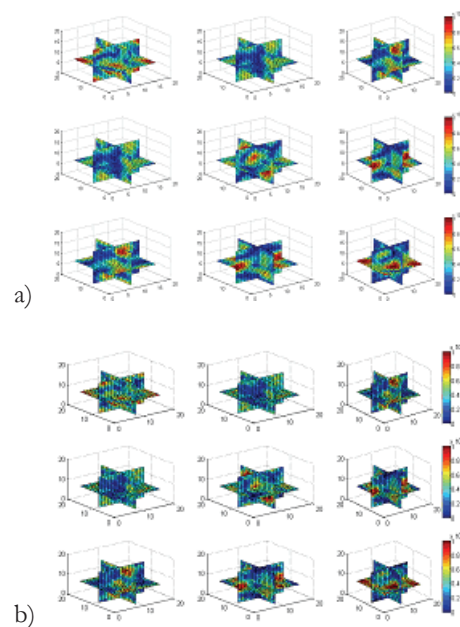


Fig. 2: **a)** One inhomogeneous element of the refractive index tensor penetrate by rays of different inclination. **b)** Real and imaginary part of the Jones transfer matrices under different inclinations

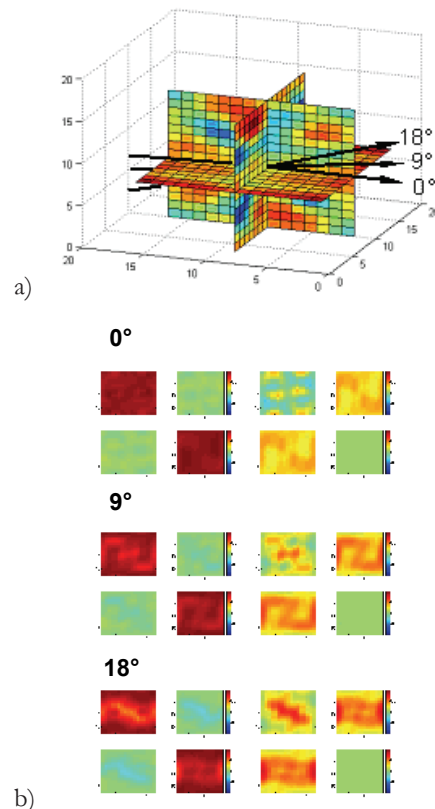


Fig. 3: **a)** One inhomogeneous element of the refractive index tensor penetrate by rays of different inclination. **b)** Real and imaginary part of the Jones transfer matrices under different inclinations

The meaning of the 3d anisotropic inhomogeneity is demonstrated in figure 3., where rays with different inclinations pass through an inhomogeneous glass blank. They are affected by different regions in the volume and by different projections of the associated refractive index ellipsoids. Figure 3b shows the real and imaginary part of the Jones transfer matrices for three different projection directions. If no tensorial volume information is available all three projections would have the same Jones matrices.

*Supported by: Landesstiftung Baden-Württemberg,
project "RISOM"*

References:

- [1] J. Kauffmann, N. Kerwien, H.J. Tiziani, W. Osten; "*3D anisotropy reconstruction: an iterative tensorial tomographic algorithm*", Proceeding of ICO 2004 Tokyo, pp.615-616

Interferometry and Diffractive Optics

Absolute Calibration of Aspheric Null Tests (CCUPOB)

Supported by: BMBF, FKZ: 13N7861

An Adaptive Null Lens using Membrane Mirrors (METAMO)

Supported by: Landesstiftung Baden-Württemberg, Project "METAMO"

An Adaptive Phase Mask for Wavefront Coding

Supported by: Landesstiftung Baden-Württemberg, Project "Wellenfrontcodierung"

Refractive and Hybrid Microoptic Design: Minimally invasive systems for combustion analysis

Supported by: Landesstiftung Baden-Württemberg, project "Mikrooptische Systeme für die mikroinvasive, Laser-gestützte Verbrennungsdiagnostik"

Fabrication of high resolution diffractive elements by direct laser writing

–

Interferometry at different optical wavelengths

–

Absolute Calibration of Aspheric Null Tests (CCUPOB)

C. Pruss, S. Reichelt, H.J. Tiziani

The state of the art in high precision aspheric surface figure testing is the interferometric null test. In most null test configurations for aspheric surfaces a null lens is required. This is a refractive, diffractive or hybrid (both refractive and diffractive) optical element that adapts the spherical or plane wave of the interferometer to the surface under test, in such a way that the light which is normally incident onto a perfect aspheric surface is retro-reflected.

In a null test setup the null lens has to be regarded as part of the reference and needs to be calibrated. However, in contrast to standard transmission spheres there exist no general calibration method.

We have developed, to our knowledge, the first complete absolute interferometric test for aspheric surfaces that includes all errors due to the null lens. This method is based on computer generated holograms (CGH) that reconstruct multiple wave fronts.

The starting point is a new absolute calibration method for binary Fresnel zone mirrors (FZM) [1] that allows the separation of the errors, introduced by the imperfectly written FZM-pattern, from the errors of the substrate and from the interferometer errors (5 position test for FZM). The wave front error, WPD, due to the CGH-pattern distortion, ζ , can be written as:

$$W_{PD}(x,y) = -m_r \lambda_0 \zeta(x,y) \cdot \nu(x,y)$$

Here m_r is the reconstruction diffraction order, λ_0 the measuring wave length and ν the line density in the CGH. Separating the errors of the substrate from the errors of the pattern distortion is the basis for the complete absolute test of aspheric surfaces. The absolute test consists of 5 steps :

Step 1: Production of a calibration CGH ("twin CGH") that is used to replace the aspheric surface under test in the interferometric null setup – This twin CGH produces two wavefronts: (1) an aspheric wavefront that is equivalent to that produced by the aspheric surface ("null mode") and (2) a spherical calibration wavefront ("FZM-mode")

Step 2: Calibration of the twin CGH in FZM-mode using the 5 position test for FZM (see fig. (a))

Step 3: Calculation of the calibration function for the aspheric wavefront of the twin CGH using the measurements of step 2 and the known line densities of the twin CGH

Step 4: Calibration of the null setup with the known aspheric wavefront reconstructed from the twin CGH in null-mode (see fig. (b))

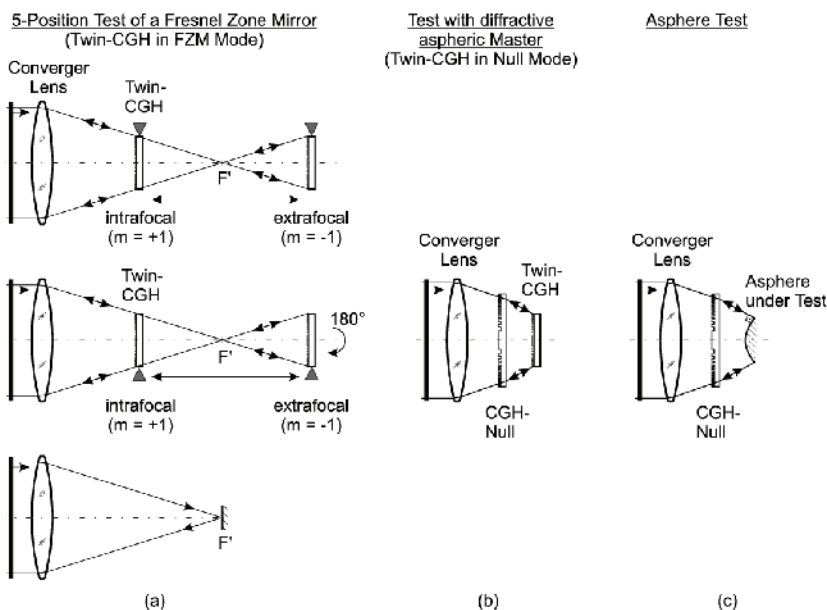
Step 5: Measurement of the aspheric surface with the calibrated setup (see fig. (c))

Of course, after the calibration procedure 1-4 has been conducted, many aspheres of the same type can be measured without recalibration, if the interferometric setup is stable.

Supported by: BMBF, FKZ: 13N7861

References:

- [1] Reichelt, S., Freimann, R. and Tiziani, H. J., "Absolute interferometric test of Fresnel zone plates", Opt. Commun. 200, 107, 2001
- [2] Reichelt, S., Pruss, C. and Tiziani, H. J., "Absolute interferometric test of aspheres by use of twin computer-generated holograms", Applied Optics, 42(22):4468-4479, 2003



An Adaptive Null Lens using Membrane Mirrors (METAMO)

C. Pruss, C. Leroux, H.J. Tiziani, W. Osten

Flexible aspheric surface testing continues to be a major topic in the optical industry. Interferometric null testing of aspheric surfaces requires a compensator element that adapts the spherical wave of the interferometer to the individual surface under test. This so called null lens might be refractive or, increasingly, diffractive as a computer generated hologram (CGH).

We are investigating a new approach for testing aspheric surfaces that avoids static, individually manufactured null lenses: an active null lens based on a computer controlled membrane mirror. It can be adapted to different aspheric shapes, thus providing much more flexibility in optical shop testing.

The concept of an adaptive null lens relies on the precise control and calibration of the active element. We use a 50 mm micromachined membrane mirror from OKO Technologies (Figure 1). The mirror is electrostatically driven. Its initial shape can be optimized with alignment screws to obtain a flat surface at 0 Volts. Our measurements show a high reproducibility of the shape of this mirror.

There are different ways to integrate the mirror into the null test setup. A setup that offers several advantages is depicted in Figure 2. In this configuration the mirror is integrated using a polarizing beam splitter and a retardation plate.

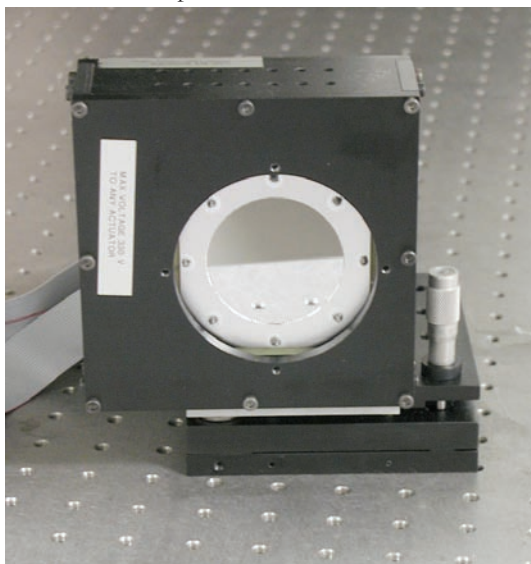


Fig. 1: Membrane mirror with a diameter of 50 mm. The mirror consists of a thin membrane (about 1 μm thickness) that is electrostatically attracted by 79 electrodes.

The mirror is used in a symmetrical way, i.e. the wave front in the test arm is reflected from the membrane mirror, to the surface under test and again from the membrane mirror, doubling the effect of the active element. Telescopes are used to relay and adjust the pupils of: the surface under test, the membrane mirror and the sensor chip. For the calibration, the retardation plate is rotated so that only the membrane mirror is observed.

The dynamic range of the membrane mirror (in terms of deflection magnitude) is given by the gap between the membrane mirror and the electrodes (up to 170 μm) and by the maximum applied voltage (up to 700 V).

The response of the membrane mirror to applied voltage can be described by the Poisson-equation for stretched membranes. For small deflections, the deflection varies to a good approximation, quadratically, with the applied voltage. For high deflections, the dependence of the gap size from the membrane deflection has to be taken into account, leading to a greater increase of the deflection. For our devices, a large deflection leads to catastrophic failure and must therefore be avoided. This restricts the usable deflection range to about 30% of the gap size.

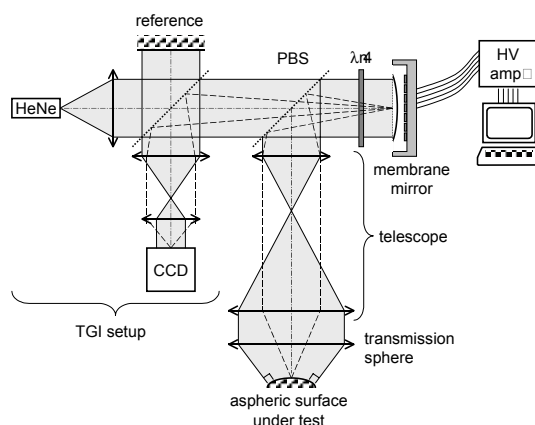


Fig. 2: Flexible interferometric null testing on the basis of a membrane mirror. The membrane mirror is integrated into the Twyman-Green interferometer (TGI) using polarizing optics.

Supported by: Landesstiftung Baden-Württemberg, project "METAMO"

An Adaptive Phase Mask for Wavefront Coding

C. Pruss, C. Leroux, H.J. Tiziani, W. Osten

In microscopy the depth of field is limited, especially for high numerical apertures. In recent years a new approach for extending the depth of field was proposed. It is based on a hybrid system, consisting of the optical system plus a numerical processing of the recorded picture. The optical system includes a phase plate that introduces aberrations (wave front coding), leading to an MTF that is almost independent of the focus position. The aberrations reduce the imaging quality of the optical system. This is compensated by the subsequent numerical processing of the image, leading to a final image with an increased depth of field.

Unfortunately, the resulting image contains artefacts that depend on the orientation and the strength of the phase plate used. We therefore proposed a variable phase mask that can be adapted to the viewed scene. This adaptive phase mask is realized with an electrostatically driven membrane mirror. Membrane mirrors offer a series of advantages for this kind of application: they introduce no chromatic aberrations, offer a smooth, non-pixelated surface profile, consume almost no electrical power, are fast (limiting frequencies up to several thousand Hertz) and offer a high reproducibility of the generated shape. They allow the adjustment of the strength and the orientation of the phase mask within milliseconds.

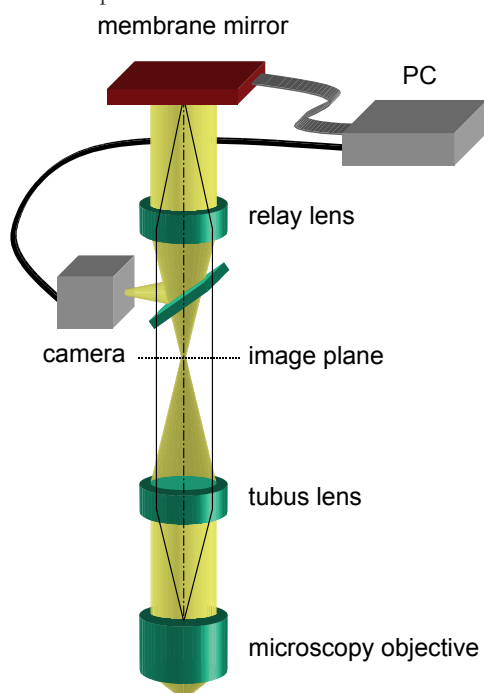


Fig. 1: Integration of the reflective adaptive phase mask into the microscopy setup – The relay lens images the pupil plane of the microscope objective onto the membrane mirror.

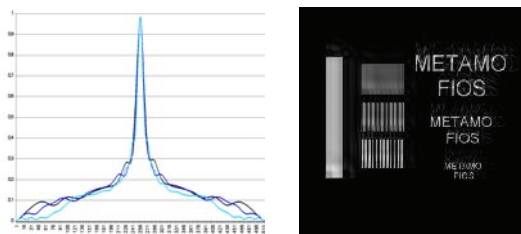


Fig. 2: Simulations of the wave front coding system based on the customized mirror. Left: MTF for three different focus positions, right: reconstructed defocused image.

The membrane mirror was specially designed for this task. It contains a customized electrode layout of 44 electrodes which are optimized for the generation of the necessary cubic wave front change of the form:

$$OPD(x,y) = \alpha (x^3 + y^3)$$

x and y are normalized pupil coordinates and α is a parameter that sets the magnitude of the cubic wave front. A typical value for α is $1.5 \cdot 10^{-6} \text{ m}^{-2}$. Membrane mirrors can be modeled, to a good approximation, as perfect, stretched membranes with fixed boundary conditions. The Poisson equation applies. In our simulations, we use a numeric, iterative method to solve this equation.

Since the boundary conditions do not allow the generation of the desired cubic shape over the whole membrane (except for the trivial case $\alpha=0$) the optical pupil diameter is required to be smaller. Our simulations showed that for a 15 mm width membrane an active optical area of 7.5 mm in diameter is a good compromise between influence of the fixed boundary and the minimum size of the electrodes that is given by the fabrication technology.

The membrane mirror is integrated into the microscopy setup with a beam splitter (see Figure 1). It is placed in a plane conjugate to the exit pupil of the microscopy objective. Figure 2 shows the first simulation results of the adaptive wave front coding system.

Supported by: Landesstiftung Baden-Württemberg, project "Wellenfrontcodierung"

References:

- [1] C. Pruss, H. Tiziani, W. Osten, T. Hellmuth, S. Rathgeb: Design eines hochauflösenden, fokusinvarianten Systems: Wellenfrontkodierung mit adaptiver Optik, DGAO Proceedings, <http://www.dgao.de/jt2004/>, 2004

Refractive and Hybrid Microoptic Design: Minimally invasive systems for combustion analysis

R. Reichle, C. Pruss, H.J. Tiziani, W. Osten, F. Zimmermann (PCI),
C. Schulz (PCI)

To optimize the combustion process in engines it is vital to get time-resolved information about fuel concentrations and temperatures. Within the scope of a joint project with PCI (Physikalisch Chemisches Institut, University of Heidelberg) new minimally invasive microoptical systems are being developed to perform these measurements in engines. In future these new sensors should speed up engine developments giving more economical fuel mixtures and cleaner exhaust gases.

For the measurement method, which is based on UV-laser induced fluorescence of tracer substances, the following systems are realized:

1.) Point measurement close to the ignition spark with a fiber optic sensor:

To perform UV-LIF spectroscopy measurements on standard engines without modifications, the combustion chamber is accessed by a modified spark plug that fulfills the dual function of ignition and microoptics sensor. The optical part performs (i) the spatially defined excitation of the tracer substances and (ii) the collection of the emitted fluorescence light.

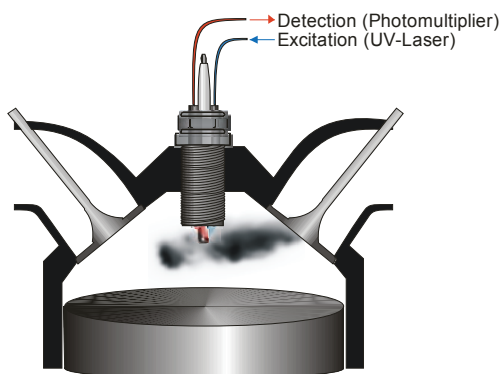


Fig. 1: Fiber optic sensor integrated in spark plug

For the design of the sensor head and its optimization both optical functions were simulated [1]. A measuring volume of a few cubic millimetres was set to average very local inhomogenities. For a simple application of the sensor the interface to the outside optics is realized with UV light transmitting fibers.

2.) 2D-Measurement of combustion parameters with refractive-diffractive (hybrid) microoptics:

For 2D UV-fluorescence measurements we are realizing a hybrid optical system adapted to the tracer concept. The system consists of excitation and observation optics. The excitation optics transform a Gaussian laser beam into a divergent light-section with top-hat profile to define the plane for the 2D-measurement.

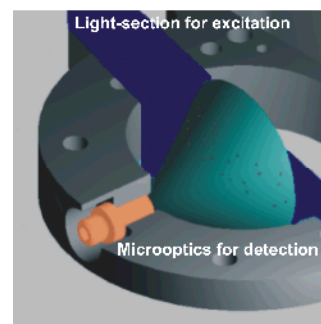


Fig. 2: Setup for the 2D-measurement

The emitted UV-fluorescence light is imaged onto a CCD-camera by a wide angle keyhole-optic. The keyhole-optic is chromatically corrected for the appropriate spectral region with the help of negative dispersion in the diffractive components. Since the phase functions of these elements can be aspherical, they are advantageous for the correction of further aberrations and thus improve the characteristics of the imaging optics.

Supported by: Landesstiftung Baden-Württemberg,
project "Mikrooptische Systeme für die mikroinvasive,
Laser-gestützte Verbrennungsdiagnostik"

References:

- [1] R. Reichle, C. Pruss, W. Osten, H. Tiziani, F. Zimmermann, C. Schulz: "Microoptical sensor for integration in a functional spark plug for combustion analysis by UV-laser induced fluorescence spectroscopy", Proc. VDI 4th Conference on Optical Analysis Technology, 2004.

Fabrication of high resolution diffractive elements by direct laser writing

C. Pruss, V. Korolkov, T. Schoder, J. Westhauser, H.J. Tiziani, W. Osten

One of the major issues that prevents the widespread use of diffractive elements in optical systems continues to be the availability of high precision diffractive elements. At the institute we maintain a long tradition of design and fabrication of diffractive optical elements – our first writing system was installed in the 1970s. In 1995 we started to produce high resolution computer generated holograms (CGH) using a direct laser writing process.

The core of our CGH fabrication is the laser writing system CLWS300, a flexible high precision tool that works in polar coordinates and is comparable to a DVD writer. This working principle offers the advantage of a high, continuous scanning speed and facilitated fabrication of rotationally symmetric structures. Yet the system is not limited to writing circles but allows to write arbitrary structures such as linear gratings, microlenses or angular scales. It is capable of writing both binary and blazed diffractive optical elements. Blazed structures are written in a grayscale mode where the writing beam intensity is varied, currently, by up to 64 levels. The substrate size can vary from a few millimeters to 300 mm in diameter and the shape can be rectangular, round or any other reasonable shape. The

system allows substrate thicknesses up to 25 mm. In 2004 we obtained a second CLWS 300 laser writing system which will serve as development system for novel writing techniques.

Binary structures are fabricated using a thermochemical process on a chromium layer that is followed by a wet etching step.

Blazed, quasicontinuous structures are written either directly into a photoresist layer or by using a grayscale mask. The exposed photoresist is subsequently processed using a low contrast developer. The resulting photoresist profile is then either used directly (e.g. for mastering) or is transferred into the fused silica substrate using dry etching (RIE).

Example applications that we have designed and developed with academic and industrial partners are:

- CGH for aspheric testing
- Custom made microlens arrays
- Beam shaping elements (e.g. Gaussian, Tophat)
- Nipkow microlens disks
- Decorative optical elements
- Master fabrication for mass replication

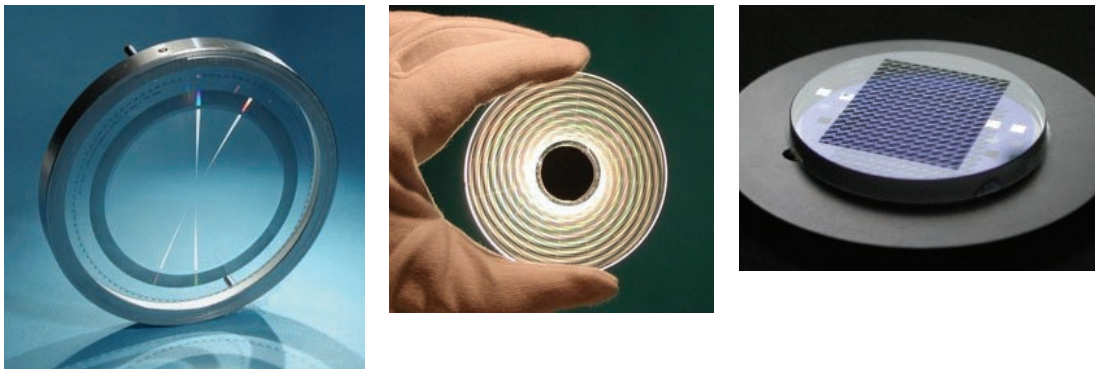


Fig. 1: Examples for diffractive elements fabricated on the laser direct writing system CLWS300. **Left:** Diffractive null lens for aspheric testing, **Middle:** microlens disk in Nipkow-arrangement, **Right:** two sided element, part of a phase shifting point source array.

References:

- [1] S. Reichelt, C. Pruss, and H. J. Tiziani "Absolute interferometric test of aspheres by use of twin computer-generated holograms" *Applied Optics*, 42(22) pp. 4468–4479, 2003
- [2] C. Pruss, S. Reichelt, V. P. Korolkov, W. Osten, and H. J. Tiziani "Performance improvement of CGHs for optical testing" *Proceedings of SPIE*, 5144, pp. 460-471, 2003

Interferometry at different optical wavelengths

C. Pruss, S. Reichelt, H.J. Tiziani

Probably the most commonly used wavelength in interferometry is the 632.8 nm line of a frequency stabilized Helium-Neon gas laser. This laser offers a long coherence length and has a known, stable wavelength with a reasonable output power of typically 1 mW.

In some cases however, this standard-laser source cannot be used. This is true e.g. for:

- Wavelength testing: the optical components need to be evaluated at the wavelengths they are designed for. One example would be the testing of IR-optics in transmission.
- Optically rough surfaces: if the roughness of the surface exceeds one half of the testing wavelength, it cannot be tested.
- Requirement for unambiguity: when measuring a single wavelength, the phase can only be determined modulo 2π . Step heights larger than half the testing wavelength cannot be measured.

We therefore operate interferometric test setups at different wavelengths ranging from 193 nm up to 10.6 μm . Among them are:

ALI 200 with Fisba $\mu\text{Phase DCI2}$: 6 inch (150 mm) interferometer of Twyman-Green type equipped with two motorized stages necessary for aspheric testing with computer generated holograms (CGH).

Kern multiple wavelength interferometer: Interferometer with selectable wavelengths, 632.8 nm, 3.39 μm and **10.6 μm** . Apertures: 80 mm and 210 mm. Suitable for measuring rough surfaces and IR-optics (see Figure 1).

Multiple wavelength interferometer: Interferometer working at three wavelengths: 632.8, 812 and 822 nm. Synthetic wavelengths up to 67 μm . Suitable for step heights measurements and aspheric testing (see Figure 2).

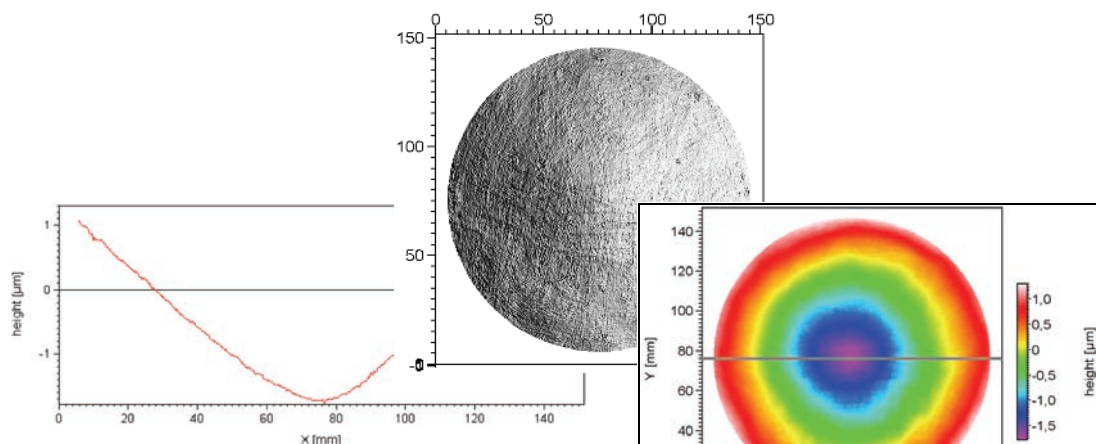


Fig. 1: Polishing carrier for semiconductor wafers – Measured for Philips Semiconductors GmbH

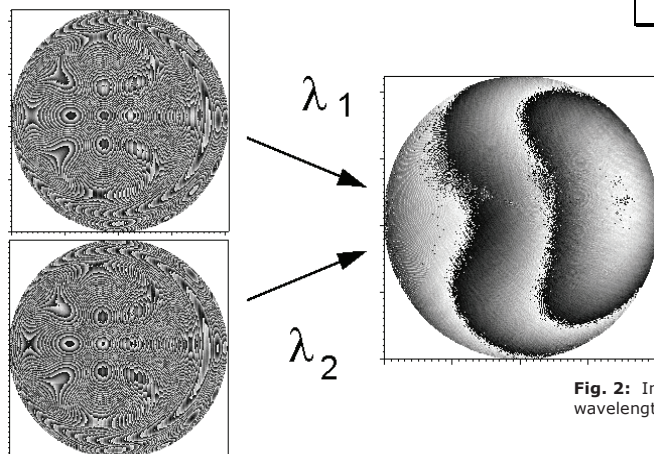


Fig. 2: Interferograms of an aspheric surface measured at two wavelengths and the resulting synthetic wavelength

Coherent Measurement Techniques

Digital holographic interferometry for the investigation of the elastic properties of bone

Project in cooperation with "The Weizmann Institute of Science" (Israel) with financial support from the "Alfried Krupp von Bohlen and Halbach Foundation"

Applications of short-coherence digital holography in microscopy

Pulsed digital holographic interferometry for endoscopic investigations (HoEnd)

Supported by: Landesstiftung Baden-Württemberg

Online surveillance of dynamical processes by using a moving system based on pulsed digital holographic interferometry

Supported by: Airbus Deutschland GmbH, Bremen

Wave front reconstruction from a sequence of holograms recorded at different planes

Supported by: Alexander von Humboldt Foundation

Compensation of unwanted deviations in Comparative Digital Holography (KOMA)

Supported by: Landesstiftung Baden-Württemberg

Digital holographic interferometry for the investigation of the elastic properties of bone

G. Pedrini, I. Alexeenko, P. Zaslansky*, W. Osten

Holography is a technique for recording and reconstructing wave fronts. Holographic interferometry allows a comparison of wave fronts recorded at different instants in time.

In recent years CCD sensors and increasing computer capabilities have enabled the development of systems such as electronic speckle pattern interferometry and digital holographic interferometry.

In this work we have shown that the digital holographic interferometry can be used for the measurement of deformation of bone. Furthermore, the fracture process of the sample can be visualised. The elastic properties of biological samples depend on their environment. It is very important to investigate the objects under natural conditions. For this reason, the investigations reported have been done by using bone samples immersed in the water. The measurement of deformation of biological samples by using optical methods is usually difficult. Due to their translucent nature, part of the light goes into the sample where it is eventually absorbed or reflected, a mechanical deformation involves a decorrelation of the microstructure, and the consequence is a decorrelation of the reflected wave front. In order to minimise this effects we recorded many digital holograms by taking care that the deformation between two successive holograms was small. The total deformation is obtained by the sum of the recorded partial deformations.

Figure 1 schematically shows the experimental set-up. Light from a laser is divided by a beam splitter (BS1) into a beam for illumination of the object and a reference beam. The object beam is carried by a fibre bundle and illuminates the object from a direction k_i . Some of the light is scattered by the object in the observation direction, k_o , towards the detector, where a positive lens forms an image of the object on a CCD sensor. An image-plane hologram is formed on the CCD as a result of the interference between the reference beam and the object beam. The aperture (AP) serves to limit the spatial frequencies of the interference pattern. A single mode optical fibre carries the reference wave. The use of fibres for illuminating the object and for the reference makes the arrangement more compact. A beam splitter BS2 is used to recombine object and reference waves on the detector. The beam splitter is adjusted in order to have a small angle between the object and reference beams.

The fringes formed by the interference between the reference and object wave need to be resolved by the sensor.

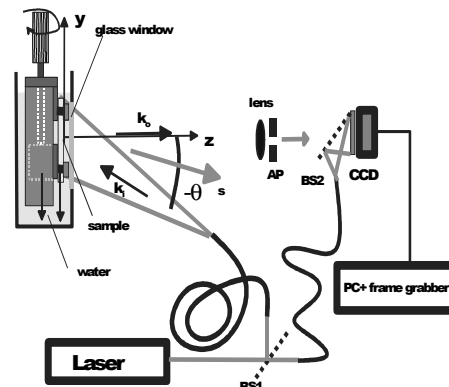


Fig. 1: Arrangement for the 1D measurement of bone deformations by using digital holography

The complex amplitude of a wave front reflected by an object, that is subjected to a dynamic deformation, is a function of time. Consider now the case where a sequence of K digital holograms of an object undergoing deformation are recorded. Each hologram is then processed individually by taking the Fourier transform of the recorded intensity, filtering and inverse Fourier transformation. By using this procedure (Fig. 2) the complex amplitude of the wavefront is obtained.

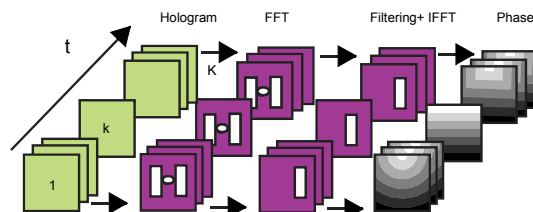


Fig. 2: Procedure for calculating the phase from a sequence of digital holograms

For each hologram, the phase of the wavefront is calculated, thus, we are able to utilize the recorded hologram intensity to obtain the phase at the time t . The phase map corresponding to the deformation of the object between the beginning of the experiment ($t=0$) and the time t can therefore be calculated by summing the phase differences.

A piece of antler immersed in water was loaded in tension by using a special device. The camera used had 690×480 pixels with an acquisition rate of 30 frames/second.

We used a 100 mW Nd:YAG with a wavelength of 532 nm. The measurements were performed within a 4 sec period (during this period the sample was loaded), and 120 holograms (30 per second) were recorded. Figure 3 shows the results of the object deformation at two different times after the

beginning of the loading process. On the left side of the bone sample (close to the notch) we see that the fringes of the phase map have a higher density of fringes. This is the part where the bone will break.

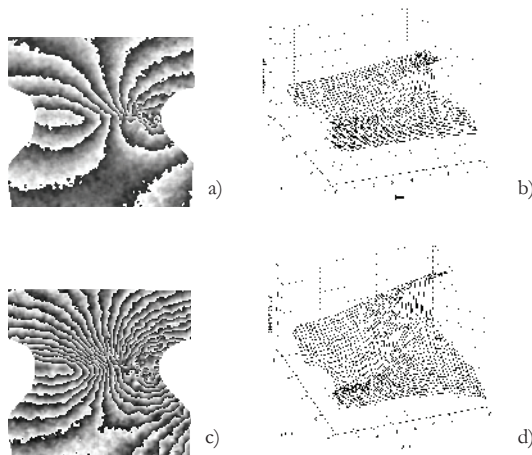


Fig. 3: Deformation of a notched piece of bone immersed in water at two different time (0.5 and 1.5 seconds after the begin of the loading process). **a)**, **c)** are the phase maps and **b)**, **d)** are the corresponding deformations.

The method presented above provides information on the deformation of the sample as a function of time, but along one direction only. In order to have more information about the object deformation, we modified the setup. Two Nd:YAG laser sources and two cameras have been used in the experiment. The object is illuminated from two different directions and two sensors acquire the information about the deformation from two sensitivity directions. The separate sensitivity vectors make it possible to calculate the in-plane and the out-of-plane deformation. The use of two independent sources prevents cross interference and allows each sensor to only record the interference between the reference wave and the desired wavefront reflected by the sample. Figure 4 shows a result of the deformation of a bone. The phase maps have been unwrapped and combined in order to obtain the deformation along the observation direction (out of plane, z-axis) and in-plane (along the loading direction y).

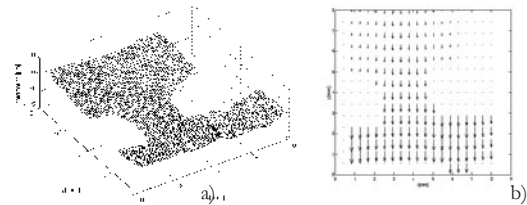


Fig. 4: Deformation of a bone. Pseudo 3D representation of the out of plane deformation **(a)**, in plane "arrow representation" of the deformation along the y direction **(b)**.

It is technically possible to add a third sensor and third illumination system to allow the simultaneous recording of the deformation along a third sensitivity vector. This can be useful when all the three components of the deformation need to be measured.

It was possible to show that the speed of deformation just before the occurrence of a fracture is very high. By using the instrument described in this paper, it was not possible to visualise the deformation at the instant of the fracture, in order to solve this problem, we will use high speed acquisition sensors for future experiments.

* P. Zaslansky is with the Weizmann Institute of Science (Israel)

Project in cooperation with "The Weizmann Institute of Science" (Israel) with financial support from the "Alfried Krupp von Bohlen and Halbach Foundation"

References:

- [1] Zaslansky, P., Pedrini, G., Alexeenko, I., Osten, W., Friesem, A., Weiner, S., Shahar, R., "Static and dynamic interferometric measurements used to determine mechanical properties of cortical bone", in: Advances in Mechanics, edited by Carmine Pappalettere, pp. 76-77, McGraw-Hill, Milano, 2004
- [2] Alexeenko, I., Pedrini, G., Zaslansky, P., Kuzmina, E., Osten, W., Weiner, S., "Digital holographic interferometry for the investigation of the elastic properties of bone", in: Advances in Mechanics, edited by Carmine Pappalettere, pp. 458-459, McGraw-Hill, Milano, 2004
- [3] Pedrini, G., Alexeenko, I., Zaslansky, P., Osten, W., Tiziani H. J., "Digital holographic interferometry for investigations in biomechanics" 8th International Symposium on Laser Metrology Macro-, micro-, and nano-technologies applied in science, engineering, and industry, February 14 – 18, 2005 Merida, Yucatan Mexico

Applications of short-coherence digital holography in microscopy

G. Pedrini, L. Martínez-León, W. Osten

Holography has proved to be a convenient method to store and reconstruct the complete amplitude and phase information of a wave front. Since the technique was invented by Gabor, extensive research has been performed on holography, to overcome the original limitations and to develop many of its applications, particularly in microscopy. In the early years of holography, the processes of recording a hologram and its reconstruction were tough and time consuming, as the former step normally involved chemical development of photographic plates. Nowadays, thanks to CCD sensors and to modern computer resources, both processes can be performed in a very short time by means of digital holographic procedures. Thus, a hologram, the interference pattern between one wave front of interest and an auxiliary reference wave, can be captured and stored digitally, and then numerically reconstructed by a computer.

Digital holography has been broadly applied to microscopy. Current research focuses on improving imaging techniques. In other studies of digital holographic microscopy, developments of particular applications, for example shape measurement, are made. Several imaging techniques, such as coherence radar or digital light-in-flight holography take advantage of low temporal coherence to examine three-dimensional objects. A combination of digital holography and short coherence interferometry provides high-resolution cross-sectional images of the microstructure of material and biological samples. Short coherence holography allows optical sectioning, the ability to discriminate light coming from different planes within a sample. Besides, digital reconstruction allows a straightforward reconstruction of each plane. The selection of the plane of interest can be simply performed by mechanical shifting of a mirror in the experimental set-up. Some advantages of this method over other imaging techniques allowing optical sectioning, like confocal microscopy or OCT, are the simplicity of the optical arrangement and the possibility to record at once the whole information about the plane of interest, without any need of lateral scanning.

Our set-up is a variation of the Mach-Zehnder interferometer, and is shown in Fig. 1. The interferometer contains three beam splitters. The first one splits the light emitted by a short coherence laser into the reference and the object beams. In the object arm of the interferometer, light is conveyed towards the sample by means of two fixed mirrors and a second beam splitter, which in addition combines the light reflected by the object with the light from the reference

arm. The third beam splitter, included in the modified Mach-Zehnder interferometer, deviates the reference beam through a delay line, where the optical path length of that arm is made approximately equivalent to the path of the object arm. Besides balancing the optical path lengths, this part has also the role of integrating a moving mirror within the set-up. The moving mirror is required by the phase-shifting technique and the axial scanning of the sample. An in-line set-up is employed, where the phase is obtained by temporal phase-shifting.

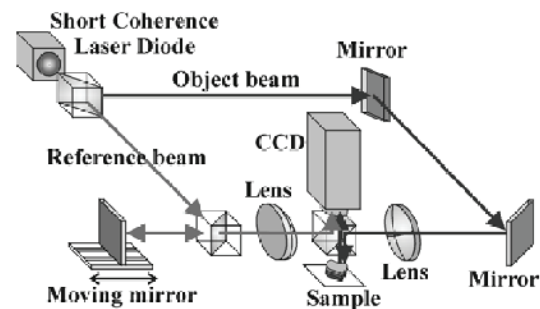


Fig. 1: Experimental set-up

When the object beam illuminates the sample, only the light reflected by certain points of the specimen can interfere with the reference onto the CCD camera. At these points, the overall optical path lengths of the reference and the object beams are matched within the coherence length of the laser. In order to select the depth of the sample to be imaged, the moving mirror placed in the reference arm of the interferometer permits the adjustment of the optical path. To measure the whole volume of our sample, a sequence of holograms must be acquired. In each recording, the position of the mirror in the reference arm is shifted precisely, and in this manner, the optical path between reference and object beams is matched. The set of reconstructed images corresponding to different planes of the object offers a complete description of its 3D structure, with an axial resolution depending on the coherence length, or equivalently, on the spectral width of the source. No lens is required in the imaging step. However, a system of lenses is introduced for focusing the beam in both reference and object arms. With the help of microoptical elements or an optical fiber, a compact set-up can be built.

We have investigated different sorts of biological samples. In Fig. 2, we present the images of different layers in a fly. The diagram shows the part of the insect that has been imaged. Several holograms from different depths of the fly have been recorded. The pictures

illustrate the optical sectioning. They show the contour of the fly at a certain level, with an interval of 0.1 mm between each image. The set of images presented allows the reconstruction of the 3D insect shape.

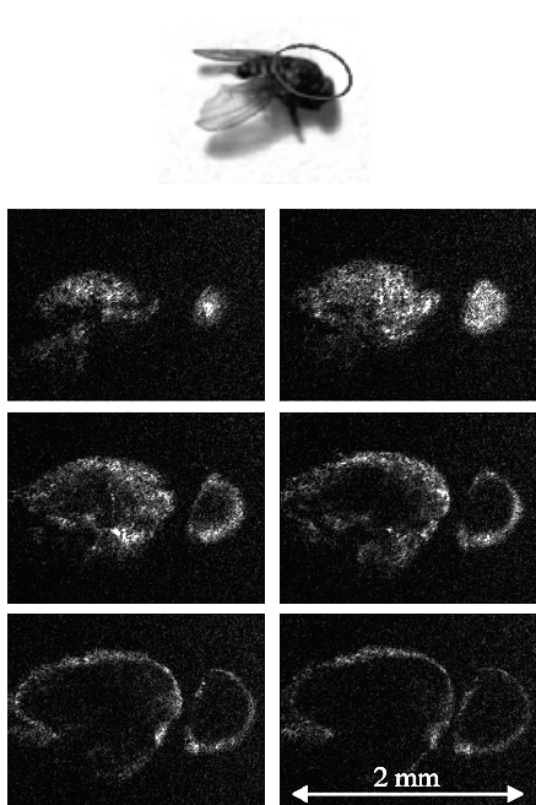


Fig. 2: Reconstructed images of a fly

In Fig. 3, a different kind of biological sample has been studied. Images taken from a bone, a piece of deer antler, are shown. As can be seen in this figure, a clear image is obtained from the top surface of the bone (with the moving mirror at its original position, 0 μm). Some details, like a big hole, can be observed. However, as we enter the sample, by moving the mirror about two hundred micrometers, the image is not as sharp as before. Again, only wave fronts coming from inside the object whose optical path length matches the reference will interfere. But, inside the volume sample, the bone absorbs, scatters and diffracts the light, preventing a clear image of the inner layers.

Since, inhomogeneities in the refraction index, absorption, multiple scattering, diffraction, or even a change in the coherence properties of the light, may influence the optical path inside the sample, actually, light might come from different sample depths. We can only assure that light arriving from

the surface, from the points reflecting light, matches the reference optical path to within the coherence length of the laser. All these effects that modify the behavior of light inside a biological sample, and produce the lack of definition which is clearly observed in the deepest layers, are included in the so-called "sample-induced aberrations". This is a common problem for all the methods of obtaining accurate and high resolution images, for instance, from a volume biological sample or a thick tissue.

A method for compensating such aberrations is under investigation.

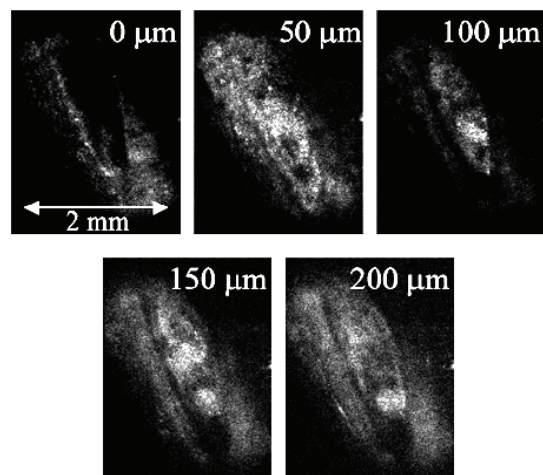


Fig. 3: Reconstructed images of a bone.

References:

- [1] Pedrini, G., Schedin, S., "Short coherence digital holography for 3D microscopy", *Optik*, Vol. 112, No. 9, S. 427-432, 2001
- [2] Martinez-Leon, L., Pedrini, G., Osten, W., "Short-coherence digital holography for the investigation of 3D microscopic samples" *Proc. SPIE*, 2004
- [3] Martinez-Leon, L., Pedrini, G., Osten, W., "Applications of short-coherence digital holography in microscopy", *Appl. Opt.*, 44, 2005
- [4] G. Pedrini and H. J. Tiziani, "Short-coherence digital microscopy by use of a lensless holographic imaging system", *App. Opt.* 41, 4489-4496, 2002

Pulsed digital holographic interferometry for endoscopic investigations (HoEnd)

G. Pedrini, I Alexeenko, W. Osten

Holographic interferometry combined with endoscopy enhances the versatility of standard 2D-endoscopic imaging as it opens up the possibility of measuring additional parameters, on hidden surfaces. Combinations of digital holography, with an endoscope for transferring the image, and a pulsed laser, as a light source, allows measurements in an industrial environment (e. g. vibration measurements, non destructive testing of technical objects) and in-vivo investigation of biological tissues. It might be useful for the detection of pathology in medicine.

Figure 1 shows schematic illustrations of rigid and flexible endoscopes combined with a system based on pulsed holographic interferometry. The optical set-up consists of the pulsed laser, the interferometer unit with the CCD-camera and the endoscope unit. Figure 1.(a) shows the arrangement for a rigid endoscope but this endoscope can be replaced with a flexible fibre endoscope, as shown in figure 1.(b). Rigid and flexible endoscopes have a lot in common. The objective lens forms an image of the subject which in turn is transferred by the relay optics and magnified by a lens system onto the sensor. The difference is in the relay itself. To allow flexibility the image is carried by a bundle of optical fibers, instead of a system of lenses as for the rigid endoscopes. The resolution of a flexible endoscope depends on the number of fibers and their diameter. More fibers of smaller diameter give higher resolution.

For both arrangements, the recording procedure and the way to process the digital holograms is exactly the same. The pulsed laser emits short (20 ns) Q-switched pulses, which are divided at the beam-splitter into the reference and the object beams. The reference beam is conveyed to the interferometer unit with a single-mode optical fibre. The object beam is coupled into a fibre bundle and conveyed to the object. Our endoscopes (the rigid and the flexible), are provided with an adapter for coupling the illumination beam. The diverging output beam illuminates the object, the light is diffusely reflected back from the object surface towards the endoscope, which brings the object image to the interferometer unit. An image-plane hologram is formed on the CCD-detector as a result of the interference between the slightly off-axis reference beam and the object beam. The aperture serves to limit the spatial frequencies of the interference pattern, in such a way that the detector resolves it. The dimensions of the aperture are chosen by considering the resolution

of the CCD-detector pixel size and the distance between the aperture and the sensor. Two or more digital holograms, corresponding to different laser pulses, are captured on separate video frames by the CCD-camera.

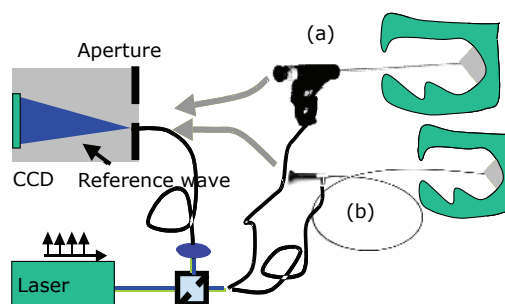


Fig. 1: Set-up with (a) rigid and (b) flexible fiber endoscope for investigations using pulsed digital Holography

We used our system to measure inside an industrial pump. At one side of the pump there are some ports where the endoscope was inserted in order to look at and to measure the vibration of the mechanical parts located inside. Figure 2.b) shows a white light image of the inside of the pump. On the right hand side of Fig. 2.b) we can see the piston. During the pumping operation, the piston is moving forward and backward at a frequency of 50 Hz. Two digital holograms were recorded, with a pulse separation of 50 μ s. Figure 2.c) shows one phase map obtained after subtraction of the phases of two holograms between the two exposures. On the right hand side of the piston there are more fringes. This means that the piston is moving more compared with the other areas around. This example shows that by using the endoscopic technique it is possible to look inside a more or less closed object and investigate vibrating parts.

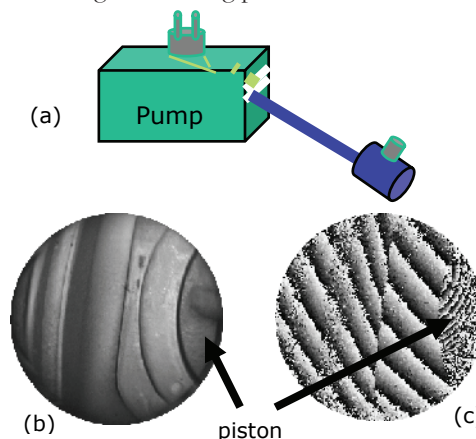


Fig. 2: Measurements inside a pump (a), Image of the object (b), Phase map obtained during the pump operation (c)

We also tested the dynamic deformation of in vivo biological tissues. The problem with measurements of biological tissues is that the reflectivity is not ideal and furthermore that any disruption of the biological tissue produces, in addition to producing the the deformation, causes alterations in the microstructure of the surface. Consequently, the correlation between the holographic patterns recorded with the two laser pulses is reduced, resulting in noise in the fringe patterns and poor image quality. Figure 3 shows phase maps obtained from measurements performed inside the oral cavity (in vivo) using a rigid endoscope.

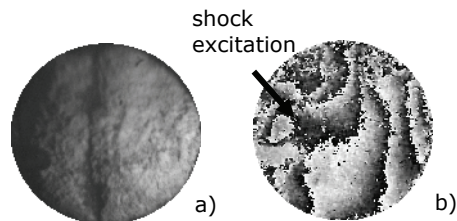


Fig. 3: In vivo investigation inside the oral cavity. **a)** Image of the investigated part (tongue). **b)** Phase map corresponding to the deformation produced by a shock excitation of the tongue

We have found that in order to measure at hidden surfaces, we can combine commercially available endoscopes with an interferometer based on digital holography. Recently, with the newer smaller CCD detector arrays, it has become possible to build the complete interferometric system (CCD included) with small dimensions. Figure 4 shows a picture of our prototype. The chip has 659×494 pixels (pixel size $7.4 \times 7.4 \mu\text{m}^2$). The sensitive area is quite small ($4.8 \times 3.6 \text{ mm}^2$) but the sensor is inserted on a mount which has much larger size ($12 \times 13 \text{ mm}^2$), in effect limiting the size of our holographic head to a diameter of 18 mm. This can be used to investigate objects which can be reached from small access holes. The prototype shown in figure 4 has been used to perform measurements inside a cavity, as shown in figure 5. A pulsed Nd:YAG laser was used for these measurements.

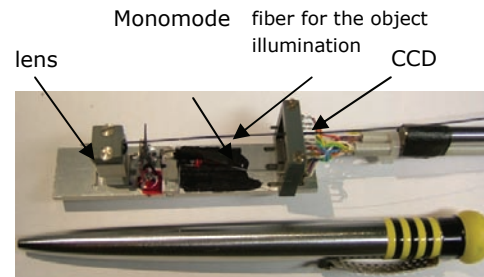


Fig. 4: Image of the prototype built at our Institute, diameter of 18 mm

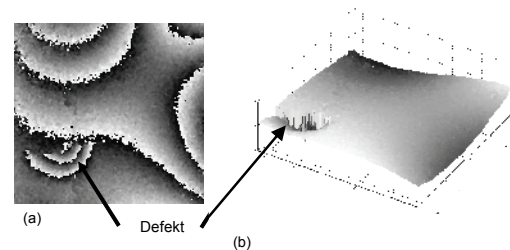


Fig. 5: Vibration measurement of an object with a defect. Vibration frequency 2350 Hz. Phase map **(a)**. Pseudo 3D representation of the vibration **(b)**

Supported by: Landesstiftung Baden-Württemberg

References:

- [1] G. Pedrini, I Alexeenko, W. Osten, H. J. Tiziani, "Temporal phase unwrapping of digital hologram sequences", Appl. Opt. 42, pp. 5846-5854, 2003
- [2] S. Schedin, G. Pedrini, H. J. Tiziani, "A comparative study of various endoscopes for pulsed digital holographic interferometry", Applied Optics-OT, Vol. 40, Issue 16, pp. 2692-2697, June 2001
- [3] G. Pedrini, M. Gusev, S. Schedin, H. J. Tiziani, "Pulsed digital holographic interferometry by using a flexible fiber endoscope", Optics and Laser in Engineering 40, pp. 487-499, 2003
- [4] G. Pedrini, I Alexeenko, H. Tiziani, "Pulsed endoscopic digital holographic interferometry for investigation of hidden surfaces", Proc. SPIE Vol. 4933, pp. 123-128, 2003
- [5] G. Pedrini, I Alexeenko, W. Osten, "Gepulste digitale Holografie für Schwingungsmessungen an schwer zugänglichen Oberflächen", Technisches Messen, 3, pp. 172-179, 2005

Online surveillance of dynamical processes by using a moving system based on pulsed digital holographic interferometry

G. Pedrini, I. Alexeenko, U. Schnars*, W. Osten

For online surveillance of dynamical processes like laser welding and friction stir welding (see Fig.1), we need a system which moves at a certain speed and measure the deformations of a surface submitted to a loading. The measurement of inhomogeneities on the deformation of the surface should allow controlling online the quality of the soldering and eventually driving the system in order to correct the soldering defects.

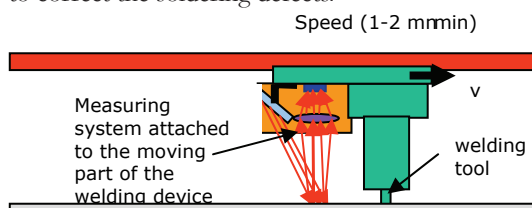


Fig. 1: Optical arrangement fixed to the moving platform

In cooperation with Airbus Bremen we developed a method based on pulsed digital holography for measuring the deformation of an object by using a system which moves at a speed of some metres/minute.

Figure 2 shows a sketch of the measuring system used for our investigations. Light from a laser is divided into a beam for illumination of the object and a reference beam. The object beam illuminates the object along a direction k_i . Some of the light is scattered by the object in the observation direction k_o towards the detector, where a positive lens forms an image of the object on a CCD sensor. An image-plane hologram is formed on the CCD as a result of the interference between the reference beam and the object beam. The aperture serves to limit the spatial frequencies of the interference pattern. A single mode optical fibre carries the reference wave. A beam splitter is used to recombine object and reference waves on the detector. The beam splitter is adjusted in order to have a small angle between the object and reference beams for the introduction of the spatial carrier. This allows the quantitative evaluation of the phase. We consider now the case where the optical measuring system is fixed to a moving device, as shown in Figure 1, and is used for measuring of dynamical deformations of the surface. The movement of the measuring head has two consequences on the phase and intensity of the recorded object:

- displacement of the object image on the CCD
- linear phase change of the wavefront reflected by the object surface

These effects of the image shift and linear phase

shift may be compensated. Holograms are recorded at a frequency of 20 Hz and the phases of the wavefronts are calculated. Each wavefront is compared with that one recorded with the precedent pulse. After compensation of the unwanted effects due to the movement, we get a phase map which contains only the information concerning the deformation of the object surface in the interval between two exposures.

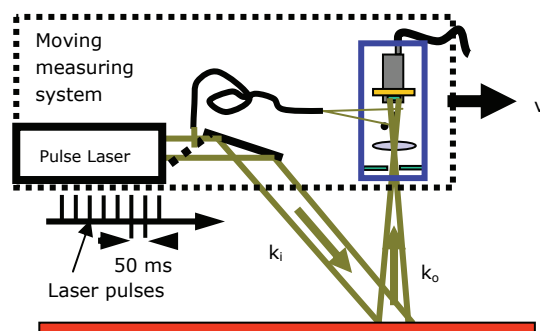


Fig. 2: Optical arrangement for pulsed digital holographic interferometry

We started our investigation by measuring the deformation of a thin metal plate ($60 \times 100 \times 0.5 \text{ mm}^3$) submitted to vibration (Fig. 3 a). A shaker was used to excite the plate at one of its vibration mode (1385 Hz). The angle between the illumination and observation direction was only few degrees, this means that we measure out of plane deformations. The table carrying the measuring head moves with a speed of approximately 1.2 m/minute (20 mm/sec). The laser emits pulses with a frequency of 20 Hz and a sequence of 100 digital holograms is recorded within 5 seconds ($100 \times 50 \text{ ms}$). Between two subsequent pulses (pulse separation 50 ms), the moving table displacement is 1 mm. From two holograms, we calculate at first the shift produced on the CCD chip by using the correlation method, we compensated the shift and the unwanted change of phase. The compensated fringes phase map calculated from two holograms taken at different times is shown in Fig. 3 b). Fig. 3 c) shows a phase map obtained when the measuring system is not moving. The quality of 3.c) is slightly better (less noise), compared with 3.b). The reduced quality of the phase map obtained from the measuring head moving at a speed of 1.2 m/min is due to two factors. If we consider the moving measuring head and the fact than two successive holograms are taken with the head at different position, it is apparent that:

- 1) the speckle pattern coming from the object and entering the aperture is not exactly the same for the two exposures (consider that the speckle pattern is stationary and the aperture moves e. g. 1 mm)
- 2) due to the shift between the two exposures, the two holograms (speckle patterns) to be compared are recorded on different area of the CCD sensor. The reflections produced by the glass covering the sensor introduce some unwanted effects.

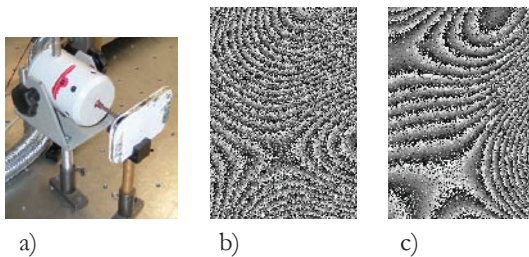


Fig. 3: Plate vibrating at 1385 Hz observed by moving head, (field investigated: $21 \times 29 \text{ mm}^2$). **a)** object, and shaker, **b)** Phase map obtained after compensation of the movement (1.2 m/min, $\Delta L=1 \text{ mm}$). **c)** Phase map obtained in the case that the measuring head is not moving.

A simulation of what happens during the welding process is given by thermal loading. We used two pieces of lead (see Fig. 4 a), and heated them by using a gas flame until some parts began to melt together (melting point $327.5 \text{ }^\circ\text{C}$). We recorded a sequence of holograms of the object during the cooling process with the measuring head moving at a speed of 1.4 m/min. Four phase maps corresponding to the deformation of the object during the melting process are shown in Figs. 4 b-e. At the centre of the phase map we see a lot of noise, this is due to the fact that in this part (where the two piece of lead are thinner), we had a large deformation and thus a lot of fringes which cannot be resolved.

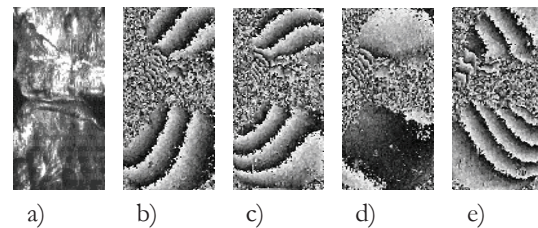


Fig. 4: Object submitted to thermal loading observed by moving head (1.4 m/min) **a)** image of the lead object, (field investigated: $21 \times 29 \text{ mm}^2$) **b-e)** 4 of the 100 phase maps obtained during the cooling process

**U. Schnars is with Airbus Deutschland*

Supported by: Airbus Deutschland GmbH, Bremen

Wave front reconstruction from a sequence of holograms recorded at different planes

G. Pedrini, Y. Zhang*, W. Osten

If the amplitude and the phase of a monochromatic wave front are known at a certain plane, it is possible by using the law of propagation to calculate the object wave front at a given distance from that plane. The problem that remains to be solved is how to obtain the complex amplitude of a wave field since it is well known that the detectors are not sensitive to the phase (the phase information is lost during the recording process).

One way to get the complex amplitude of a wave front is to overlap it to it with a reference wave and to use a detector to record the interference produced by that two waves (holography). During the last 10 years there has been an impressive development of techniques where the holograms are recorded on electronic devices (CCD, CMOS) and then digitally reconstructed (digital holography).

Even without a reference wave (as is the case in holography), from the 3D intensity distribution it is possible to get the information about the amplitude and phase. In the last years many investigations have been made with the purpose of reconstructing amplitude and phase from the intensity pattern only (in this case no reference is added to the wave front). Gerchberg-Saxton and Yang-Gu algorithms are iterative methods, which allows us to get the phase information if the intensity is known at a certain plane, and we have some additional information about the object wave front in another plane (e. g. pure amplitude object, or pure phase object). Recently it was shown that by recording two or more intensity patterns of the object at different positions and by application of iterative algorithms, it is possible to avoid the assumption of a pure absorptive or a pure phase object.

We propose a method for phase retrieval, where we increase the number of intensity patterns recorded and we decrease the complexity of the iteration procedure. The recording arrangement is shown in Figure 1. It may be used in transmission or reflection. We consider here a transmitting object, which may be an amplitude or phase object, illuminated by coherent light. The light diffracted is recorded on a CCD or CMOS sensor that at first is located at the distance z_0 from the object. After this recording we move the sensor by Δz and we record the intensity I_1 , we continue this procedure until $n+1$ interferograms are acquired.

The distances z_0 and Δz and the numbers of interferograms ($n+1$), need to be chosen according to the size of the object investigated. We will con-

sider here only small objects (several mm); In this case z_0 and Δz will be typically in the mm range. The phase of the wave front is obtained by processing the recorded intensities using following procedure:

- 1) the amplitude A_0 is calculated by taking the square root of the intensity I_0 . A constant phase ($\phi_0=0$) is assumed and a propagation of the wave front $A_0 \exp\{i\phi_0\}=A_0$ from z_0 to $z_0+\Delta z$ is calculated using the diffraction relationship. This operation gives us a complex amplitude having a phase of ϕ_1 .
- 2) The term $\exp\{i\phi_1\}$ is combined with the square root of I_1 (A_1) to form a new estimate of the complex amplitude. A propagation of $A_1 \exp\{i\phi_1\}$ from $z_0+\Delta z$ to $z_0+2\Delta z$ is calculated.
- 3) The same procedure is repeated for all the other interferograms until I_n . After this we get the phase ϕ_n at $z_0+n\Delta z$.

During this procedure, the phase of the object wave front is adjusted step by step. The reconstruction of the wave front from one plane to the next is calculated by the Rayleigh-Sommerfeld relationship.

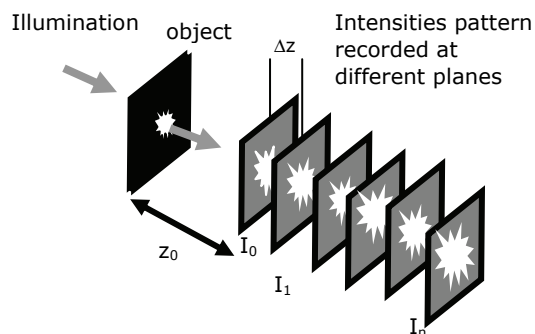


Fig. 1: Recording arrangement

In order to test the proposed method, we used at first a simulated pattern. Figure 2.a shows the input object used for the simulation. This looks like an amplitude object but in order to make the simulation more complicated and closer to reality, we added a random phase noise in the range $0-1.5\pi$ different for each pixel. For the simulation 1024×1024 pixels have been used. The wavelength used was 532 nm and the pixel size $6.7 \mu\text{m}$. The intensity was calculated at different distances from the object in intervals of 10 to 50 mm. The distance between two successive interferograms was $\Delta z=1$ mm. From the intensities $I_0 \dots I_n$, and by using the method described above, we simulated the phase retrieval. Figures 2.b-d show the reconstructions of the object obtained after 1, 3, and

20 application of the phase adjustment. To obtain Fig. 2.b, we just took the square of the intensity of I_0 (recorded at z_0), performed a propagation until the plane $z_0+\Delta z$ was reached to get ϕ_1 , multiplied $\exp(i\phi_1)$ by the square root of I_1 , and finally used this first approximation of the wave field reconstruction of the object to back propagate from the plane $z_0+\Delta z$ to the object plane ($z=0$). This first approximation do not give a clear image of the object, but by applying the procedure further and use the other recorded intensities we get a better phase adjustment and thus better reconstructions as shown in Figs. 2.c-d. Some investigations have been carried out in order to test the convergence of the technique. We found that with n increasing the quality of the reconstructed wavefield increases. This can be understood if we consider that when the number of interferograms used increases, more information is used to retrieve the phase; therefore, the recovered wave fields will be closer to the physical value. This is valid until a certain value of n . Afterwards if we record more interferograms, due to the size limitation of the detector, the quality of the reconstructed wave fronts will decrease. Investigations are in progress in order to theoretically determine the convergence of the proposed method.

An experiment has been carried out in order to verify the simulations. A transmission mask, see Fig. 3.a), was illuminated by a collimated beam with a wavelength of 532 nm (from an Nd:YAG laser). The diffraction intensities pattern were recorded by using a CCD camera having a pixel size of 6.7 μm (Teli CS 3910) and 1300 \times 1030 pixels from which only 1024 \times 1024 were used for the wave front calculation. At the beginning of the experiment, the distance, z_0 , between the mask and the sensor was 10 mm.. The CCD was translated in steps of $\Delta z=1$ mm, from z_0 to $z_0 + n\Delta z = 10 + 20 = 30$ mm, ($n=20$) at each step the intensity pattern was recorded. From the 21 intensity patterns it was possible to calculate the phase using the method described previously. From the amplitude (directly calculated from the recorded intensity) and the phase (obtained after phase retrieval) it was possible to reconstruct the focused image of the object. The result is shown in Fig. 3.b).

The advantage of this approach is that no reference wave is required when the interferograms are recorded and no time consuming iterative algorithms are used for the reconstruction. The method could be used to reconstruct the phase of wavefronts having shorter wavelength e. g. UV and X-rays.

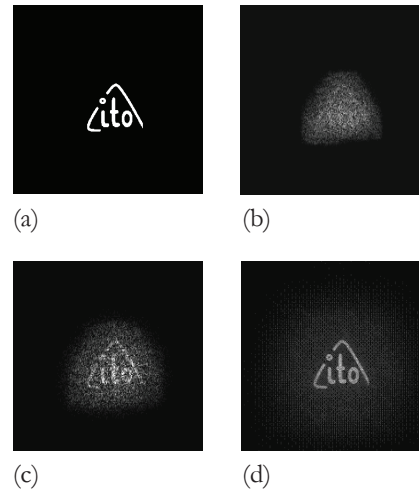


Fig. 2: a) Original image used for the simulation, b)-d) reconstructions of the object obtained after 1, 3 and 20 applications of the phase adjustment.

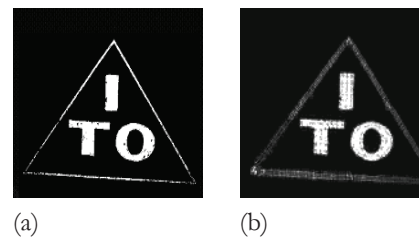


Fig. 3: a) Original mask used for the experiment b) Reconstructions of the object.

*Y. Zhang was supported by the Alexander von Humboldt Foundation

References:

- [1] Zhang, Y., Pedrini, G., Osten, W., Tiziani, H. J., "Image Reconstruction for In-Line Holography with the Yang-Gu Algorithm", Appl. Opt, 42, 6452, 2003
- [2] Zhang, Y., Pedrini, G., Osten, W., Tiziani, H. J., "Reconstruction of in-line digital holograms from two intensity measurements", Opt. Lett., 29, 1787, 2004
- [3] Zhang, Y., Pedrini, G., Osten, W., Tiziani, H. J., "Applications of fractional transforms to object reconstruction from in-line holograms", Opt. Lett., 29, 1793, 2004
- [4] Zhang, Y., Pedrini, G., Osten, W., Tiziani, H. J., "Whole optical wave field reconstruction from double or multi in-line holograms by phase retrieval algorithm", Optics Express, Vol. 11, 3234, 2003
- [5] G. Pedrini, W. Osten, Y. Zhang, "Wave front reconstruction from a sequence of interferograms recorded at different planes" Opt. Lett. 30, 833-835, 2005

Compensation of unwanted deviations in Comparative Digital Holography (KOMA)

X. Schwab, G. Pedrini, W. Osten

In industry there is an important need for measuring systems for the comparison and testing of technical objects with rough surfaces. Classical interferometry allows only the investigation of smooth surfaces. Therefore at ITO we are developing and implementing a new coherent optical technique for the comparison of the shape or deformation of two nominally identical objects which have rough surfaces (master-sample-comparison). We use the technique of Comparative Digital Holography (CDH), a combination of the principles of Digital Holography (DH) and Comparative Holography (CH). Using this method it is not necessary that both samples are located at the same place and consequently remote shape or deformation comparison between a master and a sample become possible [1].

To compare the shape, or the deformation, between a master and a test object with rough surfaces [2], double exposure of both objects and a numerical calculation of the related phase differences are needed. In contrast to the well known incoherent techniques based on inverse fringe projection, this new approach uses a coherent mask that is imaged onto the sample object, which has a different microstructure. The coherent mask is created by DH to enable immediate access to the complete information about the master object at any location. The availability of this complete optical information as a digital hologram allows comparison of both the shape and the deformation of sample objects which have different microstructures. The innovative aspect of CDH is the projection of the conjugated wave front of the master onto the sample using a liquid crystal modulator (LCD). This wave front can be considered similar to a coherent mask. The arrangement that is used to compare master and test object is shown in Fig. 1.

A transmission of the hologram to a different location can be done via a data network. At the new location, the hologram is fed into an LCD and a laser is used to read out the hologram and reconstruct the conjugated wave front of the master object, Fig. 1 (b). The wave front illuminates the sample object from the direction of observation during the recording of the master object. The new observation position of the sample object is from the direction where the master object illumination originated. Consequently, the resulting reconstruction of the second hologram indicates directly the difference between master and sample object.

One problem is the mutual positioning of the sample and master object. To minimize unwanted

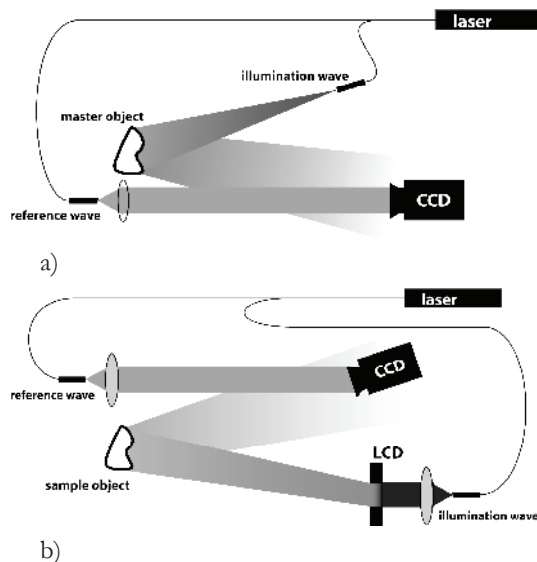


Fig. 1: Schematic representation for the experimental setup for the CDH. **a)** Recording of the hologram of the master object. **b)** Coherent illumination of the sample with the conjugated wave front of the master.

deviations between the reconstructed wavefront of the master object and the sample object, an artificial phase-shift of the reconstructed master wavefront can be generated. This phase-shift is induced by the liquid crystal modulator.

We present first the simulation of a shape difference measurement. As a master object, we simulated a pyramid with one surface microstructure and for the sample object, we simulated a pyramid containing 4 defects with a different surface microstructure. The result of the CDH simulation of the shape difference measurement between the two pyramids in Fig. 2 is shown in Fig. 3. The defects are clearly visible and quantifiable without having the need for extensive image processing after digital reconstruction of the holograms.

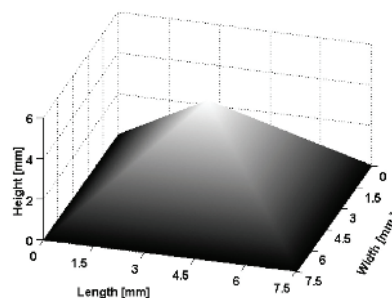


Fig. 2 a): Simulated master object for the CDH

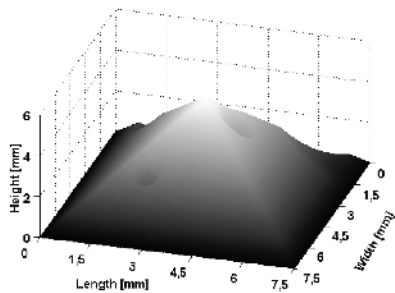


Fig. 2 b): Simulated sample object for the CDH

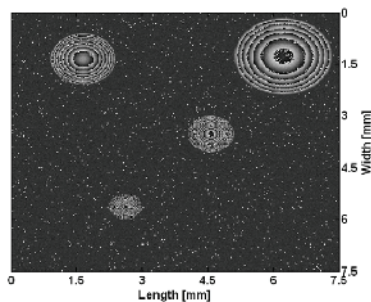


Fig. 3: Shape difference between the master and sample object of the Fig. 2

As an experimental result, we present the measurement of the deformation difference. The master and sample object were two different plastic plates and the sample object had three defects. With the holder shown in Fig. 4, we can apply a controlled deformation to the center of the plastic plate.

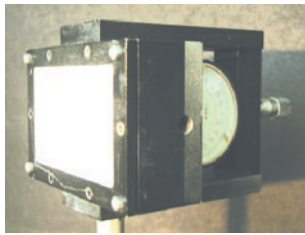


Fig. 4: Holder used to deform the master and sample object

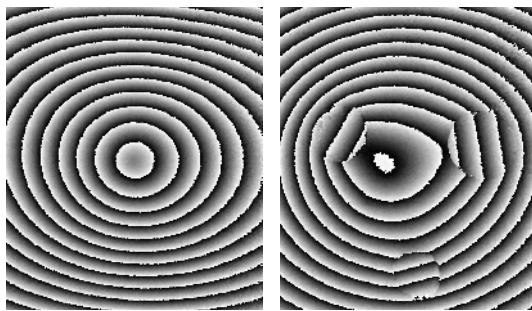


Fig. 5: Measurement of a deformation of $5 \mu\text{m}$ using the holographic set up shown on fig. 1 a) for: a) the master object and b) the sample object with three defects.

The deformation applied to both objects was $5 \mu\text{m}$. In Fig. 5, we show the holographic measurement of the deformation of the master and sample objects.

The conjugate wave front of the master in the initial state is projected onto the sample in its initial state using an LCD. The same procedure is made for the deformed state of both master and sample objects. From the resulting two holograms, we get the deformation difference between the master and the sample objects which is shown in Fig. 6. We recognize the three defects of the sample object in the fringe background pattern. The origin of this pattern is that a defect has both a local and an extended effect, as can be clearly seen in Fig. 5. b). The unwanted deviations between the reconstructed wave front of the master and the sample objects was compensated by writing an additional phase-shift to the LCD [3].



Fig. 6: Deformation difference between a master and a sample object by projecting the conjugated wave front of the master onto the sample object like shown in Fig. 1. b).

The CDH technique has the following properties: (i) interferometric accuracy of the comparison of the form or deformation of two nominally identical objects with rough surfaces, and (ii) the master hologram can be transmitted electronically, allowing the test object to be remotely located. At ITO the CDH technique includes an active compensation for repositioning errors of the sample object by an iterative self adjustment of the reconstructed conjugate wavefront of the master object that is generated by the LCD.

Supported by: Landesstiftung Baden-Württemberg

References:

- [1] Osten, W., Baumbach, T., Seebacher, S., Jüptner, W., "Remote shape control by comparative digital holography", Proc. Fringe 2001, Elsevier Science, pp. 373-382
- [2] Osten, W., Baumbach, T., Jüptner, W., "Comparative digital holography", Optics Letters 27 (2002), pp. 1764-1766
- [3] Schwab, X., Kohler, C., Osten, W., submitted for publication to Applied Optics, "Optimally tuned spatial light modulators for digital holography"

Invited lectures on international conferences

T. Haist

Dynamic holography and its application in measurement systems

SPIE Conf. "Optical Information Systems", August 4 - 5, 2003, San Diego, California, USA

N. Kerwien

Mueller matrix microscopy for high-resolution inspection of 2D-microstructures

EOS Topical Meeting Advanced Imaging Techniques, Delft, 2003

K. Körner

New approaches in depth-scanning optical metrology

SPIE Conf. "Optical Metrology in Production Engineering", April 27 - 30, 2004, Strasbourg, France

W. Osten

Trends for the solution of identification problems in holographic nondestructive testing

7th Int. Symposium on Laser Metrology Applied to Science, Industry, and Every Day Life. 9 - 13 September, 2002, Novosibirsk, Russia

W. Osten

Active metrology by digital holography

Int. Conf. Speckle Metrology 2003, 18-20 June 2003, Trondheim, Norway

W. Osten

Active approaches in optical metrology

Int. Conf. On Laser Applications and Optical Metrology, December 1 - 4, 2003, New Delhi, India

W. Osten

Modern optical nondestructive testing

2004 SEM X International Congress, June 7 - 10, 2004, Costa Mesa, USA

W. Osten

Optics beyond the limits: The future of high precision optical metrology and implications for optical lithography

ICO 2004, July 12 - 15, Tokyo, Japan

W. Osten

Optical nondestructive testing 3rd Sino-German

Symposium on Micro- and Nanotechnology, Beijing and Shanghai, PR China, 07. - 14. September 2004

W. Osten

Optics: Old questions! New answers?

Int. Colloquium "Optics - Key Technology for the Future", November 17 - 18, 2004, Aachen, Germany

C. Pruss

Metrological Features of diffractive high-efficiency objectives for laser interferometry

7th Int. Symposium on Laser Metrology Applied to Science, Industry, and Every Day Life. 9 - 13 September, 2002, Novosibirsk, Russia

Editorial Work

Osten, W. (Ed.):

Interferometry X- Applications

Proc. SPIE Vol. 4778, Bellingham 2002

Osten, W.; Novak, E. (Eds.):

Interferometry XI- Applications

Proc. SPIE Vol. 5532, Bellingham 2002

Osten, W.; Creath, K.; Kujawinska, M. (Eds.):

Optical Measurement Systems for Industrial Inspection III

Proc. SPIE Vol. 5144, Bellingham 2003

Osten, W.; Takeda, M. (Eds.):

Optical Metrology in Production Engineering

Proc. SPIE Vol. 5457, Bellingham 2004

Reviewed papers

Falldorf, C.; Osten, W.; Kolenovic, E.

Speckle shearography using a multiband light source

Optics and Lasers in Engineering 40 (2003) pp. 543-552

Haist, T.; Tiziani, H.J.

Color-coded object-adapted fringe projection for two- and three-dimensional quality control

Technisches Messen 69 (2002) pp.367-73

Kalms, M.; Osten, W.

Mobile shearography system for the inspection of aircraft and automotive components

Optical Engineering 42 (2003) 5 pp. 1188-1196

Kaysner, D.; Bothe, Th.; Osten, W.

Scaled topometry in a multisensor approach

Optical Engineering 43 (2004) 10 pp. 2469 – 2477

Kolenovic, E.; Osten, W.; Klattenhoff, R.; Lai, S.; Kopylow, C.; Jüptner, W.

Miniaturized digital holography sensor for distal three-dimensional endoscopy

Applied Optics 42 (2003) 25 pp. 5167-5172

Leonhardt K.; Droste U.; Tiziani H. J.

Interferometry for Ellipso-Height-Topometry-Part 1: Coherence scanning on the base of special coherence.

Optik 113 (2003) 12 pp. 513-519

Li, W.; Bothe, Th.; Osten, W.; Kalms, M.

Object adapted pattern projection – Part I: Generation of inverse patterns

Optics and Lasers in Engineering 41(2004) pp. 31-50

Pedrini G.; Tiziani H.J.; Alexeenko,I.

Digital-holographic interferometry with an image- intensifier system Imaging System

Applied Optics-OT 41 (2002) 4 pp. 648-653

Pedrini, G.; Gusev, M.; Schedin, S.; Tiziani, H. J.

Pulsed digital holographic interferometry by using a flexible fiber endoscope

Optics and Lasers in Engineering 40 (2003) pp. 487-489

Pedrini, G.; Schedin, S.; Tiziani, H.J.

Pulsed digital holography combined with laser vibrometry for 3D measurements of vibrating objects

Optics and Laser in Engineering 38 (2002) pp. 117-129

Pedrini G.; Tiziani H.J.

Short-Coherence Digital Microscopy by Use of a Lensless Holographic Imaging System

Applied Optics-OT 41 (2002) 22 pp. 4489-4496

Pedrini, G.; Alexeenko, I.; Osten, W.; Tiziani, H.J.

Temporal Phase Unwrapping of Digital Holograms Sequences

Applied Optics 42 (2003) 29 pp. 5846-5854

Proll, K.-P.; Nivet, J.-M.; Volland, Ch.; Tiziani, H.J.

Enhancement of the dynamic range of the detected intensity in an optical measurement system by a three-channel technique.

Applied Optics 41 (2002) pp. 130-135

Proll, K.-P.; Nivet, J.-M.; Körner, K.; Tiziani, H.J.

Microscopic three-dimensional topometry with ferroelectric liquid crystal-on-silicon displays

Applied Optics 42 (2003) pp. 1773-1777

Pruss, C.; Tiziani, H.J.

Dynamic null lens for aspheric testing using a membrane mirror

Optics Communications 233 (2004) pp. 15-19

Pruss, C.; Reichelt, S.; Tiziani, H. J.; W. Osten

Computer generated holograms in interferometric testing.

Optical Engineering 43 (2004) 11 pp. 2534-2540

Reichelt, S.; Daffner, M.; Tiziani, H. J.; Freimann, R..

Wavefront aberrations of rotationally symmetric CGHs fabricated by a polar coordinate laser plotter.

Journal of Modern Optics 49 (2002) 7 pp. 1069-1087

Reichelt, S.; Pruss, C.; Tiziani, H.J.

Absolute interferometric test of aspheres by use of twin computer-generated holograms.

Applied Optics 42 (2003) 22 pp. 4468–4479

Reichelt, S.; Tiziani, H.J.

Twin-GGHs for absolute calibration in wavefront testing interferometry

Optics Communications 220 (2003) 1 pp. 23-32

Rocktäschel, M; Tiziani, H.J.

Limatations of the Shack-Hartmann sensor for testing optical aspherics

Optics and Laser Technology 34 (2002) 34 pp. 631-637

Ruprecht, A. K.; Wiesendanger, T. F.; Tiziani, H.J
Chromatic confocal microscopy with a finite pinhole size

Optics Letters 29 (2004) pp. 2130-2132

Ruprecht, A. K.; Wiesendanger, T. F.; Tiziani, H. J.
Signal evaluation for high speed confocal measurements

Applied Optics 41 (2002) 35 pp. 7410-7415

Seifert, L.; Liesener, J.; Tiziani, H.J.
The adaptiv Shack-Hartmann sensor

Optics Communications 216 (2003) 4 pp. 313-319

Tavrov, A.; Totzeck, M.; Kerwien, N.; Tiziani, H.J.;
Rigorous coupled-wave analysis calculus of submicrometer interference pattern and resolving edge position versus signal to noise ratio

Optical Engineering 41 (2002) 8 pp. 1886-1892

Wiesendanger T.; Yasuno Y.; Ruprecht A.; Yatagai T.;
 Tiziani, H.J.
Characterization of Microoptic Arrays by Evaluation of the Axial Confocal Response

Optical Review 10 (2003) pp. 301-302.

Windecker, R.; Körner, K.; Fleischer, M.; Tiziani, H.J.
Signalverarbeitung bei tiefenscannenden 3D-Sensoren für neue industrielle Anwendung

Technisches Messen 69 (2002) pp. 251-257

Yasuno, Y.; Wiesendanger, T. F.; Makita, S.; Ruprecht, A. K.;
 Yatagai T.; Tiziani H. J.
Non-mechanically-axial-scanning confocal microscope using adaptive mirror switching

Optics Express 11 (2003) pp. 54-60

Yasuno, Y.; Wiesendanger, T.F.; Ruprecht, A.K.; Makita, S.;
 Yatagai, T.; Tiziani, H.J.
Wavefront-flatness evaluation by wavefront-correlation-information-entropy method and its application for adaptive confocal microscope

Optics Communications 232 (2004) pp. 91-97

Yasuno, Y.; Wiesendanger, T.; Ruprecht, A.; Yatagai, T.;
 Tiziani H.J.
Determination of Aberration Coefficient of Microoptic Arrays from Axial Confocal Response by Neural Method

Optical Review 10 (2003) pp. 318-320

Yasuno Y., Wiesendanger, T.F., Yatagai, T., Ruprecht, A.K;
 Tiziani, H.J.

Aberration measurement from confocal axial intensity response using neural network

Optics Express 10 (2002) pp. 1451-1457

Zhang, Y.; Pedrini, G.; Osten, W.; Tiziani, H.
Applications of fractional transforms to object reconstruction from in-line holograms

Optical Letters 29 (2004) 15 pp. 1793 – 1795

Zhang, Y.; Pedrini, G.; Osten, W.; Tiziani, H. J.
Image Reconstruction for In-Line Holography with the Yang-Gu Algorithm

Applied Optics 42 (2003) 32 pp. 6452

Zhang, Y.; Pedrini, G.; Osten, W.; Tiziani, H.
Phase retrieval microscopy for quantitative phase-contrast imaging

Optik 115 (2004) 2 pp. 94-96

Zhang, Y., Pedrini, G., Osten, W., Tiziani, H. J.
Reconstruction of in-line digital holograms from two intensity measurements

Optics Letters 29 (2004) 15 pp. 1787

Zhang, Y.; Pedrini, G.; Osten, W.; Tiziani, H. J.,
Whole optical wave field reconstruction from double or multi in-line holograms by phase retrieval algorithm

Optics Express 11 (2003) 24 pp. 3234

Conference proceedings and journals

2002

Falldorf, C.; Osten, W.; Kolenovic, E.; Jüptner, W.:

Features of multiband speckle shearography

Proc. SPIE Vol. 4900, pp. 1262-1269, 2002

Kauffmann, J.; Tiziani, H.J.

Temporal Speckle Pattern Interferometry for vibration measurement

in Vibration Measurement by Laser Techniques: Advances and Applications, E. P. Tomasini, ed.

Proc. SPIE Vol. 4827, pp. 133-136, 2002

Kerwien, N.; Totzeck, M.; Tavrov, A.; Tiziani, H.J.

Hochauflösender quantitativer Nomarski Interferenzkontrast mit Polarisationskorrektur

103. Jahrestagung der Deutschen Gesellschaft für angewandte Optik (DGaO) Innsbruck, 2002

Liesener, J.; Seifert, L.; Tiziani, H.J.

Adaptiver Shack-Hartmann-Sensor mit LCD-Mikrolinsen

Poster, 103. Jahrestagung der Deutschen Gesellschaft für angewandte Optik (DGaO) Innsbruck, 2002

Osten, W.; Baumbach, Th.; Falldorf, C.; Kalms, W.; Jüptner, W.
Some progress with the implementation of a shearography system for the testing of technical components

Proc. SPIE Vol. 4900, pp. 1299-1309, 2002

Osten, W.; Elandaloussi, F.; Mieth, U.

Trends for the solution of identification problems in holographic non-destructive testing (HNNDT)

Proc. SPIE Vol. 4900, pp. 1187-1196, 2002

Pedrini, G.; Alexeenko, I.; Gusev, M.; Tiziani, H.J.

Vibration measurements of hidden object surfaces by using holographic endoscopes

Proc. SPIE, Vol. 4827, pp. 315-322, 2002

Pruss, C.; Reichelt, S.; Tiziani, H.J.; Korolkov, V.P.

Metrological features of diffractive high-efficiency objectives for laser interferometry

Proc. SPIE, Vol. 4900, pp. 873-884, 2002.

Reichelt, S.; Pruss, C.; Tiziani, H. J.

Interferometrische Absolutmessung von Asphären

103. Jahrestagung der Deutschen Gesellschaft für angewandte Optik (DGaO) Innsbruck, 2002

Reichelt, S.; Pruss, C.; Tiziani, H. J.

New design techniques and calibration methods for CGH-null testing of aspheric surfaces

In Osten, W., editor, Interferometry XI: Applications, Proc. SPIE, Vol. 4778, pp. 158-168, 2002.

Reichelt, S.; Pruss, C.; Tiziani, H. J.

Specification and characterization of CGHs for interferometrical optical testing

In Osten, W., editor, Interferometry XI: Applications, Proc. SPIE, Vol. 4778, pp. 206-217, 2002

Reichelt, S.; Tiziani, H. J.; Freimann, R.

Interferometrischer Absoluttest von Fresnelschen Zonenplatten

103. Jahrestagung der Deutschen Gesellschaft für angewandte Optik (DGaO) Innsbruck, 2002

Tavrov, A.; Totzeck, M.; Kerwien, N.; Bohr, R.; Tiziani, H.J.

High-resolution Jones-matrix microscopy by means of interferometry and polarimetry

Poster, 103. Jahrestagung der Deutschen Gesellschaft für angewandte Optik (DGaO) Innsbruck, 2002

Totzeck, M.; Kerwien, N.; Tavrov, A.; Tiziani, H.J.

DUV-Mikroskopie: Mehr als nur eine Wellenlängenskalierung

Poster, 103. Jahrestagung der Deutschen Gesellschaft für angewandte Optik (DGaO) Innsbruck, 2002

Totzeck, M.; Kerwien, N.; Tavrov, A.; Rosenthal, E.;

Tiziani, H.J.

Quantitative Zernike phase-contrast microscopy by use of structured birefringent pupil-filters and phase-shift evaluation

Interferometry XI: Techniques and Analysis, Katherine Creath; Joanna Schmit; Eds. Proc. SPIE Vol. 4777, pp. 1-11, 2002

Totzeck, M.; Tavrov, A.; Kerwien, N.; Tiziani, H.J.

Inspection of sub-wavelength structures and zero-order gratings using polarization interferometry

Interferometry XI: Techniques and Analysis, Katherine Creath; Joanna Schmit; Eds. Proc. SPIE Vol. 4777, pp. 330-344, 2002

Wiesendanger, T.; Yasuno, Y.; Ruprecht, A.; Totzeck, M.; Tiziani, H.J.

Charakterisierung von Mikrooptikarrays durch Auswertung der axialen konfokalen Systemantwort

103. Jahrestagung der Deutschen Gesellschaft für angewandte Optik (DGaO) Innsbruck, 2002

2003

Alexeenko, I.; Gusev, M.; Pedrini, G.; Tiziani, H.J.

The applying of stroboscopic holographic interferometry to frequency-bounded vibrational investigation

Proc. SPIE, Int.Soc.Opt.Eng. Vol. 5134, pp.29-35, 2003

Berger, R.; Bohr, R.; Kerwien, N.; Pedrini, G.; Osten, W.; Tiziani, H.J.

Digitale holografische Interferometrie im DUV

104. Jahrestagung der Deutschen Gesellschaft für angewandte Optik (DGaO) Münster, 2003

Bodermann, B.; Mirandé, W.; Kerwien, N.; Tavrov, A.; Totzeck, M.; Tiziani, H.J.

Comparative linewidths measurements on Chrome and MoSi structures using newly developed microscopy methods

Recent Developments in Traceable Dimensional Measurements II, J. E. Decker, N. Brown
Proc. SPIE, Vol 5188, pp.320-330, 2003

Falldorf, C.; Hanson, S.; Osten, W.; Jüptner, W.

Fringe compensation in multiband speckle shearography using a wedge prism

Proc. SPIE Vol. 4933, pp. 82-89, 2003

Franz, S.; Windecker, R.; Tiziani, H.J.

Machine tool embedded white light interferometrical sensor for diameter measurements

Proc. SPIE, Vol. 5144, pp. 484-491, 2003

Gusev, M.; Alexeenko, I.; Pedrini, G.; Tiziani, H.J.

Mode shape separation in stroboscopic and double-pulse holographic analysis

Proc. SPIE, Vol. 5134, pp.36-42, 2003

Gusev, M.; Pedrini, G.; Alexeenko, I.; Tiziani, H.J., Malov, A.

Application of stroboscopic and double-pulse holographic interferometry to frequency-bounded vibrational investigation

Proc. SPIE, Vol. 5129, pp.80-91, 2003

Haist, T.; Osten, W.; Reicherter, M.; Liesener, J.; Seifert, L.

Dynamic holography and its application in measurement systems

Proc. SPIE Vol. 5202, pp.131-142, 2003

Kauffmann, J.; Gahr, M.; Tiziani, H.J.

Noise reduction in speckle pattern interferometry

in Speckle Metrology 2003, Gastinger K., Lokberg J., Winter, S., eds
Proc. SPIE Vol. 4933, pp. 9-14, 2003

Kauffmann J.; Tiziani, H.J.

Reduzierung der Messunsicherheit in der Temporal Speckle Pattern Interferometrie

104. Jahrestagung der Deutschen Gesellschaft für angewandte Optik (DGaO) Münster, 2003

Kerwien, N.; Rosenthal, E.; Tavrov, A.; Tiziani, H.J.

Hochaufgelöste Strukturerkennung mittels Müllermatrix-Mikroskopie

104. Jahrestagung der Deutschen Gesellschaft für angewandte Optik (DGaO) Münster, 2003

Kerwien, N.; Rosenthal, E.; Totzeck, M.; Osten, W.; Tiziani, H.J.

Mueller matrix microscopy for high-resolution inspection of 2D-microstructures

EOS Topical Meeting Advanced Imaging Techniques, Delft, 2003

Kerwien, N.; Tavrov, A.; Kauffmann, J.; Osten, W.; Tiziani, H.J.

Rapid quantitative phase imaging using phase retrieval for optical metrology of phase-shifting masks

Optical Measurement Systems for Industrial Inspection III, W. Osten, K. Creath, M. Kujawinska
Proc. SPIE, Vol 5144, pp. 105-114, 2003

Klattenhoff, R.; Kolenovic, E.; Osten, W;

von Kopylow, C.; Jüptner, W.

Miniaturized sensor head for distal holographic endoscopy

Proc. SPIE Vol 5145, pp. 137-145, 2003

Kolenovic, E.; Osten, W.; Jüptner, W.

Improvement of interferometric phase measurements by consideration of the speckle field topology

Proc. SPIE Vol. 4933, pp. 206-211, 2003

Liesener, J.; Seifert, L.; Schoder, T.; Tiziani, H.J.

Interferometer mit dynamischer Referenz

Poster 104 Jahrestagung der Deutschen Gesellschaft für angewandte Optik (DGaO) Münster, 2003

Nivet, J.-M.; Kömer, K.; Droste, U.; Fleischer, M.; Tiziani, H.J.; Osten, W.

Depth-scanning Fringe projection technique (DSFP) with 3-D calibration

Proc. SPIE Vol. 5144, pp. 443-450, 2003

Nivet, J.-M.; Körner, K.; Droste, U.; Fleischer, M.; Tiziani, H.J.; Osten, W.
Tiefenscannende Streifenprojektionstechnik (DSFP) mit 3D-Kalibrierung

3D-Nordost 2003, Tagungsband: 6. Anwendungs-bezogener Workshop zur Erfassung, Verarbeitung, Modellierung und Auswertung von 3D-Daten, Berlin, ISBN: 3-9809212-0-4, pp. 21-30, 2003

Osten, W.

Active metrology by digital holography

Proc. SPIE Vol. 4933, pp. 96-110, 2003

Osten, W.; Haist, T.; Körner, K.

Active approaches in optical metrology

Proc. Int. Conf. On Laser Applications and Optical Metrology, New Delhi 2003, pp. 9-19

Osten, W.; Kolenovic, E.; Klattenhoff, R.; Köpp, N.
Optimized interferometer for 3D digital holographic endoscopy

Proc. SPIE Vol 5144, pp. 150-161, 2003

Pedrini, G.; Alexeenko, I.; Tiziani, H.J.;

Pulsed endoscopic digital holographic interferometry for investigation of hidden surfaces
 Proc. SPIE, Vol 4933, pp.123-128, 2003

Proll, K.-P.; Nivet, J.-M.; Körner, K.; Tiziani, H. J.

Application of ferroelectric liquid crystal-on-silicon display in fringe projection setups

Proc. SPIE Vol. 5144, pp. 280-287, 2003

Pruß, C.; Reichelt, S.; Korolkov, V.P.

Diffraaktives Interferometerobjektiv.

Design, Realisierung, Performance

104. Jahrestagung der Deutschen Gesellschaft für angewandte Optik (DGaO) Münster, 2003

Pruss, C.; Reichelt, S.; Korolkov, V. P.; Osten, W.; Tiziani, H. J.
Performance improvement of CGHs for optical testing

In Osten, W., editor, Optical Measurement Systems for Industrial Inspection III

The International Society for Optical Engineering, 2003
 Proc.SPIE, Vol. 5144, pp. 460-471, 2003

Reichelt, S.; Pruss, C.; Tiziani, H. J.

Absolute testing of aspheric surfaces

In Geyl, R. and Rimmer, D. editors, Optical Fabrication, Testing, and Metrology

Proc. SPIE, Vol. 5252, pp. 252-263, 2003

Reicherter, M.; Liesener, J.; Haist, T.; Tiziani, H.J.

Advantages of holographic optical tweezers

Proc. SPIE Vol. 5143, pp. 76-83, 2003

Reicherter, M.; Liesener, J.; Haist, T.; Tiziani, H.J.

Flexible Fallengeometrie bei der holografischen Pinzette

104 Jahrestagung der Deutschen Gesellschaft für angewandte Optik (DGaO) Münster, 2003

Ruprecht, A.; Wiesendanger, T.; Tiziani, H.J.; Osten, W.

Auflösungssteigerung in einem chromatisch-konfokalen Mikroskop

104 Jahrestagung der Deutschen Gesellschaft für angewandte Optik (DGaO) Münster, 2003

Seifert, L.; Liesener, J.; Tiziani, H.J.

Adaptive Shack-Hartmann sensor

Proc SPIE Vol. 5144, pp. 250-258, 2003

Seifert, L.; Liesener, J.; Tiziani, H.J.

Der adaptive Shack-Hartmann Sensor zur Vermessung von Gleitsichtgläsern

Poster 104. Jahrestagung der Deutschen Gesellschaft für angewandte Optik (DGaO) Münster, 2003

Tavrov, A.; Kerwien, N.; Berger, R.; Tiziani, H.J., Totzeck., M.; Spektor, B.; Shamir, J.; Toker, G.; Brunfeld, A.

Vector simulations of dark beam interaction with nano-scale surface features

Optical Measurement Systems for Industrial Inspection III, W.

Osten, K. Creath, M. Kujawinska

Proc. SPIE, Vol 5144 , pp. 26-36, 2003

Wiesendanger, T.F.; Körner, K.; Ruprecht, A.; Windecker, R.; Tiziani, H.; Osten, W.

Fast confocal point sensor for in-process control of laser welding

Proc. Int. Conf. On Laser Applications and Optical Metrology, New Delhi 2003, pp. 336-339

Wiesendanger, T.; Yasuno, Y.; Ruprecht, A.; Tiziani, H.J.

Konfokale Mikroskopie mit einem adaptivem Spiegel

104. Jahrestagung der Deutschen Gesellschaft für angewandte Optik (DGaO) Münster, 2003

2004

Alexeenko, I.; Pedrini, G.; Zaslansky, P.; Kuzmina, E.;
Osten, W.; Weiner, S.

Digital holographic interferometry for the investigation of the elastic properties of bone

Advances in Mechanics edited by Carmine Pappalettere,
pp. 458-459, McGraw-Hill, Milano, 2004

Baumbach, T.; Osten, W.; Kebbel, V.; Kopylow, C.; Jüptner, W.
Set-up calibration and optimization for comparative digital holography

Proc. SPIE Vol. 5532, pp. 16-27, 2004

Baumbach, T.; Osten, W.; Kopylow, C.; Jüptner, W.
Application of comparative digital holography for distant shape control

Proc. SPIE Vol. 5457, pp. 598-609, 2004

Berger, R.; Kauffmann, J.; Kerwien, N.; Osten, W.; Tiziani, H.J.
Rigorous Beugungssimulation: Ein Vergleich zwischen RCWA, FDTD und der Finiten Elemente Methode

Poster P59, 105. Jahrestagung der Deutschen Gesellschaft für angewandte Optik (DGaO) Bad Kreuznach, 2004

Falldorf, C.; Kopylow, C.; Osten, W.; Jüptner, W.
Digital holography and grating interferometry: a complementary approach

Proc. SPIE Vol. 5457, pp. 225-231, 2004

Kauffmann J.; Kerwien N.; Tiziani, H.J.; Osten W.
3D anisotropy reconstruction: an iterative tensorial tomographic algorithm

Proceeding der ICO, pp.615-616, Tokyo, 2004

Kauffmann, J.; Kerwien, N.; Osten, W.; Tiziani, H.J.
Ein tomographisches Verfahren zur Rekonstruktion der volumenaufgelösten Verteilung des Brechungsindextensors

105. Jahrestagung der Deutschen Gesellschaft für angewandte Optik (DGaO) Bad Kreuznach, 2004

Kauffmann, J.; Kerwien, N.; Osten, W.; Tiziani, H.J.; Meining, S.
Polarisations-Mikroskopie im DUV

105. Jahrestagung der Deutschen Gesellschaft für angewandte Optik (DGaO) Bad Kreuznach, 2004

Körner, K.; Droste, U.; Schuster, Th.; Osten W.
Depth-scanning Techniques in Optical 3-D Metrology
VDI-Berichte Nr. 1844, pp.339-348, 2004

Körner, K.; Ruprecht, A.; Wiesendanger, T.

3D-Messtechnik in der mikroskopischen Skala

3D-Nordost 2004, Tagungsband: 7. Anwendungs-bezogener Workshop zur Erfassung, Verarbeitung, Modellierung und Auswertung von 3D-Daten, Berlin,

ISBN: 3-9809212-0-2, pp. 19-26, 2004

Körner, K.; Ruprecht, A. K.; Wiesendanger, T. F.

New approaches in depth-scanning optical metrology

Proc. SPIE Vol. 5457, pp. 320-333, 2004

Liesener, J.; Hupfer, W.J.; Gehner, A.; Wallace, K.

Tests on micromirror arrays for adaptive optics

SPIE Annual Meeting 2004 Denver

Proc. SPIE Vol. 5553, pp. 319-329, 2004

Liesener, J.; Pruß, C.; Tiziani, H.J.; Osten, W.

Array of phase-shifting point sources

MOC 04 Jena, Paper L61 + Poster, 2004

Liesener, J.; Seifert, L.; Osten, W.; Tiziani, H.J.

Active wavefront sensing and wavefront control with SLMs

SPIE Annual Meeting 2004 Denver

Proc. SPIE Vol. 5532, pp. 147-158, 2004

Liesener, J.; Tiziani, H.J.

Interferometer with dynamic reference

Proc. SPIE Vol. 5252, pp. 264-271, 2004

Martinez-Leon, L.; Pedrini, G.; Osten, W.

Short-coherence digital holography for the investigation of 3D microscopic samples

Proc. SPIE Vol. 5457, pp. 528-537, 2004

Nivet J.-M.; Schuster, T.; Körner, K.; Droste, U.; Osten, W.

A new calibration scheme for three-dimensional depth-scanning fringe projection measurement method

Proc. SPIE Vol. 5457, pp. 334-343, 2004

Osten, W.

Mehr Präzision und Sicherheit durch Lasermesstechnik.

Lasertechnik Journal Oktober 2004, S. 40-45

Osten, W.

Optics: Old questions! New answers?

Proc. Int. Colloquium "Optics – Key Technology for the

Future", November 17 – 18, 2004, Aachen, Germany, pp. 3-10

Osten, W.; Totzeck, M.

Optics beyond the limits: The future of high precision optical metrology and implications for optical lithography

Proc. ICO 2004, Tokyo 2004, pp. 589-592

Pedrini, G.; Alexeenko, I.

Miniaturised optical system based on digital holography

Proc. SPIE, Vol. 5503, pp. 493-498, 2004

Proll, K.-P.; Kohler, C.; Körner, K.; Osten, W.

Adaptive Microscopic 3-D Measurement with Liquid-Crystal Spatial Light Modulators

Photon 04 FASIG 3: Optical testing and New algorithms, Glasgow, 2004

Proll, K.-P.; Kohler, C.; Baumbach, T.; Osten, W.; Osten, S.; Gruber, H.; Langner, A.; Wernicke, G.

Optical characterization of liquid-crystal-on-silicon displays

Proc. SPIE Vol. 5457, pp.632-642, 2004

Reichle, R.; Pruss, C.; Osten, W.; Tiziani, H.J.;

Zimmermann, F.; Schulz, E.

Microoptical sensor for integration in a functional spark plug for combustion analysis by UV-laser induced fluorescence spectroscopy

Proc. VDI 4th Conference on Optical Analysis Technology, 2004; 23/24. Juni, Frankfurt

Reinig, P.; Dost, R.; Mört, M.; Hingst, T.; Mantz U.; Schuster, T.; Kerwien, N.; Kaufmann, J.; Osten W.

Potential and limits of scatterometry: A study on bowed profiles and high aspect ratios

Scatterometry Workshop 2004, 3.-5.5.2004 Porquerolles, Frankreich

Reicherter, M.; Gorski, W.; Haist, T.; Osten, W.

Dynamic correction of aberrations in microscopic imaging systems using an artificial point source

Proc. SPIE Vol. 5462, pp. 68-78, 2004

Ruprecht, A. K.; Körner, K.; Wiesendanger, T. F.;

Tiziani, H. J.; Osten, W.

Chromatic confocal detection for high speed micro-topography measurements

Three-Dimensional Image Capture and Applications VI

San Jose, CA, USA. 19-20 Jan. 2004

Proc. SPIE Vol. 5302-6, no.1, pp. 53-60, 2003

Ruprecht A.K.; Proll K.-P.; Kauffmann J.; Tiziani H.J.; Osten, W.

Multi Wavelength Systems in Optical 3-D Metrology

6th Int'l Conference for Optical Technologies, Optical Sensors and Measuring Techniques (OPTO 2004), Nürnberg, 25.-27. Mai 2004, pp. 101-106

Seifert, L.; Liesener, J.; Tiziani, H. J.; Osten, W.

Adaptive Shack-Hartmann Sensor

MOC 04 Jena, Paper L62 + Poster, 2004

Wiesendanger, T.; Körner, K.; Ruprecht, A.; Tiziani, H.J.; Osten, W.

Fast confocal point-sensor for in-process control of laser welding

ISMQ2004, 8th International Symposium on Measurement and Quality Control in Production, Erlangen, Germany, 2004. Proc. of Intl. Conf. on Laser Applications and Optical Metrology.

Editor C.Shakher and D:S: Mehta, pp. 336-339

Wiesendanger, T.; Ruprecht, A.; Körner, K.; Tiziani, H.J.; Osten, W.

Konfokaler Sensor zur Messung der Einschweißtiefe im Keyhole

105. Jahrestagung der Deutschen Gesellschaft für angewandte Optik (DGaO) Bad Kreuznach, 2004

Zaslansky, P.; Pedrini, G.; Alexeenko, I.; Osten, W.; Friessem, A.;

Weiner, S.; Shahar, R.

Static and dynamic interferometric measurements used to determine mechanical properties of cortical bone

Advances in Mechanics edited by Carmine Pappalettere, pp. 76-77, McGraw-Hill, Milano, 2004

Patents

2003

Körner, Klaus; Osten, Wolfgang
Verfahren und Sensor zur hochgenauen optischen Abtastung
 DE 10321883 A1, Anmeldedatum 07.05.2003

Körner, Klaus; Ruprecht, Aiko
Anordnung und Verfahren zur hochdynamischen, konfokalen Technik
 DE 10321885, Anmeldedatum: 07.05.2003

Körner, Klaus
Robuster interferometrischer Sensor und Verfahren zur Objektabtastung
 DE 10321886A1, Anmeldedatum: 07.05.2003

Körner, Klaus; Osten, Wolfgang
Robuster optischer Sensor und Verfahren zur Hochgeschwindichkeits-Detektion
 DE 10321887 A1, Anmeldedatum: 07.05.2003

Körner, Klaus; Osten, Wolfgang
Messverfahren und Sensor, insbesondere zur optischen Abtastung bewegter Objekte
 DE 10321888 A1, Anmeldedatum:07.05.2003

Körner, Klaus
Verfahren und Anordnung zur interferenziellen und hochdynamischen Keyhole-Tiefen-Detektion
 DE 10321894 A1, Anmeldedatum:07.05.2003

Körner, Klaus; Osten, Wolfgang
Interferometrischer Sensor zur chromatischen Objektiefenabtastung
 DE 10321895 A1, Anmeldedatum:07.05.2003

Körner, Klaus
Optischer Sensor und Verfahren mittels Triangulation, insbesondere zur chromatischen Objekt-Tiefenabtastung
 DE 10321896 A1, Anmeldedatum:07.05.2003

Körner, Klaus; Osten, Wolfgang
Multifokales konfokales Verfahren und konfokale Anordnung für wenig kooperative Objekte
 AKZ 10356412.8, Anmeldedatum: 24.11.2003

Körner, Klaus; Wiesendanger, Tobias; Osten, Wolfgang
Verfahren und Anordnung zur interferenziellen und hochdynamischen Keyhole-Tiefen-Detektion
 AKZ 10356415.2, Anmeldedatum:24.11.2003

Körner, Klaus; Osten, Wolfgang
Verfahren und Anordnung zur simultanten, multifokalen, optischen Anordnung
 AKZ 10356416.0, Anmeldedatum:24.11.2003

Liesener, Jan; Pruß, Christof
Schaltbares Punktlichtquellen-Array und dessen Verwendung in der Interferometrie
 DE 10325601, Anmeldedatum:5.6.2003

2004

Liesener, Jan; Pruß, Christof
Schaltbares Punktlichtquellen-Array und dessen Verwendung in der Interferometrie
 Internationale Anmeldung PCT/DE2004/001114,Anmeldedatum: 1.6.2004

HymoSens-Patentanmeldung: Lehmann, Peter; Lücke, Peter; Mohr, Jürgen; Moran-Iglesias, Carlos Javier; Osten, Wolfgang; Ruprecht, Aiko; Schönfelder, Sven
Optischer Messkopf
 AKZ 102004011189.8, Anmelder:Fa.Mahr, Anmeldedatum: 04.03.2004

Körner, Klaus; Ruprecht, Aiko; Lehmann, Peter; Osten, Wolfgang
Verfahren und Anordnung zur konfokalen Abtastung von bewegten Datenträgern
 AKZ 102004043992.3, Anmeldedatum: 08.09.2004

Körner, Klaus; Kohler, Christian; Osten Wolfgang
Streifenprojektions-Triangulationsanordnung zur dreidimensionalen Objekterfassung, insbesondere auch zur dreidimensionalen Erfassung des Gesichts eines Menschen
 AKZ 102004052199.9, Anmeldedatum: 20.10.2004

Körner, Klaus; Wiesendanger, Tobias; Berger, Reinhard; Ruprecht, Aiko; Droste, Ulrich; Pruß, Christof; Osten, Wolfgang
Interferometrischer Multispektral-Sensor und interferometrisches Multispektral-Verfahren zur hochdynamischen Objekt-Tiefenabtastung oder Objekt-Profilerfassung
 AKZ 102004052205.7, Anmeldedatum: 20.10.2004

Doctorial Thesis, Diploma Thesis & Student Research Projects

Doctorial Thesis

Proll, Klaus-Peter

Optische Topometrie mit
räumlichen Lichtmodulatoren

10/2004

Reichelt, Stephan

Interferometrische Optikprüfung mit
computergenerierten Hologrammen

9/2004

Fleischer, Matthias

Signalverarbeitung in der
optischen 3D-Messtechnik

5/2003

Daffner, Michael

Asphärische Korrekturlemente zur
Strahlformung von Leistungslaserdioden

2/2003

Rocktäschel, Martin

Wellenfrontanalyse mittels
diffraktiver optischer Elemente

1/2003

Hofbauer, Ulrich

Zweiwellenlängeninterferometrie
mit Laserdioden

10/2002

Haist, Tobias

Einsatz räumlicher Lichtmodulatoren
zur Defekt- und Mustererkennung

9/2002

Wegner, Michael

Konfokale Mikroskopie zur
Topografiebestimmung technischer Oberflächen

5/2002

Diploma Thesis

Berger, Reinhard

Rekonstruktionsalgorithmen
für die digitale Holografie

3/2004

Meining, Stefan

Hochauflösende Phasenfrontmessung
mittels Phasere retrieval

1/2004

Kohler, Christian

Polarisationsoptische Charakterisierung
reflektiver Flüssigkristall-Lichtmodulatoren
(zum Einsatz in der Holografie)

10/2003

Frey, Katharina

Mehrwellenlängeninterferometrie
an asphärischen Oberflächen

04/2003

Rosenthal, Eva

Müllermatrix- Mikroskopie zur
hochauflösenden Strukturerkennung

2/2003

Kauffmann, Jochen

Untersuchung und Anpassung der Temporal
Speckle Pattern Interferometrie (TSPI) an die
Schwingungsmessung

8/2002

Schillings, Michael

Softwareentwicklung für eine
Laserlithographieanlage

10/2002

Student Research Projects

Rüth, Birgit
Charakterisierung adaptiver
Flüssigkristall- und Electrowettinglinsen
9/2004

Tepes, Paul
Optischer Fasersensor zur
Verbrennungsdiagnostik
6/2004

Weiger, Ulrich
Modellierung des Aufbaus
einer holografischen Pinzette
5/2004

Buckmüller, Peter
Simulation konfokaler Sensoren unter
Einbeziehung von Mikrooptiken
10/2003

Kohler, Christian
Charakterisierung einer CMOS-Kamera und
Aufbau eines adaptiven Messsystems
12/2002

Liebing, David
Konzeption und Realisierung eines neuartigen
faseroptischen TSPI-in-plane-Sensors
12/2002

Schmid, Peter
Prüfstand zur Charakterisierung von LCDs
5/2002

Liebing, Markus
Entwicklung eines Gitter-Shearing-Interferometers
zur Wellenfrontcharakterisierung von
Hochleistungslaserdioden
5/2002

Schillings, Michael
Testbetrieb einer ultrapräzisen
Laserlithographieanlage
4/2002

Rosenthal, Eva
Eignung verschiedener polarisationsoptischer Filter
für die quantitative Phasenkontrastmikroskopie
1/2002

Fest-Kolloquium Optik 2003

„optics and optoelectronics: state of the art and future development“

Optik und Optoelektronik: Stand und zukünftige Entwicklung

mit Abschiedsvorlesung von Herrn Prof. Dr. H.J. Tiziani und

Antrittsvorlesung von Herrn Prof. Dr. W. Osten

am 19. Februar 2003, Teilnehmer: ca. 400

| | |
|--|--|
| Begrüßung und Einführung | Prof. Dr. W. Osten ITO, Universität Stuttgart Prof. Dr. R. Gadow Fakultät für Maschinenbau, Universität Stuttgart Prof. Dr. H.J. Tiziani ITO, Universität Stuttgart |
| Grundlagenforschung an Halbleiter-Nanostrukturen | Prof. Dr. K. von Klitzing Nobelpreisträger Max-Planck-Institut für Festkörperforschung, Stuttgart |
| Entwicklung der optischen Systeme für die Mikrolithographie | Dipl.-Pfys. Winfried Kaiser Carl Zeiss, 73446 Oberkochen |
| Moderne Optiksysteeme für die 3D-Vermessungstechnik | Dr. B. Braunecker Leica Geosystems, 9435 Heerbrugg; CH |
| Satelitten-Kommunikation mit Laserlicht | Dr. Z. Sodnik esa, ESTEC, Keplerlaan 1, 2200AG Noordwijk ZH, NL |
| Eröffnung der Festveranstaltung | Prof. Dr. D. Fritsch Rektor der Universität Stuttgart |
| Der Innovationsprozess bei Carl Zeiss | Dr. A. Siegel Carl Zeiss, 73446 Oberkochen |
| Laudatio für Herrn Prof. Tiziani | Prof. Dr. W. Karthe Fraunhofer Institut für Angewandte Optik und Feinmechanik, 07745 Jena |
| Faszinierende Optik und optische Messtechnik, Rückblick und Ausblick | Prof. Dr. H.J. Tiziani ITO, Universität Stuttgart |
| Optische 3D-Messtechnik: von der Idee zum System | Prof. Dr. W. Osten ITO, Universität Stuttgart |

Optik-Kolloquium 2004

„optical production measurement technology - challenges and future directions“

Optische Fertigungsmesstechnik – Herausforderungen und Perspektiven

am 18. Februar 2004, Teilnehmer: ca. 300

| | |
|---|--|
| Begrüßung und Einführung | Prof. Dr. W. Osten ITO, Universität Stuttgart |
| Prozessfähigkeit durch optische Messtechnik- Herausforderungen und Chancen | Prof. Dr.-Ing. T. Pfeifer Dipl.-Wirt.-Ing. K. Schneefuß Fraunhofer-Institut für Produktionstechnik, IPT Aachen |
| Vergleichbarkeit optisch und taktil gemessener Gestaltabweichungen | Dr. P. Lehmann Mahr GmbH, Göttingen |
| Optische Messtechnik in den Mikro- und Nanotechnologien | Prof. Dr. G. Wilkening Physikalisch-Technische Bundesanstalt, Braunschweig |
| Hochauflösende interferometrische Messtechnik in der Fotolithografie | Dr. B. Dörband Carl Zeiss SMT AG, Oberkochen |
| Laserinterferometrische Mess- und Sensortechnik in der Fertigung | Prof. Dr.-Ing. G. Jäger TU Illmenau, Illmenau |
| Optische Messtechnik in der modernen Gleitsichtglasfertigung | F. Gruna Rodenstock, Messtechnik Brillenoptik, München |
| Informationstheoretische Optimierung von 3D-Sensoren- oder : Wieviel darf ein Sensor kosten? | Prof. Dr. G. Häusler Universität Erlangen und 3D-SHAPE GmbH, Erlangen |
| Das Prinzip der Phasogrammetrie- flexible automatisierte Erfassung komplexer Objektgeometrien | Dr. G. Notri Fraunhofer-Institut für angewandte Optik und Feinmechanik IOF, Jena |
| Stiefenprojektionen in der Fertigungsmesstechnik am Beispiel präzisionsgeschmiedeter Zahnräder | Prof. Dr. -Ing. E. Reithmeier Dr.-Ing. J. Seewig TU Hannover, IMR Hannover |
| Anwendung optischer Messtechniken im Flugzeugbau | Dr. U. Schnars, R. Henrich, D. Scherling A. Kück, Dr.-Ing. S. Seebacher Airbus Deutschland GmbH, Bremen |
| Anwendung optischer Messtechniken in der Automobilindustrie | Dr.-Ing H. Steinbichler Steinbichler Optotechnik GmbH, Neubeuren |
| Diagnostik von Turbomaschinen mit optischen Messtechniken | Prof. Dr. J. Woisetschläger Technische Universität Graz, Österreich |
| Physikalisch-optische Effekte in der optischen CD-Metrologie | N. Kerwien, Prof. Dr. W. Osten ITO, Universität Stuttgart |
| Neue Ansätze bei tiefenscannenden Verfahren in der dimensionellen Messtechnik | Dr.-Ing. K. Körner, Prof. Dr. W. Osten ITO, Universität Stuttgart |

Organized International Conferences: 2002 – 2004

W. Osten:

Interferometry XI. SPIE Congress,
10 – 11 July 2002, Seattle, USA

W. Osten:

**Optical Measurement Systems for Industrial
Inspection III, SPIE Congress,**
23 – 26 June 2003, Munich, Germany

W. Osten:

**Optical Metrology in Production Engineering.
SPIE Congress Photonics Europe,**
27 – 30 April 2004, Strasbourg, France

W. Osten:

Interferometry XII: Applications. SPIE Congress,
4 – 5 August 2004, Denver, USA

W. Osten:

**Optical Nondestructive Testing
ICEM 12, International Conference on
Experimental Mechanics**
31. August 2004, Bari, Italy

Impressum:

Publisher: Institut für Technische Optik (ITO)
Universität Stuttgart
Pfaffenwaldring 9
D - 70569 Stuttgart
www.uni-stuttgart.de/ito

Editor: Dipl.-Ing. (FH) Erich Steinbeißer..... steinbeisser@ito.uni-stuttgart.de
Dipl.-Des. Matthias Staufer, ma•ma design (Graphic & Layout)..... mail@mamadesign.net

Printing: f.u.t. müllerbader gmbh

Print run: 400

ISBN 3-923560-52-4

